Physiological MR imaging of small bowel: Implementation, validation and interpretation

Dr. Aser Soliman Ahmed Farghal

A thesis submitted for the degree of

Doctor of Medicine

School of Medicine, Health policy and Practice

University of East Anglia

Norwich, England

2011

Table of contents

List of Tables

List of Figures

Statement of originality

Unless otherwise noted or referenced in the text, the work described in this thesis is that of the author.

Acknowledgement

The writing this thesis was undoubtedly one of the most challenging tasks I have ever had to face in my entire career. If it were not for the support of enthusiastic supervisors, sincere colleagues and a special loving family, I would never have got that far.

I am deeply and forever indebted to my parents for their love, support and encouragement throughout my entire life and for them I dedicate this thesis.

I cannot express my full gratitude to Dr Andoni Toms who has been an outstanding supervisor despite his many other professional commitments. He has everything one could want in a supervisor.

I am also deeply indebted to Mr Bahman Kasmai, our excellent computer scientist, for his tireless effort in developing the software.

I would like to thank the Norfolk and Norwich Radiology Department for funding and approving this project.

My sincere thanks go to, Dr Paul Malcolm for his invaluable advice, support and also for being a volunteer in this work.

I would like to deeply thank Dr Stuart Williams, Dr Ben Simpson, Dr Mathew Tam and Dr James Hathorn for being volunteers in this study.

I am proud to record that I had several opportunities to work with an exceptionally excellent MR radiographers. Angela, Cheryl, Richard, and Shelly, your help and patience are appreciated.

I am very grateful to the Norwich Radiology Academy staff for their help and support.

I am also very grateful to my brother Ahmed, who helped me in no time when I needed him.

Words fail me to express my appreciation to my wife Sherwit, without whom; this effort would have been worth nothing. Your love, support, and persistent confidence in me have taught me so much about sacrifice and compromise.

To my daughters, Noureen and Lamar, I am deeply sorry for the time we spent apart.

Finally, I would like to thank everybody who was important to the success of this thesis, as well as expressing my apology that I could not mention personally one by one.

Abstract

The complex shape and biomechanics of small bowel make it difficult to obtain quantitative measures of its function using conventional imaging approaches. The aims of this thesis were to examine the feasibility, optimization, reliability and validity of a novel approach to evaluating small bowel peristalsis using dynamic MRI.

Dynamic abdominal MR images were acquired from healthy volunteers. Parametric maps were generated depicting the mean change in signal amplitude per voxel. Correlation of parametric maps and raw cinematic MR data was assessed by two independent observers.

To optimise the MR protocol, an index of peristalsis was generated by dividing the sum of the mean pixel values of the resulting parametric images divided by the number of pixels per image. ANOVA tests were performed to determine the optimum MR protocol to reproduce the peristaltic Index.

In the reliability study, Total Voxel Activity (TVA: the sum of all mean signal amplitude changes per voxel) was measured. Five studies were repeated with the same parameters and reliability was measured using interclass correlation coefficient.

In the validity study, three sets of cinematic images were acquired covering the whole abdomen. TVA per slice and the global TVA were compared before and after injection of an anti-cholinergic agent.

Results demonstrated that applying increasing sequential thresholds on the histogram could segment out small bowel activity from other

movement and noise. In order to reproduce the peristaltic index acquisition should be 15 frames or more and the whole abdomen should be covered. The reliability study revealed excellent correlation between the test and re-test studies. Global TVA reduced significantly after the hyoscine injection by a mean of 66%. These results described in this thesis suggest that automated segmented quantification of small bowel peristalsis from dynamic MR is feasible, and probably valid technique for measuring small bowel peristalsis.

Introduction

Background

The small bowel is an anatomically and bio-mechanically complex organ. The complex shape and distribution of the bowel loops and its constant complex movement make it difficult to obtain quantitative measures of its function using conventional imaging tools. Up until now most developments in the imaging of small bowel have focused on developing techniques that outline anatomical details from which disease can be inferred (Husebye). There has been limited focus on using radiological imaging for generating measures of function due to restrictions of ionizing radiation use, and also invasiveness of most of these techniques. Normal small bowel function results in multiple morphological changes, in three dimensions, at multiple points in space at any one time (Maglinte, Lappas, Heitkamp, Bender, & Kelvin), Therefore analysis using conventional anatomical imaging is often overwhelmed by data which makes manual interpretation an unreliable method (Fig 1.1).

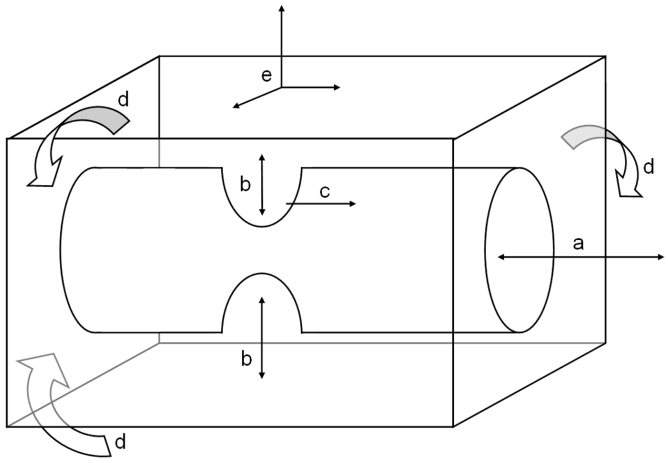

Figure (1.1) demonstrating the complexity of small bowel movements consisting of luminal content (a), peristaltic contraction (b), propagation (c), as well as rotation (d) or translocation (e) of small bowel loop in any of the three dimensions of space.

Aim of the study

The aim of this study was to investigate automated techniques of measuring small bowel motility using dynamic MRI; in particular the optimal imaging parameters will be evaluated, the reliability of the technique will be validated, and the application of various mathematical analyses will be assessed. In the long term the aim is to see if a robust technique can be developed that will enable measuring global function of peristalsis, which could initially be used to define a normal range in healthy volunteers, and then be used for monitoring disease.

Site of the study

The MR scanning was performed in the radiology department at the Norfolk and Norwich University Hospital, and image processing occurred in the imaging laboratory at the Norwich Radiology Academy.

Ethical approval

Ethical approval was obtained from the East Norfolk and Waveney Research Committee Ref: 2008RAD05S (186-12-08) (Appendix 3).

Literature Review

Small bowel anatomy and physiology

The small bowel is a tubular structure measuring approximately 600 cm in length. The duodenum and jejunum forms approximately 40%, and the ileum forms approximately 60% of its length. Its main function is to receive and digest nutrients from the stomach and deliver the undigested residue to the large bowel.

Two major movements of the luminal contents occur in the small bowel; these are mixing and propulsion. These movements are facilitated by the presence of two major layers of smooth muscles, the muscularis externa, and the muscularis mucosa. The muscularis externa has an outer longitudinal layer and an inner circular layer perpendicular to each other. The circular layer is further subdivided into inner and outer layers. The function of the muscularis mucosa layer has not been discovered yet.

The two major movements, mixing and propulsion, occur mainly as a result of contraction of the muscularis externa, however the exact function of each group has yet to be understood (Bass & Wiley; Tasaka & Farrar).

The time taken for the luminal content to travel from the duodenum to the ileo-caecal valve is called the transit time, however this definition is variable in the literature. The transit time depends mainly on propulsion. Changes in luminal calibre, amplitude of phasic contraction and luminal wall tone are the main factors affecting propulsion. The transit time is variable between subjects and ranges from 78 to 264 minutes in human (Argenyi, Soffer, Madsen, Berbaum, & Walkner; Gryback, Blomquist, Schnell, Jacobsson, & Hellstrom; Sadik, Abrahamsson, & Stotzer).

Argenyi et al., (Argenyi, et al.) and Gryback et al., (Gryback, Jacobsson, Blomquist, Schnell, & Hellstrom) studied the variability of transit time in 10 adult volunteers and reported a slightly higher range of 322 min. Sadik et al., studied the effect or gender and transit time and reported slower transit time in female subjects (Sadik, et al.). One study reported accelerated transit time in association with increasing age (Graff, Brinch, & Madsen). The transit time doesn't seem to alter between liquids and solids as demonstrated in a study using solid I^{131} and ^{99m}Tc-DTPA mixed with water (Hammer, Hammer, & Kletter; Malagelada, et al.). Small bowel transit, however, is dependent on caloric content, being slow in high caloric and lipid contents (Lin, Zhao, & Wang).

Small bowel peristalsis occurs as a result of contractions of smooth muscles in response to slow-wave of depolarisation and re-polarisation which oscillate at a rate of 11 to 12 cycles per min in the duodenum, and at a lower frequency more distally, as well as neuro-humeral stimuli and other excitatory stimuli (Barrett).

The small bowel is innervated normal by two groups of neurons, the extrinsic and intrinsic group. The intrinsic group is divided into myenteric and submucosal plexuses. The extrinsic group arises mainly from the vagus and splanchnic nerves. Another group of specialised cells that take part in regulating small bowel motility are the interstitial cells of Cajal (ICCs). The ICCs act as pacemakers for the small bowel and they also regulate immediate neurotransmission (Suzuki, Prosser, & Dahms; Wang, Sanders, & Ward). The myoelectric activity of small bowel is propagated and regulated by intrinsic electrical coupling. Propagation of the slow-wave of depolarization along the length of the bowel requires bowel continuity as a slow wave cannot travel more than 6 mm (Connor, Mangel, & Nelson). Slow-wave generally propagates distally, however a retrograde can occur very rarely (Diamant & Bortoff).

Factors regulating small bowel peristalsis

The main stimuli that affect peristalsis are the small bowel the mucosal pinching and mechanical distension either with gas, liquid or solids. Two simultaneous phases have been demonstrated in peristaltic movement. When the mucosa is stimulated a proximal excitatory (the ascending phase) and distal inhibitory (the descending phase) reflexes occur. In the ascending phase, the circular muscle group contract and the longitudinal muscles relax simultaneously proximal to the stimulus (usually by distension). In the descending phase, the longitudinal muscles contact and the circular muscles relax distal to the stimulus (Sarna, et al.). The resulting movement of both phases is

propulsion of the luminal content distally. This activity is moderated by the luminal content. Localised bowel distension seems to increase the contraction length but decreases regional propagation velocity (Larson & Schulze). This is slightly different with distension with air where there is a short segment of contraction and rapid propagation wave. This radial stretch is very potent in generating the peristaltic circular contraction and facilitated by receptors located in the mucosal surface (Brookes, Chen, Costa, & Humphreys; Der-Silaphet, Malysz, Hagel, Larry Arsenault, & Huizinga).

Pattern of small bowel motor activity

1- Migrating motor complex

The small bowel has a pattern of motility during fasting which is different from the one that occurs in the postprandial state. This fasting state is characterised by the presence of periodic intense contractions, which travel from the duodenum to the ileum. This organised movement is called the migrating motor complex (MMC) which acts as a bowel cleaner, as it tends to clear the bowel from food residue (Nieuwenhuijs, et al.). The MMC consists of four different phases lasting approximately 100 minutes. Phase I, is the static or the quiescent phase, which lasts approximately half of the cycle. Phase II is a period of uncoordinated irregular motility. Phase III is a period of forceful rhythmic contractions that travels distally and lasts for approximately 5 to 10 minutes (Dalenback, et al.) (Fig 2.1). The MMC is quite variable between subjects however they are

reproducible within subjects (Penning, Gielkens, Hemelaar, Lamers, & Masclee). Phase III occurs at least once in six hours in normal individuals (Soffer, Thongsawat, & Ellerbroek). People above the age of 80 tends to have a slower phase III (Fich, Camilleri, & Phillips). Complex neural and chemical mediators control the MMC. The vagus and the extrinsic nerves have regulatory effects on the speed of contractions (Heppell, Kelly, & Sarr; Marik & Code) (Soffer, et al.)

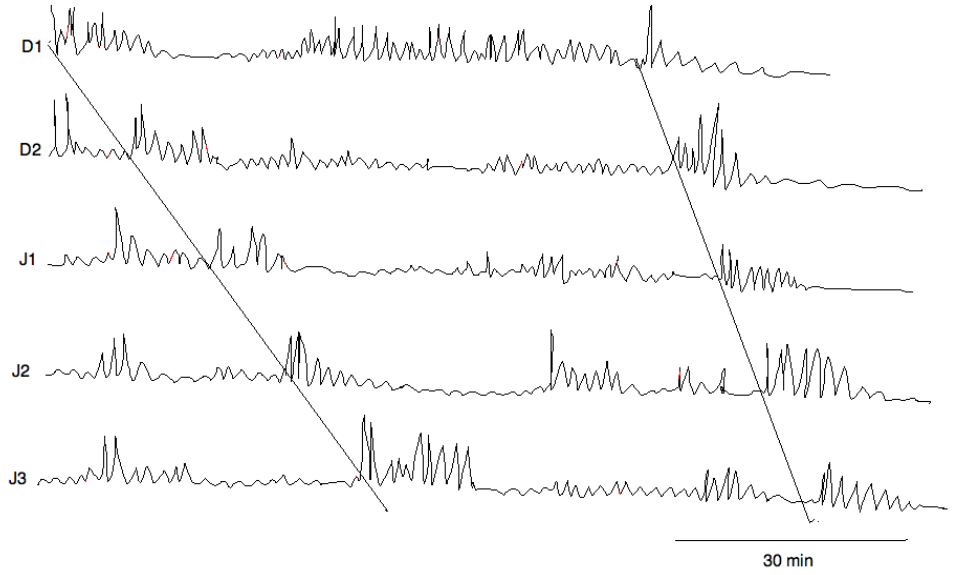

Figure (2.1) demonstrating a graph of the monomeric recordings of the human MMC in the duodenum (D1-d2) and jejunum (J1 – J3) (Adapted from Soffer at al. (Soffer, et al.))

2- Post prandial motor activity

Feeding changes the pattern of bowel motility to the fed, or the postprandial state in which the MMC is replaced by irregular forcible activity. The duration of this state depends on the caloric content (von Schonfeld, Evans, Renzing, Castillo, & Wingate). The pattern of

movements is similar to phase II of the MMC however they are slightly greater in intensity (McCoy & Baker). In both conditions, about 20% of the time contractions are stationary which pushes the content to and fro movement (Ehrlein & Schemann). It is believed that the purpose of this movement is to mix the chyme with the digestive secretions and also to expose the content to the mucosal surface for absorption.

There is another type of peristaltic activity that occurs in certain circumstances especially in reaction to toxic conditions, called the peristaltic rush or giant migrating contractions. These are fast contractions, which are approximately 2 to 3 times stronger in amplitude and 4 times longer in duration than the normal phasic contractions and travels at a speed of 1 cm per second (Kruis, Azpiroz, & Phillips; Sarna). There is also a retrograde peristaltic contraction, which leads to vomiting and retching, however these do not occur in normal circumstances.

History of small bowel imaging

Plain Radiography

On the 22nd of December 1895, Wilhelm Rontgen succeeded in imaging his own hands using x-rays. Since then, the world of radiological imaging has emerged. Plain film examination remains the most commonly performed study in medical imaging, due to its availability, low cost and non-invasiveness. Bowel obstruction, perforation, foreign bodies and pneumatosis intestinali remain the main indications for using plain films in the investigation of small bowel (Herlinger H).

Transit studies

Functional assessment of small bowel by plain radiographs is limited and restricted to transit time studies using radio-opaque markers where a series of radiographs is taken over 6 day period. There is a wide variability in the literature about the exact definition of small bowel transit time. Some authors define it as the duration of time it takes for barium, during the barium follow through examinations, to travel from the jejunum to the Ileocecal valve (IC). Others defined it as the time taken of the second cup of barium swallow to reach the IC valve (Gerson; Kim; Thompson, Halvorsen, Shaw, Bates, & Shemano).

Transit time can be measured by direct visualization using barium, radio-opaque markers (Abrahamsson, Antov, & Bosaeus) , with scintigraphic methods (Jones, et al.), or by indirect methods such as

the lactulose-hydrogen breath test (Kellow, Borody, Phillips, Haddad, & Brown; Mishkin & Mishkin)

Scintigraphic techniques have been used more often for measuring oesophageal and colonic transit times, as well as gastric emptying (Bestetti, Carola, Conciato, Marasini, & Tarolo) (Jones, et al.; Naslund, Bogefors, Gryback, Jacobsson, & Hellstrom).

Hung et al., used activated charcoal labelled with Tc-99m pertechnetate and loaded in a gastric acid resistant capsule to measure the transit time in ten healthy volunteers (Hung, Tsai, & Lin). These techniques are time consuming (takes at least 8 hours in Hung et al., study), and also involves ionizing radiation which has its own restrictions (Gryback, Blomquist, et al.).

Lactulose breath test is another test used to measure the intestinal transit time by measuring the exhaled hydrogen after oral dose of lactulose. The exhaled hydrogen is the end result of the metabolism of lactulose by the colonic bacterial flora. The transit time is measured by calculating the duration required to reach the peak concentration of hydrogen in the exhaled air (C. E. King & Toskes; C. E. King, Toskes, Spivey, Lorenz, & Welkos; Lieb & Draganov).

Sharpstone et al., studied the transit time in AIDS patients using another indirect technique, by assessing the rate of rise in serum 3-O-methyl-D-glucose (which is normally absorbed in the jejunum) and Sulphasalazine (which is metabolized in the caecum to 5-aminosalicylic acid and sulphapyridine) following their oral administration (Sharpstone, et al.). The limitations of this type of

study are that they rely on the metabolism of the substrate by colonic bacteria, which is deficient in 25% of the population due to lack of the proper colonic bacterial strain. Also overgrowth of colonic bacteria in certain diseases like inflammatory bowel disease can cause false rapid transit time.

Small bowel follow-through

Small bowel follow through was the primary method for diagnosing diseases of the small bowel until the 1990's (Rubesin & Maglinte). The barium examination of the small intestine remains an important examination and is more challenging to perform than the barium meal or barium enema, mainly because of the small bowel length, and the difficulty in manipulating the contrast medium so that all segments are well visualized (Nolan & Traill).

The barium follow-through can either be performed following a barium examination of the upper gastrointestinal tract (Marshak, Maklansky, & Lindner), or as a dedicated examination of the small bowel (Diner, Hoskins, & Navab); For this dedicated small bowel examination, a large volume of dilute barium suspension is administered orally, and fluoroscopy with spot filming are performed frequently by the radiologist, who is available throughout the examination. Effervescent agents, that release gas in the small intestine, may also be used during the barium follow-through in an attempt to give double-contrast views (Fraser & Preston).

The barium follow-through has the disadvantage of being time-consuming for patients, radiologists and the radiology department; also the use of ionizing radiation has its implications and restrictions

particularly in children, and pregnant women. Moreover, the functional information recorded during screening is subject dependant and lacks the accurate quantification.

Enteroclysis (small bowel enema)

Enteroclysis was introduced in the 70's and with the SBFT remained the main methods of investigating the mesenteric small intestine to late 90's.

Sellink et al., worked during the last decade on enteroclysis so that it has been widely used and also developed the ideal density of the barium suspension (Sellink). Bilbao-Dotter developed the tube by which infusion of barium reduced the time of the procedure, and also improved the quality of information obtained when compared to the conventional barium follow through method (Bilbao, Frische, Dotter, & Rosch). Some centres use double contrast (air - barium) for better visualization of bowel loops (Ekberg).

The main advantage of the enteroclysis technique is that the jejunum and ileum are distended by the barium contrast medium, making any morphological abnormality easier to identify. Distending the lumen of the intestine tests the elasticity of the wall and abnormal narrow segments can easily be detected (Theoni).

Herlinger et al., modified the double contrast technique by injecting 200ml of moderate-density barium suspension (85% to 100% weight/volume) followed by 1-2 Litres of 0.5% aqueous suspension of methylcellulose (Herlinger). This gives excellent mucosal detail of the normal small intestine, but abnormal segments are better demonstrated

by the barium suspension at the head of the column. Compression spot views are an important part of the examination (Scholz) to separate overlapping loops of intestine. Localized abnormalities can only be adequately demonstrated by applying proper compression, and spot views of the separated segments should be taken. This technique is invasive and uncomfortable for patients. It is also used purely for anatomical localization of disease within the bowel rather than for functional assessment. Ionizing radiation remains another issue in this method. The mean effective patient radiation dose for enteroclysis is about 1.5 mili Severts (Hart, Haggett, Boardman, Nolan, & Wall), which is equivalent to approximately 250 chest radiographs.

Ultrasonography and small bowel

Ultrasonography has been used widely for imaging the abdominal solid organs. Visualizing small bowel with ultrasound is difficult due to luminal gas (C. F. Dietrich, et al.). Recent studies aimed to visualise small bowel by hydrodilation using non-absorbable electrolyte solutions, in order to avoid gas interference and to give anatomical details. The technique of ultrasonography using orally ingested iso-osmolar, non-absorbable solution for optimal distension was initially developed by Plotta et al., (Pallotta, Baccini, & Corazziari). They used systematic ultrasonographic review of the superficial part of the abdomen before and after oral ingestion. Their main interest was to demonstrate the ability of ultrasound to demonstrate the site and type of pathological lesions leading to unexplained abdominal pain, and bowel disorders. Their results were very similar to the corresponding barium follow-through. Nagi et al., examined 45 patients using

sonoenteroclysis to demonstrate bowel wall thickening, distensibility, and filling defects, however they used a nasojeujenal tube (modified Billabo Dotter tube) to administrate the nonabsorbable solution (Nagi, Rana, Kochhar, & Bhasin).

Haruma et al., used real time ultrasonography to assess the gastro duodenal motility post liquid provocation, using 400 mls of meat soup, and solid provocation, using a controlled watery meal. They also used Doppler to assess the degree of duodenogastric reflux (DGR) by measuring the distance of the coloured signal in the stomach resulting from the duodenogastric reflux (Haruma, et al.). King et al., studied gastroduodenal motility by assessing the reflective echoes from the bran movement using orange juice as an oral contrast(P. M. King, Adam, Pryde, McDicken, & Heading). Ultrasonography also has been used to diagnose and assess celiac disease (Castiglione, et al.; Dell'Aquila, et al.). The advantages of percutaneous ultrasonography are simplicity, availability and safety. However, the disadvantages are operator dependency and the requirement of certain body habitus, as subcutaneous fat can dramatically reduce image quality.

CT Enterography and enteroclysis

Since the introduction of the first CT in 1973, diagnosis of different causes of intestinal obstruction and inflammatory bowel disease was possible by single slice CT. The introduction of the helical CT technology in 1989 and subsequently multi-slice CT further changed small bowel imaging.

The development of the multi-detector CT in 1998 allowed faster acquisition with thinner collimation and multiplanar reformatting (Silverman, Kalender, & Hazle).

CT enterography has been defined as imaging of small bowel by CT scan following administration of high volume of high density oral contrast. Approximately 1.6 L of 2% barium-based on 2-2.5% water-soluble iodine-based contrast is given over 1-2 hours (Raptopoulos, et al.). This technique is not necessarily needed in case of bowel obstruction as the bowel is already distended with gas and fluid (Furukawa, et al.). Images are then reconstructed at different slice thickness. Water can be given as an oral contrast, however in most cases intravenous contrast would be needed in this technique (Mazzeo, et al.).

CT enteroclysis is performed after insertion of a nasoduodenal tube beyond the ligament of Treitz, and distension of the small bowel by using approximately 2 Litres of 2% diluted barium. Water-soluble contrast can also be used (Mako, Mester, Tarjan, Karlinger, & Toth). CT enterography provides less distension of the bowel; however it's more comfortable for patients than intubation. Both techniques require distension of the bowel, which is non-physiological, and any attempt to study the bowel motility using these techniques will be affected by this factor.

Due to the high radiation of CT, these techniques are only limited to study the anatomical and pathological conditions rather than bowel function and motility.

Wireless Capsule endoscopy

Capsule endoscope is a new device used to directly visualise the small bowel mucosa. Iddan et al., developed the Video Capsule Endoscope (VCE) in 2001, and it was subsequently approval by the FDA as a first line investigation for detection of small bowel abnormalities. This technique revealed a high diagnostic yield when compared to other diagnostic modalities of the small intestine. The capsule endoscope contains a miniature colour video camera, illumination sources, lens, transmitter/controller, antenna, and a power source (Iddan, Meron, Glukhovsky, & Swain). It is small enough to swallow (11 x 26 mm), and it is propelled through the gastrointestinal (GI) tract by peristalsis. This tool expanded applications of the VCE to additional parts of the GI tract, adding physiological aspect to small bowel examinations (Iddan, et al.). Images produced by the capsule endoscopy reviewed by a physician which make the sensitivity of the test dependant on image quality, as well as the person reviewing these images. This examination produces approximately 57,000 images that make human interpretation a very tiring and time-consuming process. Thus, there is an active research to make the interpretation process computer assisted and near fully automated (Li & Meng) (Bashar, Kitasaka, Suenaga, Mekada, & Mori).

Capsule endoscopy has been used to diagnose Crohn's disease in endoscopic negative patients (Herrerias, Caunedo, Rodriguez-Tellez, Pellicer, & Herrerias), gastrointestinal bleeding (Appleyard, et al.), specially originating from small intestine. The technique has also been tried on children with successful results (Ma, et al., 2009) (Kavin, Berman, Martin, Feldman, & Forsey-Koukol, 2006).

Transit time has been a new area of studies recently using capsule endoscopy. Vu et al., (Vu, et al.) Studied the feasibility of an automated system to detect small bowel contractions by analysing images acquired from capsule endoscopy.

Capsule endoscopy remains a foreign body ingested by the patient and could cause complications. Parikh et al., (Parikh, Parikh, Albers, & Chandler) reported a case of intestinal perforation in a patient with crohn's disease following capsule endoscopy. Capsule retention is another potential complication which occurs in approximately 1-2% and requires surgical intervention (Karagiannis, Faiss, & Mavrogiannis, 2009).

Small intestinal endoscopy

Small intestinal endoscopy is performed in some specialist centres but it is a time-consuming and difficult procedure that is unlikely to become a practical alternative to challenge the barium examination in the same way that upper gastrointestinal endoscopy, and colonoscopy have (Nolan & Traill).

MRI of small bowel

MRI is a non-ionizing radiation technique that has also been used to image small bowel especially with the use of fast sequences that can overcome the movement artefacts (Schwizer, Fox, & Steingotter) (Froehlich, et al.; Torkzad, Vargas, Tanaka, & Blomqvist).

Imaging of the gastrointestinal tract has been limited because of image degradation due to gut wall movement. Investigators have resorted to paralysing the gut with pharmacological smooth muscle inhibitors in order to obtain sharp images. This is not only un-physiological, but also affects any attempt to study GI tract physiology with dynamic imaging.

It is now possible to capture decent sharp images in a non-paralysed state due to development in technology in acquiring MR images, using ultra-fast sequences.

MR Sequences

Unlike other imaging modalities MR image is the result of complex variables. Each of these variables can change the image characteristics. MR sequences in gastrointestinal tract depend on the presence or absence of intravenous and/or oral contrast. The following are some examples of these sequences:

Echo-planar sequences

Echo-planar MR sequences are one of the earliest methods in MR imaging of small bowel. Evans et al., (Evans, et al.) studied five volunteers using MBEST (Modulus Blipped Echo-planar Single pulse Technique) sequence to demonstrate peristalsis in the gastro duodenal

junction. He used respiratory gating and the temporal resolution was 20 frames per minute. After increasing the temporal resolution in another study images were degraded by off resonance artefacts caused by the presence of gas in the lumen (Mugler & Brookeman).

Gradient echo sequences

These sequences require enough bowel distension and contrast in order to delineate bowel details, even with the use of short echo time (TE) they are still slow to acquire, and liable to movement artefacts (Low & Francis). True-FISP (true fast imaging in steady state precession) is a relatively new sequence, which has a mixed T1W and T2W characteristics. This technique uses a balanced gradient waveform. Due to the speed, high spatial resolution and the relative insensitivity to motion artefacts, this technique has been used heavily in cardiac MR (Hawkes & Patz). It has also been recently used to assess small bowel motility with manual post processing techniques (Lang, et al.). The acquisition takes approximately 15 to 20 seconds.

Spin echo sequences

Conventional T2W sequences suffer from the problem of motion artefact. Other modifications however, have been used like the half-Fourier acquisition turbo spin-echo (HASTE), and fast spin echo (FSE). HASTE offers another short scanning alternative to True FISP but with a slightly lower resolution. The acquisition time is approximately 1 second per slice (Beall & Regan; Ha, et al.). In order to overcome the motion artefact problem with the conventional spin echo sequences a rapid sequence has been developed called the rapid acquisition with relaxation enhancement (RARE) (Hennig, Nauerth, &

Friedburg). This has allowed the development of a new technique which is called MR- Hydrography, by using a longer echo time (TE of 600-100 ms) (Laubenberger, et al.). Bilecen et al., (Bilecen, Scheffler, Seifritz, Bongartz, & Steinbrich) studied the stomach motility by using ultrafast RARE sequences to image to whole stomach. The temporal resolution of this technique is approximately one frame per second.

Parallel imaging

Parallel imaging is another new method that has been developed in recent years. The basic idea of parallel imaging is to use several independent coil elements in parallel to reduce the number of phase-encoding steps and hence the total scanning time. Despite the short acquisition time, the signal to noise ratio (SNR) is reduce dramatically in larger volumes (Lomas).

Oral contrast and bowel distension

For most MR small bowel imaging studies, adequate bowel distension and oral contrast is needed in order to delineate bowel wall pathology. In functional bowel imaging with MR, almost all studies used bowel distension, which again is not physiological. There are two ways of delivering contrast to the bowel, the first via the normal oral route and the second by using naso-jeujenal tube. Each method has it own benefits and disadvantages, which will be discussed, in the next section.

The idea of oral contrast is to change signal intensity (SI) of the region of interest from the surrounding structures so it can be easily

visualized. To achieve this, factors that affect SI need to be identified. These factors include (p) spin density, T1 and T2 relation times, TE (echo time) and TR (repetition time). This is expressed by:

$$SI = p \times e^{(-TR/T1)} \times [1 - e^{(-TE/T2)}]$$

Thus, contrast media that decrease T1 and increase p will increase SI and form a positive contrast medium (hyperintense) and vice versa (Giovagnoni, Fabbri, & Maccioni). Water and Gadolinium are examples of positive oral contrast media as they increase (SI) within the bowel (Lomas & Graves), however, barium and particulate iron oxides are negative ones (Kivelitz, et al.; Kraus, Rappaport, Ros, & Torres).

The ideal oral contrast should be safe, palatable, cheap, distribute homogenously, as well as doesn't change in character on dilution or concentration (Giovagnoni, et al.). Many positive and negative contrast media have been used in small bowel MR, but they all aimed at anatomical visualization of the bowel rather than physiological assessment of bowel motility. In order to reliably, and accurately assess the bowel motility, contrast media should be physiological and should not interfere with bowel reflexes (i.e. the effect of over distension). Water, baby milk (lyophilized milk) and Nutritional support formula have been tried as physiological cheap oral contrast agents (Balzarini, et al.; Lomas & Graves; Mirowitz & Susman). Water is easily and rapidly absorbed and hence MR scanning should start immediately after drinking (Lomas & Graves). Lyophilized milk doesn't distribute homogenously in the bowel and hence is not ideal (Balzarini, et al.).

MR Enterography and enteroclysis

The differentiation between MR enterography (or sometimes called MR follow-through) and MR enteroclysis, depends on the route of administration oral contrast. In the MR enterography contrast is administered orally, however in MR enteroclysis contrast is given through a nasoduodenal tube.

Nasoduodenal tube requires fluoroscopic guidance for its insertion, and hence exposes patients to ionising radiation (Martin, Danrad, Herrmann, Semelka, & Hussain). Negaard et al., compared the patient acceptance between the oral method and nasojejunal intubation in 38 patients. Immediate Abdominal pain was significantly higher in the enteroclysis group. More patients were willing to repeat the examination using the oral method rather than re-experiencing intubation. There was no significant difference between both groups in the procedure related diarrhoea and vomiting (Negaard, et al.).

As distension is an important factor when it comes to diagnosing pathological conditions of small bowel using MRI, the choice between conventional MR enterography and MR enteroclysis, depends on which part it is necessary to examine. It has been reported that conventional MR enterography using an oral contrast can cause under distension of the proximal small bowel (Negaard, et al.; Schreyer, et al.), however, Schryer et al., suggested that, the under distension of the proximal bowel loops might be due to the delay of acquiring imaging following administration of the oral contrast (Schreyer, et al.).

Inflammatory bowel disease remains the main indications for examining the small bowel using MRI. The sensitivity and specificity using both techniques are comparable, however MR enteroclysis using nasojeujenal tube is preferred when assessing proximal small bowel (Lawrance, Welman, Shipman, & Murray).

Dynamic MR imaging of the gastrointestinal tract

Quantification of small bowel peristalsis using MRI has not been established due to the technical difficulties and the complexity, and unpredictability of small bowel motility (Schwizer, et al.). Wright et al., (Wright, Evans, Gowland, & Mansfield) studied the antroduodenal motility of 10 healthy volunteers using modulus blipped Echo planar single pulse technique (MBEST), combined with a conventional manometry tube. Froehlich et al., (Froehlich, et al.) manually assessed the motility of small bowel using dynamic MR by selecting region of interests after adequately distending bowel loops, and measured the change in the lumen diameter. Other studies (Patak, et al.) (Kitazume, Satoh, Hosoi, Noguchi, & Shibuya) assessed the small bowel motility after abdominal surgery in patients with crohn's disease, using the same technique by manual measuring the luminal diameter, after reviewing the Dynamic MR images. To our knowledge none of the current techniques have been fully automated.

Other methods of assessing bowel motility

Intestinal manometry

Small bowel motility can also be assessed using gastroduodenojejunal manometry. This is facilitated by insertion of a multi lumen catheter, which can detect pressures from various aspects of the bowel. The catheter is inserted via fluoroscopic or endoscopic guidance. Qualitative and quantitative measures of the intestine motility can be achieved with this technique remains invasive, and involves the use of ionising radiation. It is unknown whether the presence of this tube within the lumen affects the behaviour of the bowel motility or not. Sedation might be required in some cases, which might affect the physiological pattern of the bowel motility, although this has not been assessed by formal studies (Camilleri, Hasler, Parkman, Quigley, & Soffer; Hansen).

Cutaneous electrogastrography

The idea of this technique is to measure the myoelectric activity at the abdominal surface with cutaneous electrodes. It has been used mainly for assessment of the gastric motility, however it has not been widely available in the clinical practice, as it lacks robust clinical studies, also due to the high cost of the initial equipment set up, and the vague clinical indication for its use (Camilleri, et al.).

Image segmentation

Image segmentation is defined as the process of dividing an image into multiple regions that share the same signal properties. The uses of medical imaging segmentation are variable, and include defining anatomical or pathological regions, measuring volumes, and helping in radiotherapy planning. Many algorithms have been developed for this reason. Signal inhomogeneity, noise artefact, partial voluming and closeness of the grey level of the tissue of interest to the surrounding tissues are the main problems facing medical imaging segmentation (Sharma & Aggarwal). Different classification systems have been adapted (Sharma & Aggarwal), although in general, they can be classified into automated and semi-automated methods. One example of segmentation methods is thresholding, which is an attempt to determine a suitable threshold for the signal intensity of the organ or region of interest, and group the pixels into two groups (above and below this threshold). Thresholding is effective in simple images, however it is sensitive to signal inhomogeneity, and noise (Pham, Xu, & Prince).

Summary of main findings of literature review:

- The small bowel is a notoriously complex organ to study and image.
- Two main distinctive motility patterns are recognised (The migrating motor complex and the post prandial motor activity).
- Studying the function of small bowel in-vivo was never an easy task as most of these techniques are invasive or expensive.
- The development of the ultrafast MR sequences enabled researchers to apply MRI in studying bowel physiology, however most of these attempts are done in manual and non-physiological methods.
- Thresholding is a simple way of image segmentation, but has a high sensitivity to noise and signal inhomogeneity.

Materials and Methods

Study design and objectives

Design:

This study is an experimental or pilot study performed on a small number of volunteers to test a number of hypotheses which will be mentioned below.

Objectives:

The study was divided into five parts:

1- Preparatory work:

A. Peristalsis assessment software development (PERASS):

The aim of this step was to develop software that could measure the overall peristalsis from a dynamic MR series (PERASS) by measuring the changes in pixel values and present them as a parametric map. Also it allows adding these changes into a single metric number.

B. MR scanning protocol adaptation:

This step aimed at adaptation of MR sequence from previously published work, (Froehlich, et al.; Kitazume, et al.; Patak, et al.) for the Siemens 1.5 Tesla machine to obtain suitable set of dynamic MR series for the automated analysis.

C. Optimizing the data set before testing the hypothesis

In this step the dynamic dataset was reviewed critically analysed with respect to different noise and artefacts. Some suggested solutions for the background noise were implemented

2- Proof of concept study:

The aim of this study was to determine if it might be possible to quantify small bowel activity using a non-invasive automated method by analysing data derived from MR cine images using the overall change in pixel values as a peristalsis or activity index.

3- MR Protocol optimisation study:

The aim of this study was to determine the optimum MR protocol required to reproduce a peristaltic index.

4- Reliability study and quantification of the bowel activity:

The aim for this study was to measure the test-retest reproducibility, or reliability , of the dynamic MR peristaltic index.

5- Validation of the peristaltic index: The aim of this study was to test the validity of the MR peristaltic index.

1. Preparatory work:

A. Peristalsis assessment software (PERASS):

(PERASS) is an in-house built software tool (Matlab version 7.8, The Mathworks, Natick, Massachusetts, USA) designed by Mr Bahman Kasmai, a principle clinical scientist in the department of Radiology at the Norfolk and Norwich University Hospital (Fig 3.1).

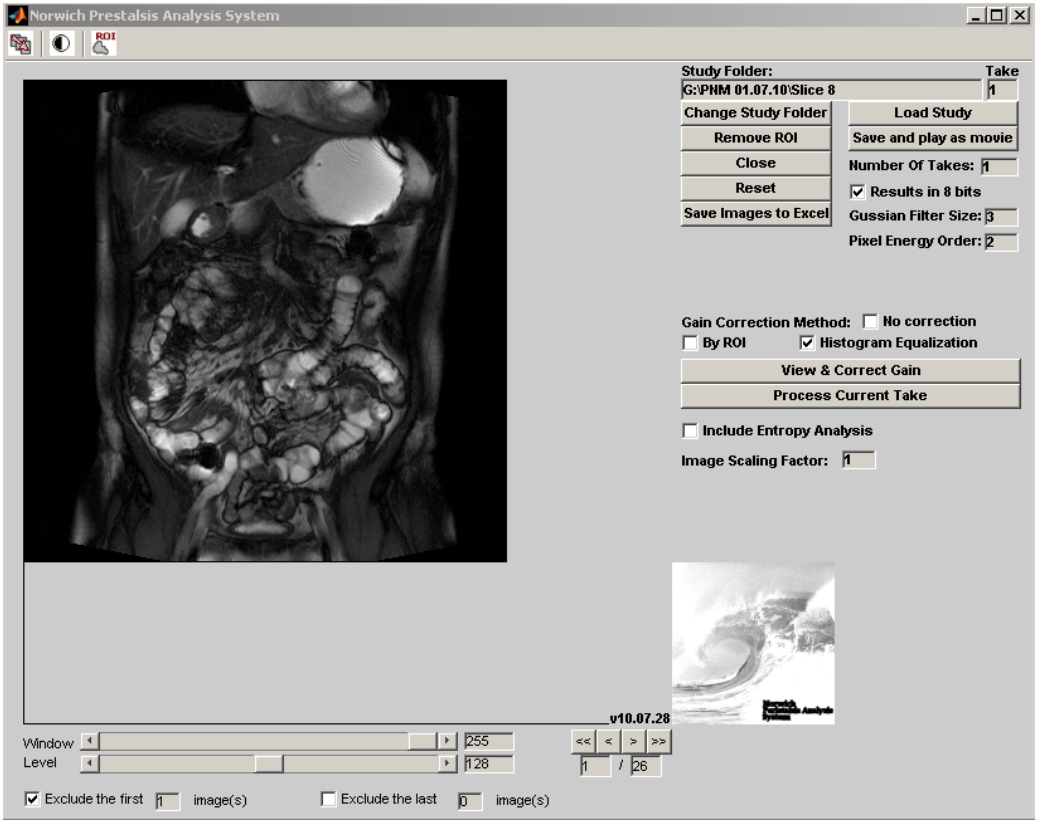

Figure (3.1) Front screen of PERASS software

PERASS calculates and creates parametric images representing the movement activity that occur in each MR cine, created from the sum of the absolute values of the pixel value difference between two (or more) consecutive images in the cine (Fig 3.2 – 3.3).

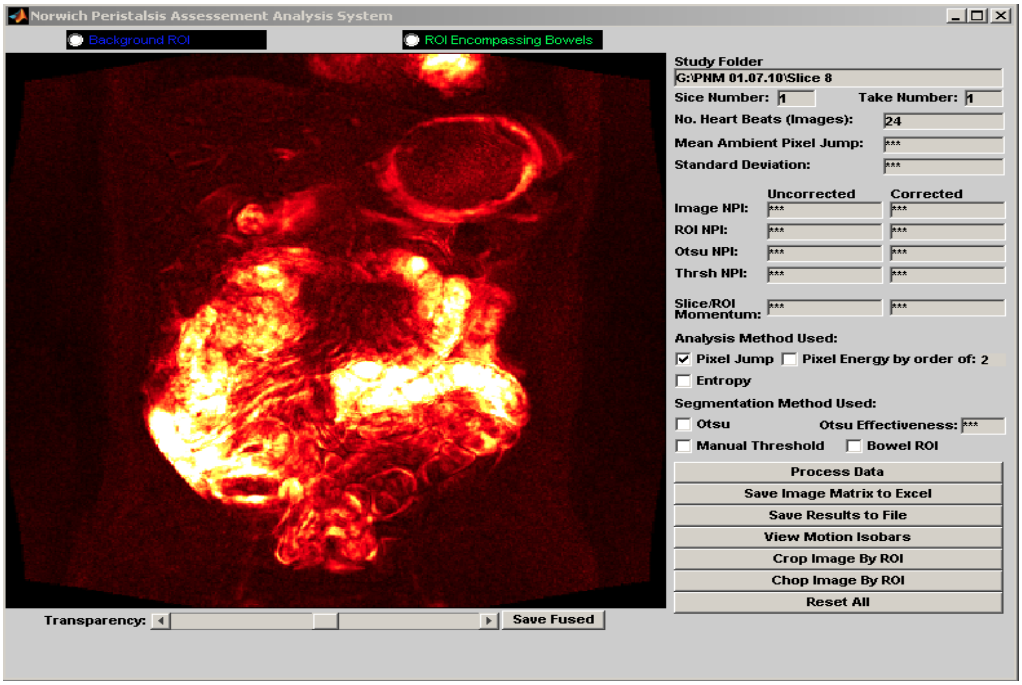

Figure (3.2) Parametric map generated from the cine

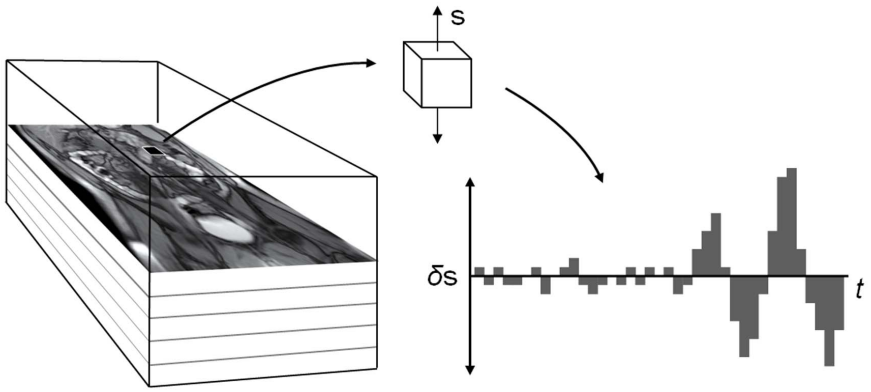

Figure (3.3) Diagram demonstrating how each voxel of the parametric map is depicted from mean signal change of the dynamic MR series (δs) in during (t) number of frames

The mathematical explanation of how software works is demonstrates as follows:

If the matrix size **(r x c)** per slice is made of **r** numbers of rows and **c** numbers of columns, the number of frames of the dynamic MR cine per slice is **n**. The pixel intensity value at row **a** and column **b** of frame no **f** is $\mathbf{I_{f,a,b}}$

The mean of the pixel value change between two consecutive frames **(f & f+1)** will be:

$$\boldsymbol{\Delta_{f,a,b}} = | \boldsymbol{I_{f,a,b}} - \boldsymbol{I_{f+1,a,b}} |$$

Each pixel in the initial parametric map will represent the sum of the means throughout the dynamic cine **P** normalized to the 256 grey shades and represented in a yellow to red scale (Fig 3.2). In the case of $\mathbf{P_{a,b}}$ it will be:

$$\mathbf{P_{a,b}} = \left(\sum_{f-1}^{n-1} \boldsymbol{\Delta_{f,a,b}} \right) / (\boldsymbol{n-1})$$

The software is then calculates the sum of the means of all pixel differences divided by the number of pixels in the entire field of view (FOV). This new number was called the Total Image Norwich peristaltic index (NPI).

$$\textbf{Total image NPI} = \sum_{n-1} |P_{(rxc)}| \div (r \times c)$$

Methods of reducing background noise

The software also allows correction for the background noise by various methods:

1. Background region of interest (ROI) thresholding

On of the ways of excluding background noise is to choose a region of interest (ROI) manually of an area in the background. The software will calculate the NPI after excluding the noise values and call it (Corrected NPI).

Corrected NPI = Sum of the pixel mean differences for all pixels >threshold (greater than mean of ambient pixels in ROI)/ Number of pixels that have pixel mean difference > threshold mean of ambient pixels in ROI ($\boldsymbol{m}$).

$$\textbf{Corrected NPI} = \sum_{n-1} | \boldsymbol{P}_{\textbf{(P> mean at ROI)}} | \; / \; m$$

2. Manual thresholding

The software is also capable of filtering the background noise by a manual segmentation technique (manual thresholding). This method segments the resulting parametric image depending on a user pre-selected level on the image histogram normalised from 1 to 8 (Fig 3.3). The resulting NPI is called the Threshold NPI.

Threshold NPI = Sum of the pixel mean differences for all pixels (per cine) that have values above the selected threshold $\mathbf{P_{th}}$/Number of pixels within the seleced threshold area $\mathbf{m_{th}}$

$$\textbf{Threshold NPI} = \sum_{n-1} |\mathbf{p_{th}}| \ / \mathbf{m_{th}}$$

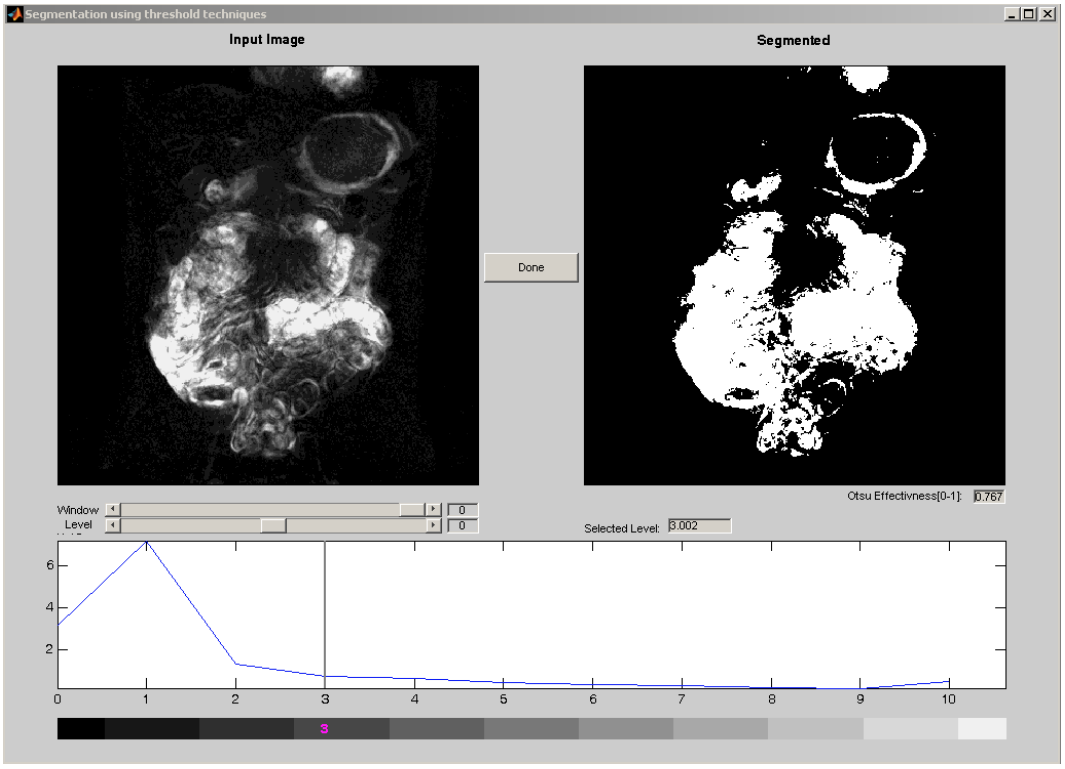

Figure (3.4) demonstrating the thresholding technique on the image histogram. The left sided image is the input unprocessed parametric image, and the right sided image is the resulting parametric map after manual thresholding.

The software also allows exclusion of certain slices, review the cine images and save cine as movie file.

Gain variability

This function was created to demonstrate, and to overcome the change in gain within the dynamic MR (as will be explained in the next study). Graphical visualisation facility of gain variability was added and correction technique was also implemented by normalizing each consecutive images histogram (Fig 3.5, 3.6). Each point in the graph represents the mean pixel value in the ROI (the groin in this instance) normalised against the mean pixel value of the same ROI of the whole cine.

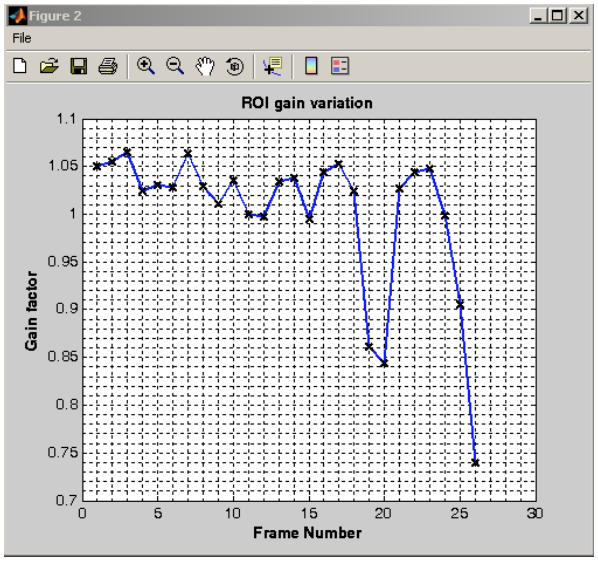

Figure (3.5) demonstrating the effect of gain variability

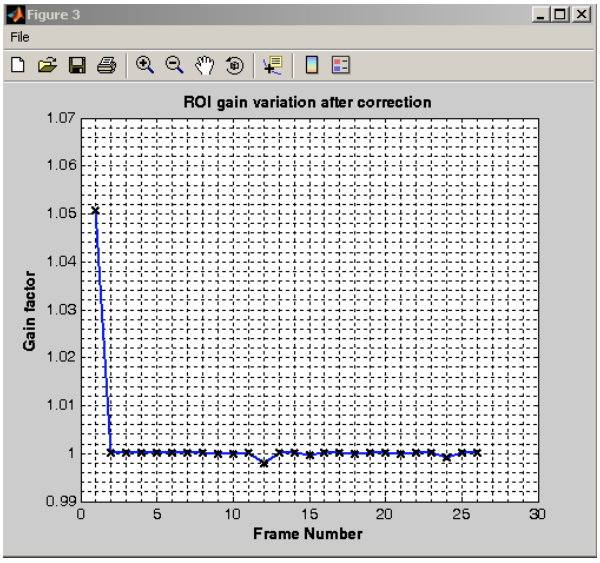

Figure (3.6) demonstrating the change in gain after correction

Peristalsis quantification

In order to quantify the global peristaltic activity, this metric measure was added to calculate the sum of the absolute difference in pixel value in either a manually selected area or an automatically generated area using the thresholding technique. A threshold value (**T**) for the mean pixel jump is selected by a user to filter noise.

The resulting number after applying the threshold technique (**T**) is called Total Voxel Activity (**TVA**)

$$\text{TVA} = \sum_{a=1}^{r} \sum_{b=1}^{c} (\mathbf{P_{a,b} > T})$$

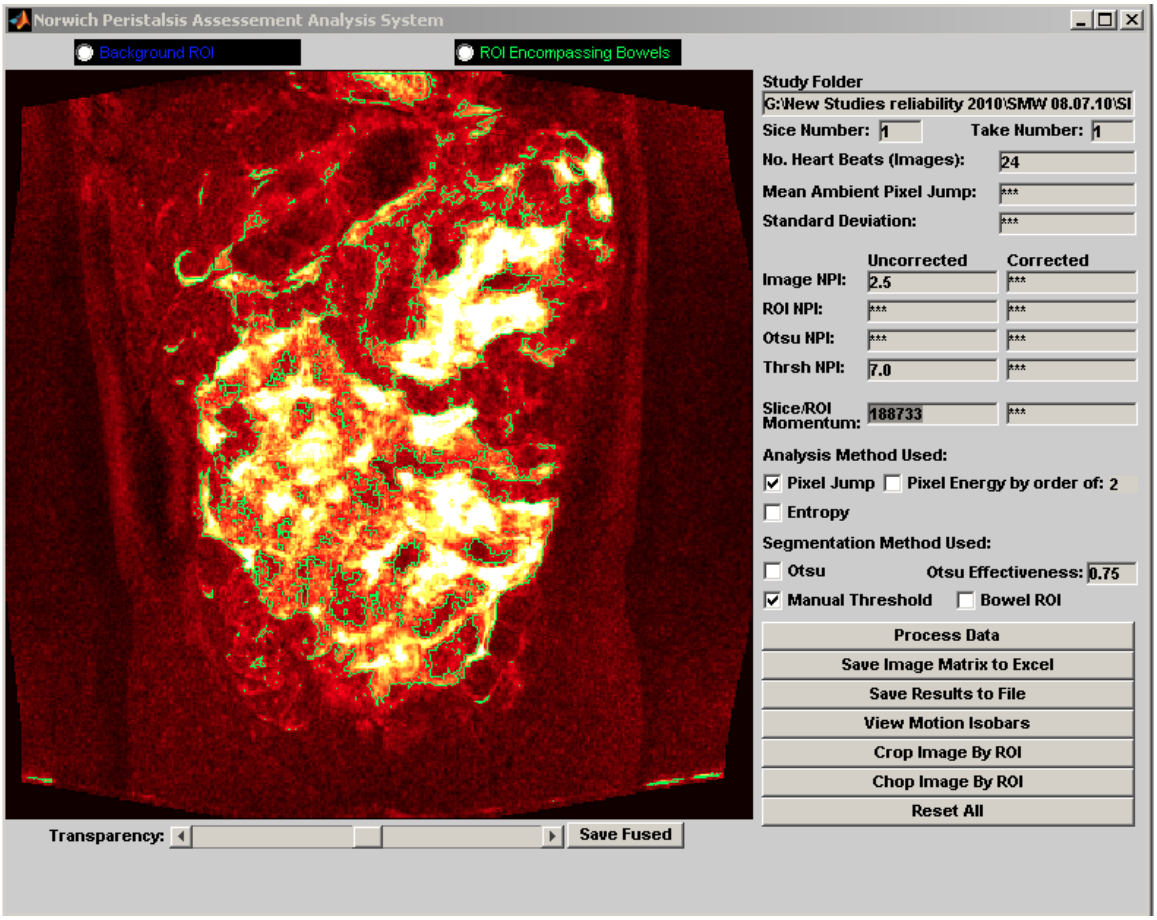

Figure (3.7) demonstrating the TVA calculated (marked as Slice momentum).

Pre-scan preparation

Inclusion and exclusion criteria

Due to the experimental nature of the study, all volunteers were medically qualified professionals; in fact all of them were either radiology trainees or consultants. The study design was fully explained to them and all the possible complications or adverse effects were discussed. Three Radiology Consultants and three Radiology Specialists registrars were recruited.

Oral contrast

Throughout the study tap water at room temperature was chosen as a physiological oral contrast. Each volunteer was asked to fast for 6 hours prior to the scan. The volunteer was then given 1 Litre of tap water to drink over 15 minutes.

B. MR sequence selection and optimizing cine prior to testing the hypothesis

All volunteer were scanned in the supine position with feet facing the magnet.

1) MR Sequence selection

A. HASTE (half-Fourier acquisition single-shot turbo Spin-Echo) Versus True- FISP (true fast imaging with steady-state precession) Cine MR imaging with Breath-hold and gentle breathing:

Research question:

Which of the two ultrafast protocols (True-FISP versus HASTE) produced the dynamic MR series most suitable for motion analysis.

MR

True-FISP sequence was used (TE 1.31 ms, TR 3.28ms, slice thickness 10 mm, echo spacing 2.9 ms, bandwidth 490 Hz/Px, FOV 590 x 302 mm, resolution 192x144, flip angle 59°, ET 256). One Coronal image was selected in the mid abdomen to produce the cine (approximately 4 cm posterior from anterior abdominal wall). 80 images were acquired in 42 seconds on a single breath-hold. The temporal resolution was approximately 1.9Frames/Sec.

HASTE sequence was tried for the same slice (TE 79 ms, TR 1000 ms, slice thickness 10 mm, echo spacing 2.9 ms, bandwidth 390 Hz/Px, FOV 590 x 302 mm, resolution 256x195, flip angle 150°, ET 256). 80 images were acquired in 79 seconds. The temporal resolution

was approximately 1.01 Frames/Sec. This scan was done on gentle breathing.

Analysis:

Images were tested by visual assessment of the dynamic data set on OsiriX® (Osirix®, version 3.7.1; OsiriX Foundation, Geneva, Switzerland) work station and the generated parametric maps using PERASS. Noise was also measured by calculating the signal to noise ration (SNR). This was calculated by drawing similar sized circular ROI in the right groin in both sequnces and using the SNR = $0.655 \cdot S/\sigma$ formula (O. Dietrich, Raya, Reeder, Reiser, & Schoenberg; Kaufman, Kramer, Crooks, & Ortendahl)

Where (S) is the mean pixel intensity value in a region of interest (ROI), and the noise to be the standard deviation (σ) in pixel intensity in background air. The 0.655 factor is due to the Rayleigh distribution of the background noise in a magnitude image.

B. True-FISP with and without Fat suppression

Research question:

Whether True-FISP with fat suppression added any value to the resulting cine.

Scanning protocol:

Two MR acquisitions were obtained from a single volunteer. The first acquisition was done with breath holding and the second was with free breathing. The volunteer was positioned supine and the whole abdomen was scanned coronally.

MR

True FISP

True FISP sequence was used (TE 1.31 ms, TR 3.28 ms, slice thickness 10 mm, echo spacing 2.9 ms, bandwidth 490 Hz/Px, FOV 590 x 302 mm, Resolution 192x144, flip angle 59°, ET 1). 80 images were acquired in 42 seconds during a single breath. The temporal resolution was approximately 1.9 frames/sec.

True FISP with Fat-suppression

True FISP sequence was used with Fat-suppression (TE 1.31 ms, TR 3.28 ms, slice thickness 10 mm, echo spacing 2.9 ms, bandwidth 490 Hz/Px, FOV 590 x 302 mm, Resolution 192x144, flip angle 59°, ET 1). 80 images were acquired in 37 seconds during a single breath. The temporal resolution was 2.16 frame/sec.

Analysis:

Visual assessment of noise was done on OsiriX® software and SNR ratio was calculated. Parametric maps were also assessed visually.

C. True FISP with and without ECG gating

The initial assessment of the cine demonstrated a considerable artefact from vascular structures due to flow and vessel wall movement. This trial was to compare the True-FISP sequence with and without cardiac gating on the resulting parametric map.

Research question:

The aim of this experiment was to test the ability of the cardiac gated sequence in reducing the vascular artefact.

Scanning protocol:

One volunteer was scanned coronally. Six coronal slices were acquired at equal intervals from the anterior abdominal wall. The aorta and para-aortic region were included in these slices.

MR

True FISP with ECG cardiac gating

True FISP sequence was used (TE 1.31 ms, TR 3.28 ms, slice thickness 10 mm, echo spacing 2.9 ms, bandwidth 490 Hz/Px, FOV 590 x 286 mm, Resolution 192x144, flip angle 59°, ET 1). 40 images were acquired during a single breath-hold over 35 seconds with ECG triggering (Prospective gating) (Average cycle 709 ± 101 ms – Acquisition window 887 ms – Trigger delay 736 ms) with a temporal resolution of approximately 1.14 frame/sec.

Analysis:

Comparison was made between images using True FISP with and without ECG gating acquisition**.** The para-aortic region was assessed visually by reviewing the cine and parametric maps were generated by PERASS.

2) Optimizing the Dynamic MR quality before testing the hypothesis

On manual reviewing the dynamic dataset on a workstation, there was a considerable variation in the contrast (gain) level of each image causing flashing artefact. This is a well recognised in prospective cardiac gating imaging affecting usually the first image of the dataset. The cause of this artefact is that there is enough time during the first acquisition for the longitudinal magnetization to recover after the initial RF pulse. Stabilization of the longitudinal magnetization only occurs in the subsequent images (Donald W McRobbie). Similar artefact however, occurred in some of the subsequent images affecting the quality of the parametric images. This resulted into over-representation of some of the non-moving parts of the abdomen on the parametric map. An example of this was the unexpected relatively high signal of the subcutaneous fat demonstrated in the parametric image (Fig 3.8). We have called this change in the dataset (change in gain).

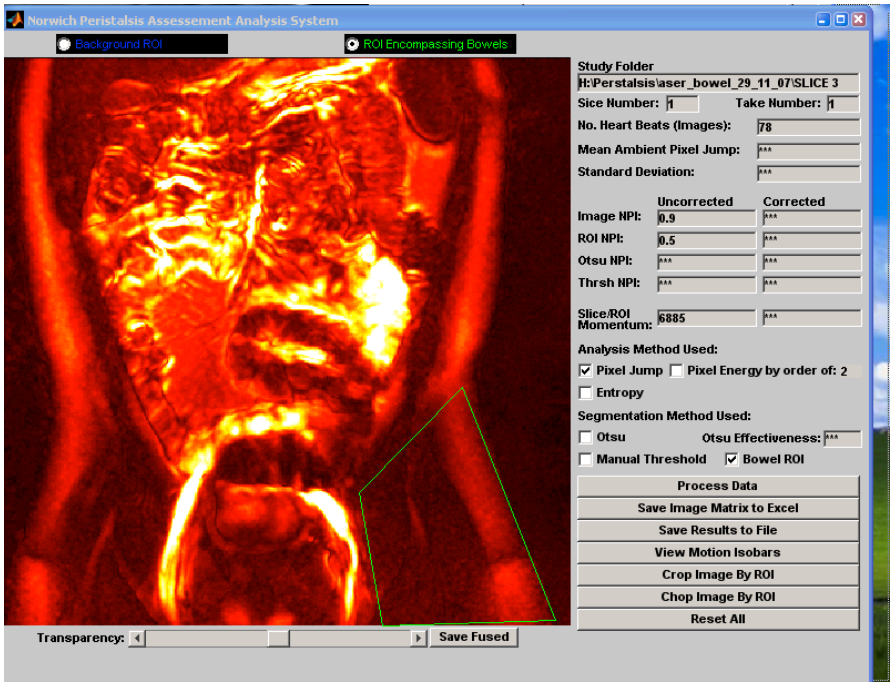

Figure (3.8) demonstrating the high signal of subcutaneous fat in the parametric map (as an example of a non-moving structure), due to the effect of (gain change) artefact.

The first image from each dataset was excluded from the subsequent analysis. As this artefact occurred not only in the first image but also in some of the middle images within the dataset, it was important to quantify this artefact by the following experiments:

Gain change artefact assessment

Scanning protocol:

A 33 years old healthy male volunteer participated in this study.

Nine coronal cines at equal distances covering the whole abdomen were acquired using True FISP sequence (TE 1.21ms, TR 277.9 ms, slice thickness 10 mm, echo spacing 2.9 ms, bandwidth 965 Hz/Px, FOV 40 x 40 cm, Matrix 192x118, flip angle 80°, ET 1). Cine sequences were acquired during a single breath-hold for 31 seconds with ECG triggering (Prospective gating) (Average cycle 709 ± 101 ms – Acquisition window 887 ms – Trigger delay 736 ms) with a temporal resolution of approximately 1 frame/sec.

Research question:

Two questions had to be answered. Theses question were (Is this artefact homogenous within the image? Is it homogenous between each image in the dynamic series?). In order to answer these questions the following were performed:

A. Changes in gain between dynamic series.

These were analysed by plotting mean contrast changes as a result of flashing in selected region of interest (ROI) over the left groin (where change in voxel values were not expected to vary considerably) as (gain factor) against time (slice number). This study was performed on a single cine and a single slice from the middle of the abdomen (approximately 40 mm from anterior abdominal wall). Pearson's correlation coefficient was performed between these means. Values were expressed in a histogram. .

B. Changes in gain within the dynamic series.

To assess the variability in gain change across the image, a region of interest was drawn over the left groin, right groin, and the liver. Changes in the mean gain (gain factor) were plotted against time (frame number). Correlation of gain changes in these three areas was compared using Pearson's correlation coefficient.

2. Proof of concept study

Study design & aim:

The aim of this phase was three folds:

a. To prove the ability of the NPI thresholding technique to separate small bowel from surrounding background noise.
b. To define the optimum threshold to be used for peristalsis analysis.

Volunteer

One healthy male volunteer, aged 32 years, who had no history of previous gastrointestinal illness or previous surgery, was enrolled in the study and informed written consent was obtained.

Preparation

The volunteer fasted for nine hours, after which, he drunk 1L of tap water over 15 minutes and waited 15 minutes before acquisition of MR data.

MR

Imaging was performed on a 1.5T MR (Siemens Avanto – Siemens Medical Solution, Erlangen, Germany) using two body phased array coils (anterior elements). The volunteer was positioned supine. Coronal images covering the whole abdomen were acquired from the anterior abdominal muscular wall to the posterior border of L3/L4 disc. True-FISP sequence was used (TE 1.21ms, TR 277.9 ms , slice thickness 10 mm, echo spacing 2.9 ms, bandwidth 965 Hz/Px, FOV 40 x 40 cm, matrix 192x118, flip angle 80°, ET 1). Dynamic MR cine sequences were acquired during a single breath-hold for 30 seconds with ECG triggering (prospective gating) (Average cycle 709 ± 101

ms – Acquisition window 887 ms – Trigger delay 736 ms) with a temporal resolution of approximately 1 frame/sec.

Parametric maps

Images were post processed using (PERASS). A single cine sequence through the mid abdomen (31 frames, over 36 seconds) was used to generate 7 parametric maps. A histogram of pixel "activity" for the parametric map representing the cine was produced and normalised from 0 to 10 (Fig 3.4). This histogram was used to set 7 threshold levels, at equal intervals, from which seven different parametric maps were generated. The first image of each dynamic dataset was excluded to eliminate the flashing artefact.

Analysis

Each parametric map was viewed by 2 independent experienced consultant radiologists, alongside with a movie of the original dynamic MR dataset. Each parametric map was compared to the MR cine (visualised as a repeatable movie) using a 9 x 9 grid to score each part of the image (Fig 3.9).

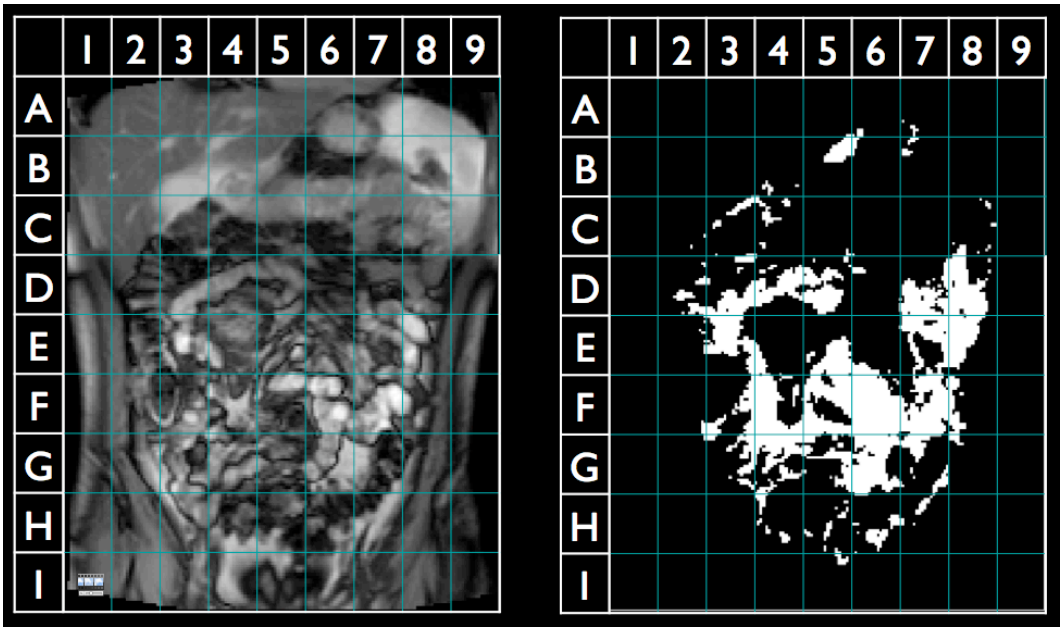

Figure (3.9). The left image demonstrates the MR cine. The right image demonstrates the parametric map at threshold level 3. Both images overlaid by a 9x9 grid for the rating purpose.

The instructions given to the assessor were:

On the MR cine image:

To rate each cell with either 0 or 1 where:

0 = No small bowel in the cell.

1= Small bowel activity present in the cell.

On the parametric image:

To rate each cell from 0 to 3 where:

0 = No signal and no small bowel activity present

1 = The movement within the cell is under-represented (less than expected visually)

2 = Good correlation i.e. the parametric map matches the degree of the small bowel activity.

3 = Over represented small bowel activity.

Inter-rate reliability for the anatomical correlation was done by Kappa correlation coefficient. Correlation between parametric maps and movie data was measured using Spearman's rank Correlation coefficient and inter-observer reliability for assessment of the parametric map was measured using a Kappa coefficient.

3. MR protocol optimization study

Aim of the study:

The aim of this study was to optimize the MR protocol for evaluating the global small bowel peristalsis. The following parameters were assessed:

a. The minimum duration required for each cine (acquisition time) to produce a reproducible threshold NPI.
b. The minimum number of slices (covering the abdomen) needed per scan and whether NPI would change per slice.
c. The minimum number of repetitions of each slice to obtain reproducible threshold NPI.
d. Whether the effect of fasting would change the results of these parameters.

Volunteers

Three healthy male volunteers aged 34, 43 and 48 years were recruited in this study after obtaining their written consent.

Preparation

Volunteers were asked to fast for six hours prior to the scan. Two volunteers were scanned while fasting and then asked to drink 1 Litre of tap water over 15 minutes before rescanning. The third volunteer was scanned only post drink.

MR

Images obtained on a 1.5T scanner (Siemens Avanto – Siemens Medical Solution, Erlangen, Germany). Two anterior elements body arrays coils were used. Coronal images were acquired to cover the entire abdomen with a slice thickness of 10mm starting from the anterior abdominal wall to the level of L3/L4 intervertebral disc; this resulted into 10 dynamic coronal acquisitions.

True-FISP sequence was used (TE 1.21 ms, TR 277.9 ms, slice thickness 10 mm, echo spacing 2.9 ms, bandwidth 965 Hz/Px, FOV 590 x 286 mm, resolution 192x118, flip angle 80°, ET 1). In two volunteers 31 images were acquired during a single breath-hold over 35 seconds with ECG triggering (Prospective gating) (Average cycle 709 ± 101 ms – Acquisition window 887 ms – Trigger delay 736 ms). Each slice was repeated 5 times with a 2 minutes interval. The acquisition time for the third volunteer was slightly shorter (21 frames).

The temporal resolution was depended on the heart rate; in volunteer A the heart rate was 80 beat/minute hence the temporal resolution was approximately 1.3 frame/sec; in volunteer B the heart rate was 64 beat/minute hence the temporal resolution was approximately 1.07 frame/sec; in volunteer C heart rate was 70 beat/minute hence the temporal resolution was approximately 1.17 frame/sec.

Analysis:

The resulting twenty five studies were post processed using the following technique:

Each dataset was loaded on the (PERASS) software. The first image from each set was excluded resulting in 30 images (frames) per cine for two volunteers, and 20 frames for the third volunteer. Parametric map was generated from each cine. Background noise was excluded by thresholding technique using level 3 on the histogram (Level 3 was taken from the result of the previous study). Analysis of variance tests (ANOVA) were performed to determine the shortest acquisition time, minimum number of slices and the minimum number of study repetition required for a reproducible threshold NPI.

So the study was divided into:

I. Repetition test

Threshold NPI per slice was calculated. ANOVA test was done between the five thresholded NPIs of the five repetitions.

II. Acquisition time test:

This is to test the minimum possible acquisition time required to produce a reproducible NPI. The duration of each cine was reduced by factor of 5 (from 30 frames to 5 frames) producing 6 different studies for each repetition for two volunteers, and four different studies for the third volunteer. Threshold NPI was calculated for each slice for three repetitions. ANOVA test was done between the resulting data.

III. Number of slices per study:

This is to test the minimum number of abdominal coronal slices required for a reproducible threshold NPI. Reducing the number of slices by choosing alternate slices of the dataset (resulting into two sets of five coronal slices per volunteer); then reducing the number of slices by choosing one slice and skip three (resulting into three sets of three coronal slices). Then more reduction to the number of slices was made by choosing one slices and skip five slices (resulting into five sets of two coronal slices). ANOVA test was performed between the 5,3 and 2 slices threshold NPI.

4. Reliability study and quantification of the bowel activity

Aim of the study:

The aim of this study was to quantify the global bowel activity and to assess the test-retest reliability of this technique.

Study design

Five healthy volunteer (age range 34 – 48, median 41.4 years) were recruited in this study after obtaining their written consent. The volunteers were asked to fast for six hours and drink 1 litre of tap water at room temperature. The abdomen was covered from front to back using cinematic coronal images. In volunteer A, 11 coronal images required to cover the whole abdomen, whoever 13, 13, 16 and 15 images were required in volunteers B, C, D, and E consecutively. This resulted in a 68 ECG triggered dynamic coronal images with no gaps. The study was repeated with the same parameters with at least two weeks gap.

MR

Volunteers were scanned on a 1.5T MR (Siemens Avanto – Siemens Medical Solution, Erlangen, Germany) using two body phased array coils (anterior elements).

True-FISP sequence with a single breath hold was used (TE 1.6 ms, TR 803.71 ms, slice thickness 10 mm, echo spacing 3.7 ms, bandwidth 930 Hz/Px, FOV 40 x 40 cm, resolution 384x384, flip angle 73°, ET 1). ECG triggering (Prospective cardiac gating) (Average cycle 985 ± 7 ms – Acquisition window 845 ms – Trigger delay 41 ms). Each cine was 26 frames long.

The temporal resolution was depended on the heart rate; in volunteer A the average heart rate was 80 beat/minute hence the temporal resolution was approximately 1.3 frame/sec; in volunteer B the heart rate was 64 beat/minute hence the temporal resolution was approximately 1.07 frame/sec; in volunteer C heart rate was beat/minute hence the temporal resolution was approximately 1.17 frame/sec. In volunteers D and E the average heart rate was 60 hence the temporal resolution was approximately 1 frame per second.

Analysis:

Images were fed into (PERASS). Using the thresholding technique on the histogram a specific value was used to eliminate the noise. Due to the relative high resolution of this study, there was a relative high noise level at the posterior slices requiring different threshold level to minimize its effect. The majority of the slices were set to threshold 3 however in the posterior slices in three volunteer levels 4 and 4.5 were

required to eliminate the noise (table 4.23). The same thresholding technique was used in all the slices in the second study. The total voxel activity (TVA) and the standard deviation per slice were then calculated in the resulting image. Correlation was made between each slice TVA in the first study and the second study. Descriptive statistics were performed on each study using (MedCalc® version 9.3.0.0). Reliability was measured using intraclass correlation coefficient comparing slice by slice in the two studies as well as total abdominal voxel activity of each study. The Bland Altman test could not be used here as the data was not normally distributed.

5. Validation of the peristaltic index (intervention with anticholinergic para-sympatholytic agent)

Aim of the study:

The aim of this study was to assess the validity and the reproducibility of the total voxel activity (TVA) as a mean of global assessment of small bowel activity.

Study design

Five healthy volunteer (age range 32 – 48, median 38.2 years) were recruited in this study after obtaining their written consent. The volunteers were asked to fast for six hours and drink 1 litre of tap water at room temperature over 15 minutes. Volunteers were scanned immediately. The abdomen was covered from front to back using cinematic coronal images. While on the scanner, each volunteer was then injected with 20 mg of Hyoscine Butylbromide (Buscopan®) intramuscularly. There was a pause for 10 minutes to allow the Hyoscine Butylbromide to suppress the bowel motility. Volunteers were then scanned using the same parameters as the pre-intervention scan. There was another pause for 20 minutes (while volunteers on the MR table) to allow the effect of Hyoscine Butylbromide to wear off, then volunteers were rescanned again with the same

MR

True-FISP sequence was used (TE 1.22ms, TR 803.71 ms, slice thickness 10 mm, echo spacing 2.9 ms, bandwidth 930 Hz/Px, FOV 40 x 40 cm, matrix 192x146, flip angle 73°, ET 1). Cine sequences were acquired during a single breath-hold for 30 seconds with ECG triggering (Prospective gating) (Average cycle 977 ± 6 ms – Acquisition window 916 ms – Trigger delay 112 ms) with a temporal resolution of 1.15 frame/sec.

Analysis:

Images were fed into PERASS. Using the thresholding technique on the histogram a specific value was used to eliminate the noise (in this case it was level 3). The total voxel activity (TVA) per slice was then calculated in the resulting image. Correlation was made between each slice TVA in the pre-intervention, intervention and the post intervention studies. Descriptive statistics were performed on each study using (MedCalc® version 9.3.0.0). Graphical comparison was used for each volunteer to demonstrate the effect of Hyoscine Butylbromide on the slice-by-slice TVA and the total TVA.

Data collection and entry

Data was collected in Excel® spread sheets for each study and saved in Norwich Radiology Academy Research server.

Statistical analysis

Statistical analysis was done using (MedCalc® version 9.3.0.0) and (SPSS® version 16.0).

Volunteer information and consent form

All volunteers were given a printed version of (Volunteers information sheet) (Appendix 1) and were asked to sign a consent form prior to the study (Appendix 2).

Summary of methods

- Study was designed and divided into Five steps:
    a. Preparatory work
        i. Software development (PERASS)
        ii. MR scanning protocol adaptation
    b. Proof of concept study
    c. MR protocol optimization study
    d. Reliability and quantification of the bowel activity.
    e. Validation of the peristaltic index
- Ethical approval sought and granted.
- Volunteers selected and consented.
- Data loaded to PERASS software.
- Statistical analysis was done using SPSS v16.0.

Results

In this chapter the following results will be discussed:

I-Preparatory work:

1. MR sequence selection

A. HASTE versus True-FISP – Breath hold and gentle breathing

B. True FISP with and without Fat suppression

C. True FISP with and without ECG triggering.

2. Optimizing the MR Cine quality before testing the hypothesis

Gain change (Flashing) artefact assessment

A. Changes in gain between dynamic series.

B. Changes in gain within the dynamic series.

II- Proof of concept study

III-MR Protocol optimization study

1.Repetition test

2.Acquisition time test:

3.Number of slices per study

IV-Reliability study and quantification of the bowel activity

V-Validation of the peristaltic index (intervention with anticholinergic para-sympatholytic agent)

1. Preparatory work:

1. MR sequence selection

A. HASTE versus True-FISP – Breath hold and gentle breathing

Visual assessment of the True FISP versus HASTE parametric maps demonstrated an increase in the background signal intensity in HASTE indicating high level of noise.

SNR in True FISP sequences was 62.842 and it was 31.776 in the HASTE sequence. Moreover, free breathing had a negative effect on the resulting parametric image, which demonstrated an increase in the overall amplitude of bowel signal as well as the abdominal wall (Fig 4.1). The temporal resolution of the True FISP images was faster (1.9 Frames/Sec) than the HASTE (1.01 Frames/Sec).

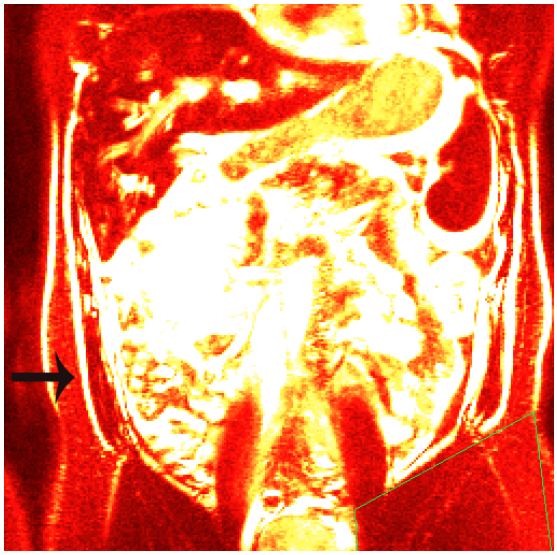

Figure (4.1) demonstrating the effect of breathing on the resulting parametric image (arrow).

B. True FISP with and without Fat suppression

Visual Comparison of both parametric maps of True-FISP with and without Fat-Suppression demonstrated increase in the background signal amplitude in the Fat supressed images (Fig 4.2), indicating increased noise level. The SNR in the True FISP image was 62.750 and it was 50.452 in the True FISP with Fat suppression.

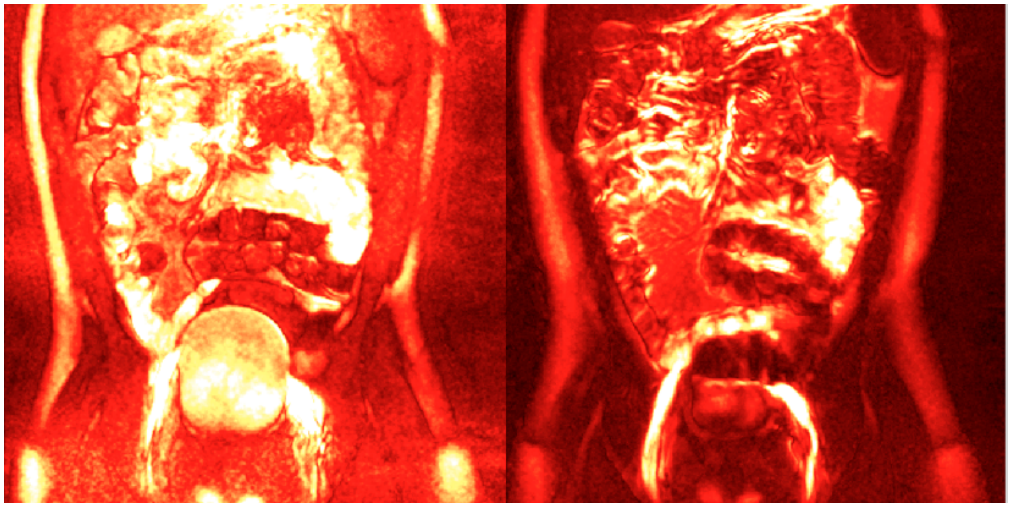

Figure (4.2) The left side image(true-FISP with fat-suppression) demonstrated increased background noise when compared to the right image (True-FISP without fat-suppression).

C. True FISP with and without ECG triggering.

Visual assessment of the parametric map generated from the ECG triggered dynamic MR dataset demonstrated marked reduction of the vascular artefact in the para-aortic region (Absence of signal within the aorta and iliac vessels) (Fig 4.4) when compared with the non-gated imaged (Fig 4.3) The temporal resolution in the gated images is dependent on the heart rate which was 1.14 frame/Sec, compared to a 1.9 frame/sec in the non-gated images.

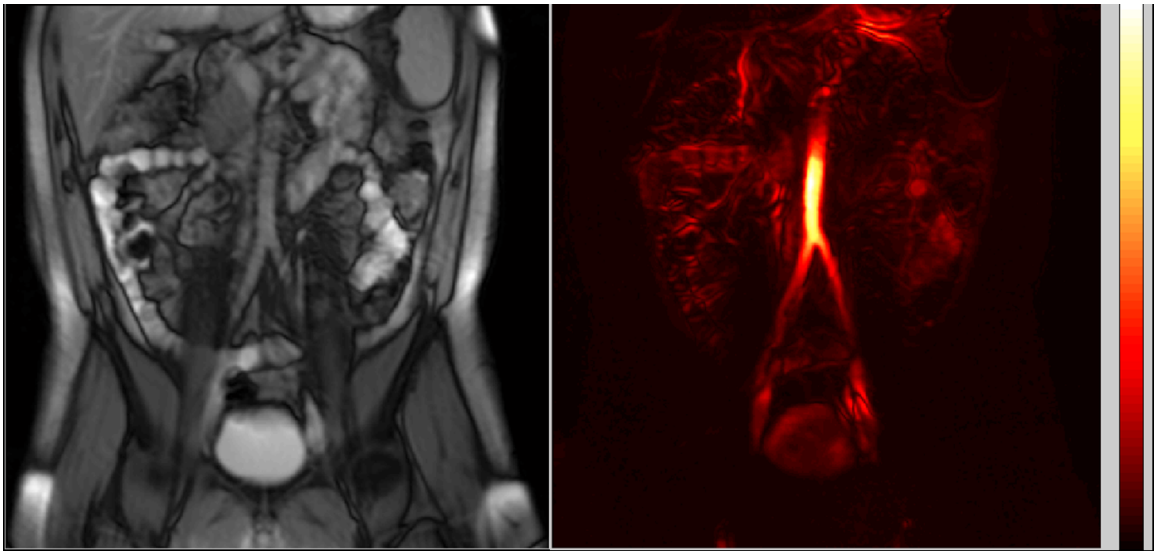

Figure (4.3) demonstrating the effect of the vascular artefact on the parametric image before applying the ECG triggering.

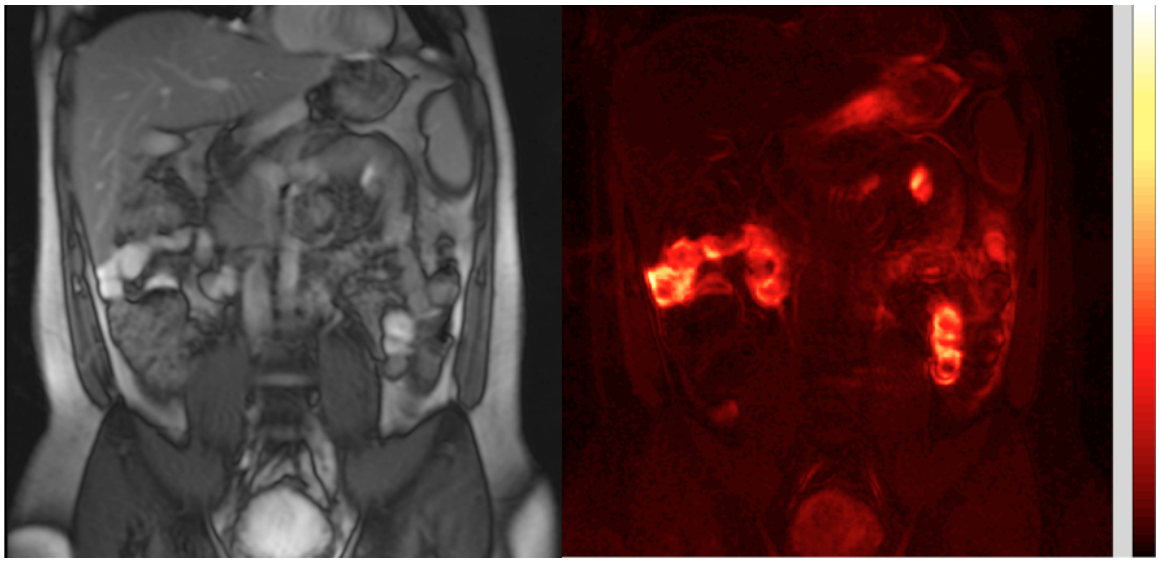

Figure (4.4) demonstrating the marked improvement on the vascular artefact on the parametric image after applying the ECG triggering.

2. Optimizing the MR Cine quality before testing the hypothesis

Gain change (Flashing) artefact assessment

A. Changes in gain between dynamic series.

Pearson's correlations of the 9 dynamic MR series were performed (Tab 4.1). The distribution of Pearson's correlation coefficients, of the mean receiver gain change in the left groin across the series, demonstrated a normal parametric distribution (Fig 4.5). This suggests that there is no systematic correlation in the gain changes, which occur within a series, between dynamic series.

Pearson's Correlations

		Slice 1	Slice 2	Slice 3	Slice 4	Slice 5	Slice 6	Slice 7	Slice 8	Slice 9
Slice 1	Pearson Correlation	1.000								
	Sig. (2-tailed)									
Slice 2	Pearson Correlation	.154	1.000							
	Sig. (2-tailed)	.410								
Slice 3	Pearson Correlation	.067	.001	1.000						
	Sig. (2-tailed)	.720	.995							
Slice 4	Pearson Correlation	.325	-.094	-.065	1.000					
	Sig. (2-tailed)	.075	.616	.729						
Slice 5	Pearson Correlation	-.252	.008	-.082	.064	1.000				
	Sig. (2-tailed)	.172	.965	.660	.732					
Slice 6	Pearson Correlation	-.253	-.730**	-.002	.193	.192	1.000			
	Sig. (2-tailed)	.169	.000	.992	.297	.302				
Slice 7	Pearson Correlation	-.149	-.822**	-.025	.205	.226	.856**	1.000		
	Sig. (2-tailed)	.423	.000	.895	.268	.222	.000			
Slice 8	Pearson Correlation	.063	-.878**	-.052	.238	.022	.780**	.923**	1.000	
	Sig. (2-tailed)	.735	.000	.783	.197	.906	.000	.000		
Slice 9	Pearson Correlation	.254	-.466**	-.180	.249	.148	.430*	.580**	.689**	1.000
	Sig. (2-tailed)	.167	.008	.331	.177	.426	.016	.001	.000	

**. Correlation is significant at the 0.01 level

*. Correlation is significant at the 0.05 level

Table (4.1) Demonstrates the Pearson's correlation of the mean receiver gain change between the dynamic series.

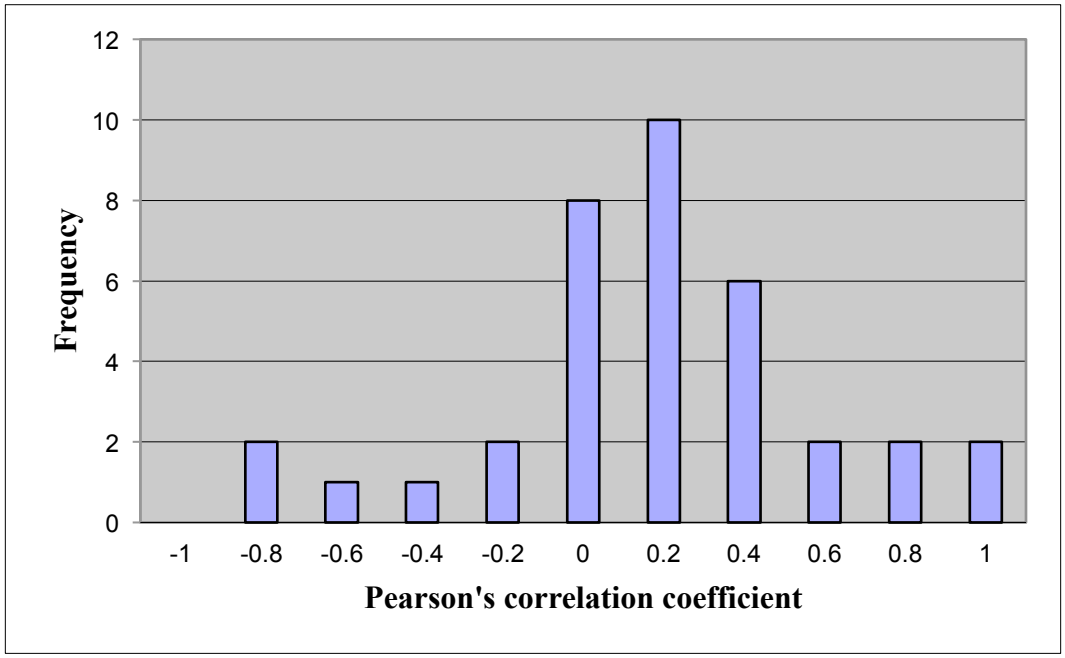

Figure (4.5) Demonstrates the normal distribution of Pearson's correlation coefficients, of the mean receiver gain change in the left groin across the series.

B. Changes in gain within the dynamic series.

Changes in gain from image to image within a dynamic series were constant for different regions of the mage. Correlation of gain between different areas of the same image (left groin – Right groin – Liver) was excellent (Pearson correlation coefficient: (0.793 – 0.944), 95% confidence intervals 0.955 – 0.974, P <0.0001) (table 4.2). The first image in every cine demonstrated high gain factor and hence it was excluded from analysis (Fig 4.6).

	Left Groin	Right Groin	Liver
Left Groin Pearson correlation	1	.936	.944
Sig. (2-tailed)		.000	.000
N	31	31	31
Right Groin Pearson correlation	.936	1	.793
Sig. (2-tailed)	.000	.000	.000
N	31	31	31
Liver Pearson correlation	.944	.793	1
Sig. (2-tailed)	.000	.000	
N	31	31	31

**. Correlation is significant at the 0.01 level (2-tailed).

Table (4.2) demonstrates the strong correlation between the gain factor measured at right groin, left groin and the liver.

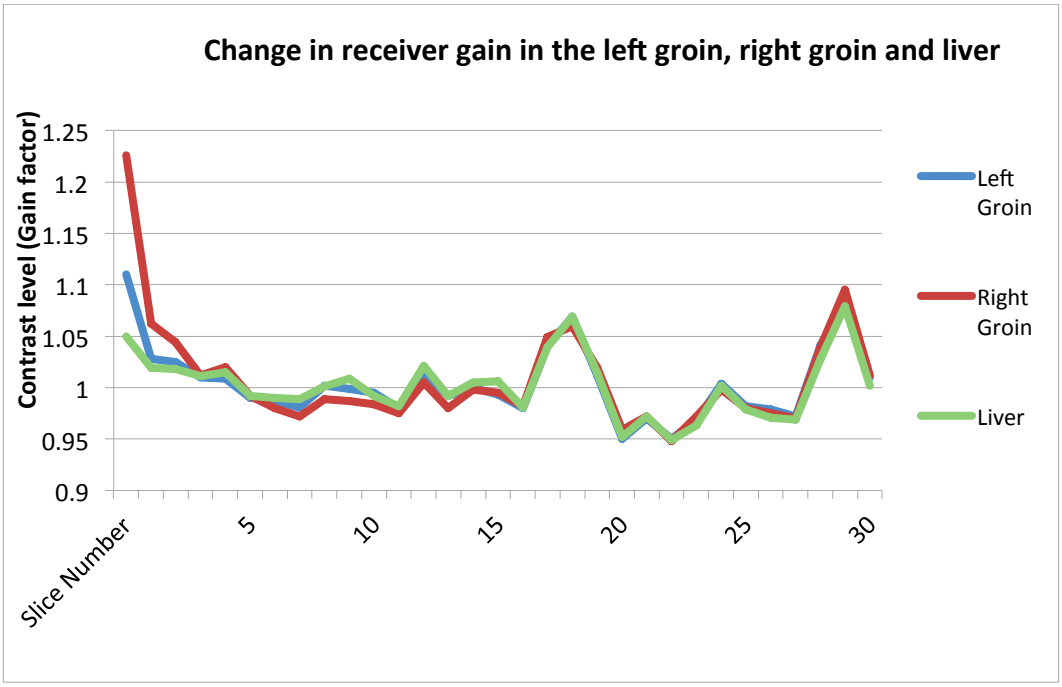

Figure (4.6) demonstrates the strong correlation in gain variation at three different areas within the same dynamic series. Note the significantly high gain factor in the first image.

2. Proof of concept study

Anatomical correlation

The inter-rater reliability for defining active small bowel on the dynamic MR was (almost perfect agreement) (κ= 0.825, 95% CI 0.61-1.0).

Correlation of the parametric maps with anatomical movie

The Spearman's ranked correlation coefficient comparing the dynamic MR with the parametric map at different thresholds of the first rater demonstrated (moderate agreement) in thresholds 1 to 4. This has increased to (substantial agreement) in threshold 5, and was (almost perfect agreement) in thresholds 6 to 7 (Fig 4.7).

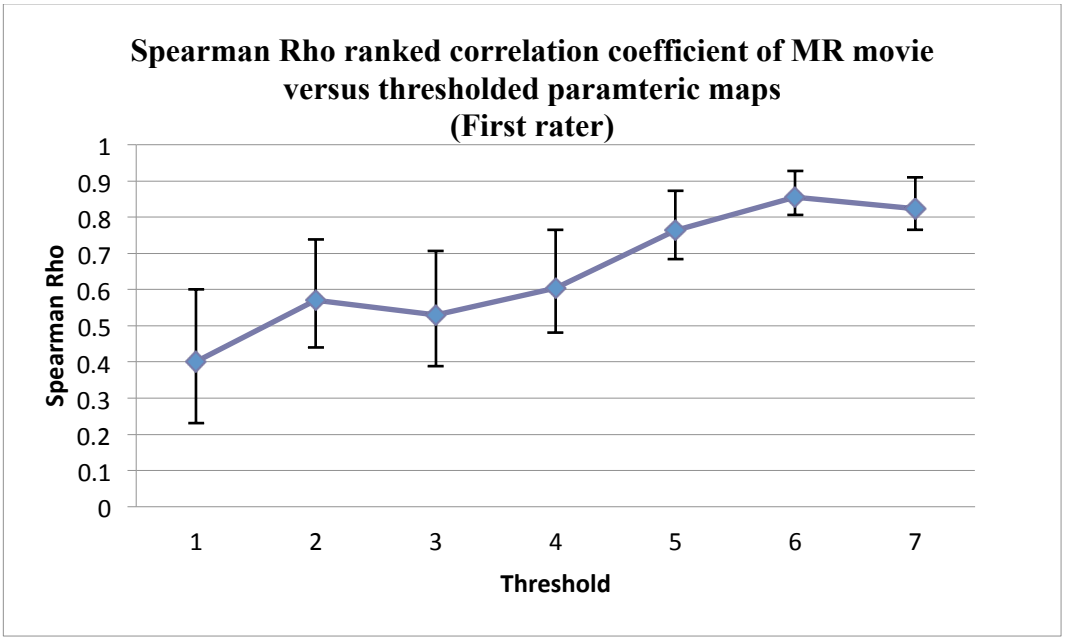

Figure (4.7) demonstrates the Spearman's correlation between the MR movie and the parametric maps at different thresholds (First rater).

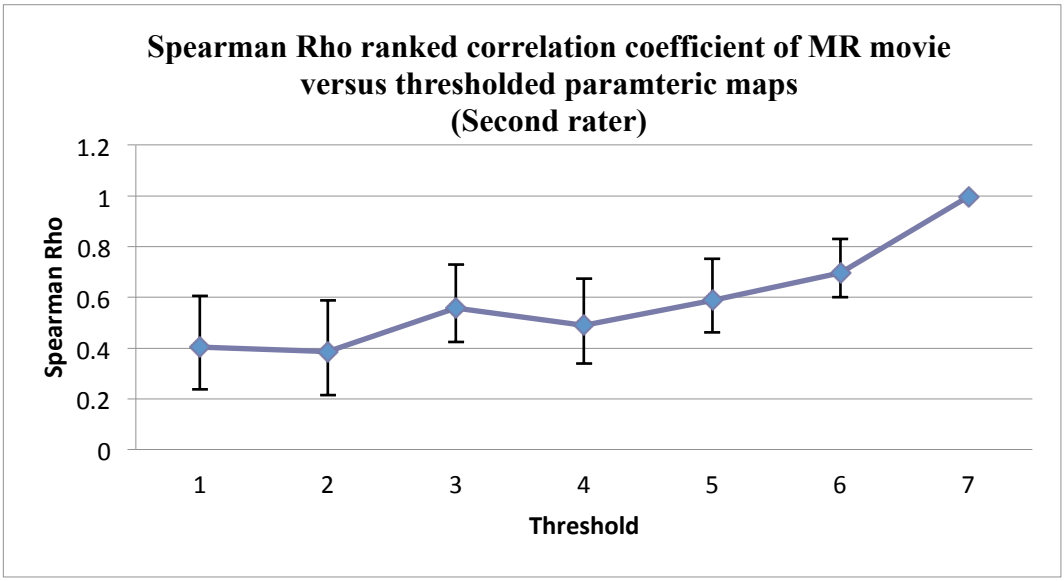

Figure (4.8) demonstrates the Spearman's correlation between the MR movie and the parametric maps at different thresholds (Second rater).

The second rater Sperman's correlation coefficient demonstrated (moderate agreement) in thresholds 1 to 5, but increased to (substantial agreement) in threshold 6, and was (almost perfect agreement) in threshold 7 (Fig 4.8).

Analysis of a single rater's observations correlating the parametric map, segmented at increasing thresholds with the dynamic MR data, revealed that with increasing thresholds there was a gradual decrease in the number of cells where small bowel activity was over represented. There was also a gradual rise in the number of cells where small bowel was under represented. At threshold 5 the two curves of (over represented and under represented small bowel) cross each other (Fig 4.9).

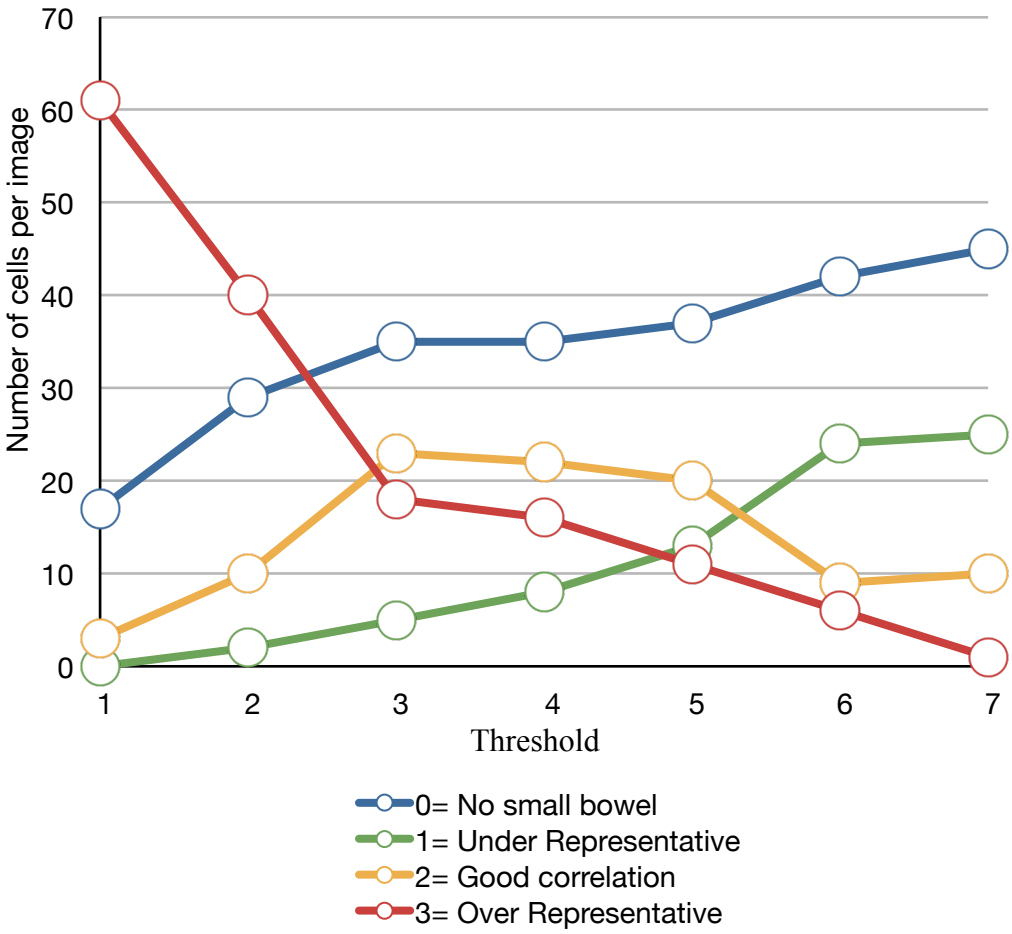

Figure (4.9) demonstrates the single rater's observations correlating the parametric map segmented at increasing thresholds with the dynamic MR. Note at threshold 3 is the peak for good correlation curve. The threshold for the maximal number of good correlation cells was 3.

Inter-rater reliability for assessment of the parametric maps

The inter-rater reliability for assessment of the parametric maps was (substantial) at the extremes of thresholds and dropped to (moderate) at thresholds 5 and 6, then raised to (substantial) for the threshold intervals 6 and 7. (κ range 0.524 – 0.808) (Fig 4.10).

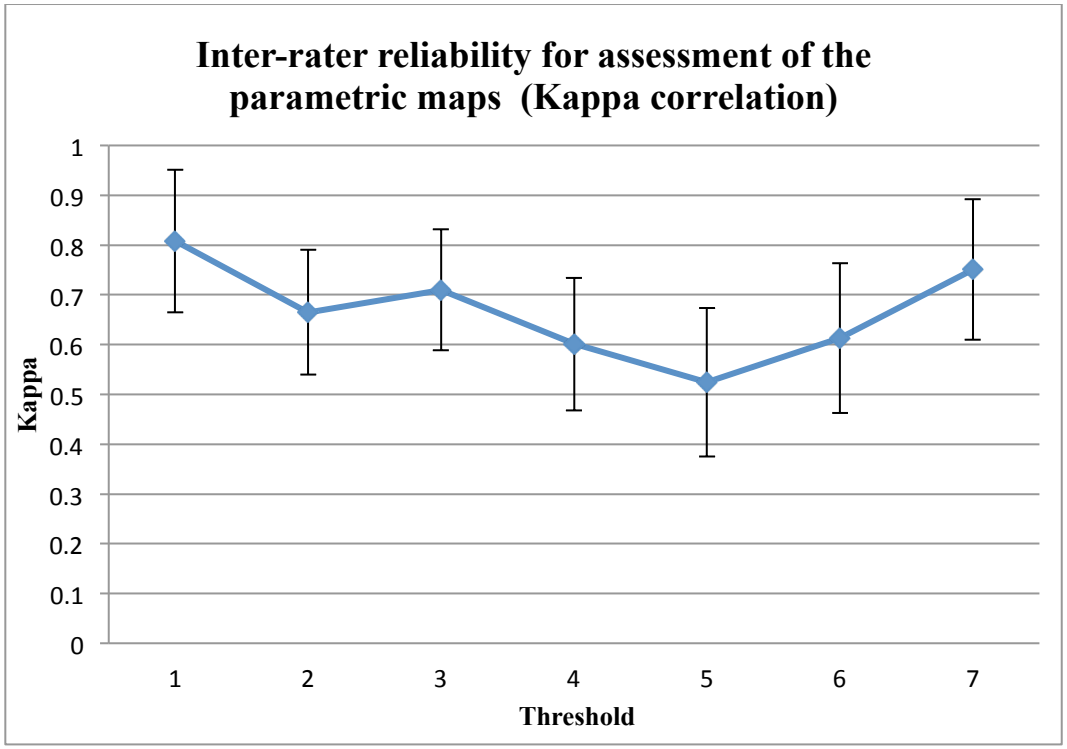

Figure (4.10) demonstrates the strong correlation of inter-rater reliability coefficient for assessing the parametric map especially at the extremes thresholds.

3. MR Protocol optimisation study

1. Repetition test

Before testing the data, normalization was checked by the Q-Q plot of each repetition. The following graphs (Fig 4.11 – 4.15) represents the Q-Q plots for volunteer A (post drink).

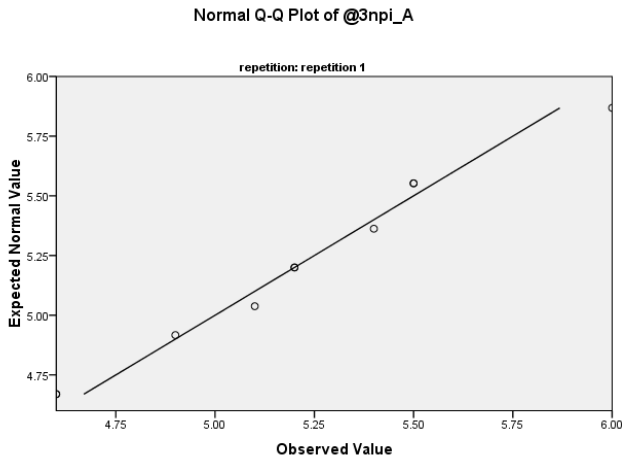

Figure (4.11) demonstrates the Q-Q plot demonstrating the normal distribution of data of the first repetition in volunteer A (post drink)

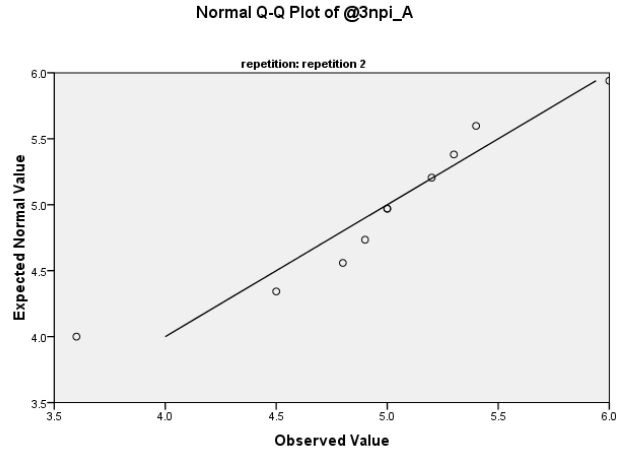

Figure (4.12) demonstrates the Q-Q plot demonstrating the normal distribution of data of the second repetition in volunteer A (post drink)

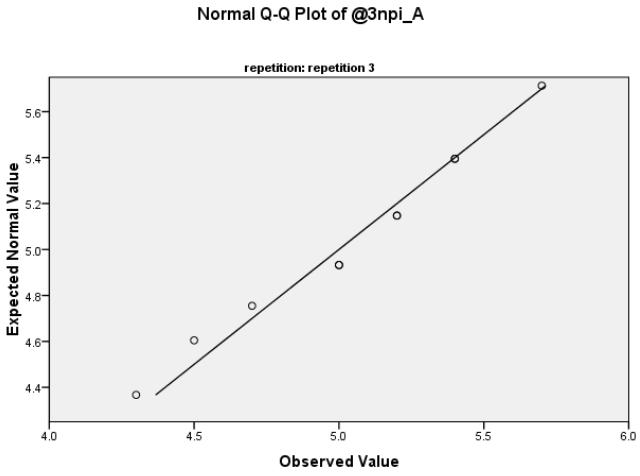

Figure (4.13) demonstrates the Q-Q plot demonstrating the normal distribution of data of the third repetition in volunteer A (post drink)

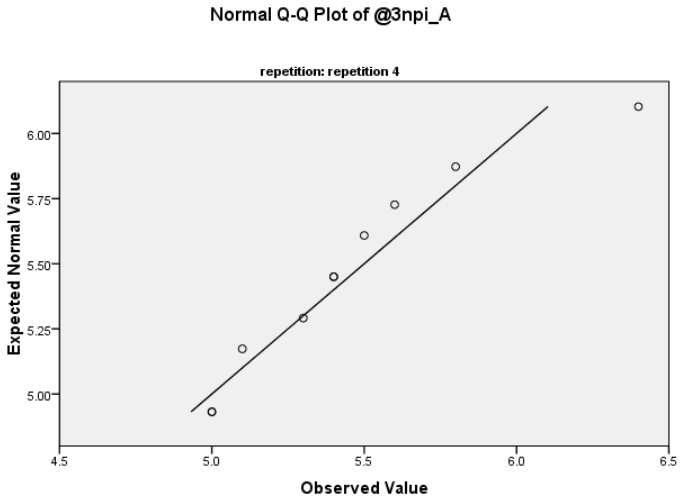

Figure (4.14) demonstrates the Q-Q plot demonstrating the normal distribution of data of the fourth repetition in volunteer A (post drink)

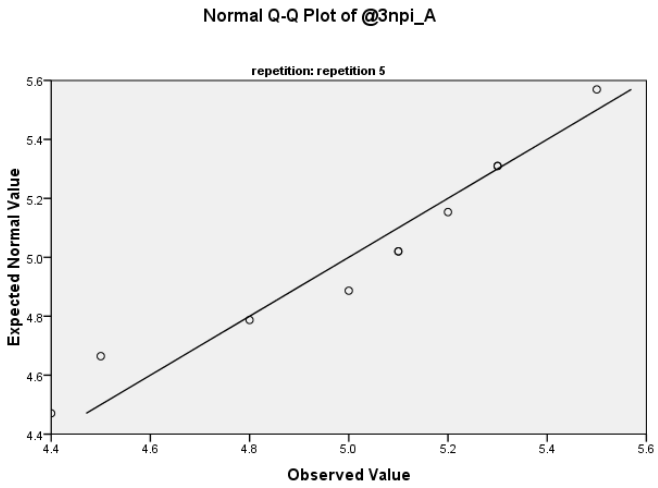

Figure (4.15) demonstrates the Q-Q plot demonstrating the normal distribution of data of the fifth repetition in volunteer A (post drink)

The (ANOVA) test of the thresholded NPIs between the five repetitions demonstrated no statistical significance between each repetition for the three volunteers (tables 4.3 – 4.12).

The following table demonstrating the ANOVA test between all the repetitions in the three volunteers in the fasting state and the post drink state. These results demonstrated no statistical significance between all the repetitions and there was no difference between the fasting and the post drink status.

ANOVA

	Sum of Squares	df	Mean Square	F	**Sig.**
Between Groups	1.006	4	.252	.590	**.671**
Within Groups	19.174	45	.426		
Total	20.180	49			

(Table 4.3) demonstrates the ANOVA test of the threshold NPI at threshold 3 between the 5 repetitions in ***volunteer A (post drink)***

Multiple Comparisons

Repetition		Mean Difference	Std. Error	**Sig.**	95% Confidence Interval	
					Lower Bound	Upper Bound
Repetition 1	Repetition 2	.440	.292	**.687**	-.498	1.378
	Repetition 3	.220	.292	**.966**	-.718	1.158
	Repetition 4	.190	.292	**.980**	-.748	1.128
	Repetition 5	.150	.292	**.992**	-.788	1.088
Repetition 2	Repetition 3	-.220	.292	**.966**	-1.158	.718
	Repetition 4	-.250	.292	**.946**	-1.188	.688
	Repetition 5	-.290	.292	**.910**	-1.228	.648
Repetition 3	Repetition 4	-.030	.292	**1.000**	-.968	.908
	Repetition 5	-.070	.292	**1.000**	-1.016	.868
Repetition 4	Repetition 5	-.040	.292	**1.000**	-.978	.898

(Table 4.4) Comparison between each repetition in ***volunteer A (post drink)***

ANOVA

	Sum of Squares	df	Mean Square	F	**Sig.**
Between Groups	.258	4	.064	.182	**.946**
Within Groups	12.383	35	.354		
Total	12.640	39			

(Table 4.5) demonstrates the ANOVA test of the threshold NPI at threshold 3 between the 5 repetitions in ***volunteer A (Fasting).***

Multiple Comparisons

Repetition		Mean Difference	Std. Error	**Sig.**	95% Confidence Interval	
					Lower Bound	Upper Bound
Repetition 1	Repetition 2	.113	.298	**.997**	-.854	1.079
	Repetition 3	.151	.298	**.992**	-.817	1.117
	Repetition 4	-.013	.298	**1.000**	-.979	.954
	Repetition 5	-.063	.298	**1.000**	-1.029	.904
Repetition 2	Repetition 3	.038	.298	**1.000**	-.929	1.004
	Repetition 4	-.125	.298	**.996**	-1.091	.848
	Repetition 5	-.175	.298	**.986**	-1.142	.792
Repetition 3	Repetition 4	-.163	.298	**.989**	-1.129	.804
	Repetition 5	-.213	.298	**.971**	-1.179	.754
Repetition 4	Repetition 5	-.050	.298	**1.000**	-1.017	.917

(Table 4.6) demonstrating the comparison between each repetition in ***volunteer A (Fasting)***

ANOVA

	Sum of Squares	df	Mean Square	F	**Sig.**
Between Groups	.526	4	.132	.346	**.845**
Within Groups	13.290	35	.380		
Total	13.816	39			

(Table 4.7) demonstrating the ANOVA analysis of the threshold NPI at threshold 3 between the 5 repetitions in ***volunteer B (post Drink)***

Multiple Comparisons

Repetition		Mean Difference	Std. Error	**Sig.**	95% Confidence Interval	
					Lower Bound	Upper Bound
Repetition 1	Repetition 2	-.138	.308	**.995**	-1.139	.864
	Repetition 3	-.263	.308	**.946**	-1.264	.739
	Repetition 4	-.338	.308	**.876**	-1.339	.664
	Repetition 5	-.188	.308	**.984**	-1.189	.814
Repetition 2	Repetition 3	-.125	.308	**.997**	-1.127	.877
	Repetition 4	-.200	.308	**.980**	-1.202	.802
	Repetition 5	-.050	.308	**1.000**	-1.052	.952
Repetition 3	Repetition 4	-.075	.308	**1.000**	-1.077	.927
	Repetition 5	.075	.308	**1.000**	-.927	1.077
Repetition 4	Repetition 5	.150	.308	**.993**	-.852	1.152

(Table 4.8) demonstrating the comparison between each repetition in ***volunteer B (post drink)***

ANOVA

	Sum of Squares	df	Mean Square	F	**Sig.**
Between Groups	1.529	4	.382	1.780	**.150**
Within Groups	9.666	45	.215		
Total	11.195	49			

(Table 4.9) demonstrating the ANOVA analysis of the threshold NPI at threshold 3 between the 5 repetitions in ***volunteer B (fasting)***

Multiple Comparisons

Repetitions		Mean Difference	Std. Error	Sig.	95% Confidence Interval	
					Lower Bound	Upper Bound
Repetition 1	Repetition 2	.230	.207	**.871**	-.436	.896
	Repetition 3	.160	.207	**.963**	-.506	.8267
	Repetition 4	-.250	.207	**.833**	-.916	.416
	Repetition 5	.180	.207	**.943**	-.486	.846
Repetition 2	Repetition 3	-.070	.207	**.998**	-.736	.596
	Repetition 4	-.480	.207	**.270**	-1.146	.186
	Repetition 5	-.050	.207	**1.000**	-.716	.616
Repetition 3	Repetition 4	-.410	.207	**.429**	-1.076	.256
	Repetition 5	.020	.20727	**1.000**	-.646	.686
Repetition 4	Repetition 5	.430	.20727	**.380**	-.235	1.096

(Table 4.10) demonstrating the comparison between each repetition in ***volunteer B (Fasting)***

ANOVA

	Sum of Squares	df	Mean Square	F	Sig.
Between Groups	.111	4	.028	.077	.989
Within Groups	16.282	45	.362		
Total	16.393	49			

(Table 4.11) demonstrating the ANOVA analysis of the threshold NPI at threshold 3 between the 5 repetitions in ***volunteer C (post Drink)***

Multiple Comparisons

Repetition		Mean Difference	Std. Error	**Sig.**	95% Confidence Interval	
					Lower Bound	Upper Bound
Repetition 1	Repetition 2	.070	.269	**.999**	-.794	.934
	Repetition 3	.090	.269	**.998**	-.774	.954
	Repetition 4	.040	.269	**1.000**	-.824	.904
	Repetition 5	.140	.269	**.991**	-.724	1.004
Repetition 2	Repetition 3	.020	.269	**1.000**	-.844	.884
	Repetition 4	-.030	.269	**1.000**	-.894	.834
	Repetition 5	.070	.269	**.999**	-.794	.934
Repetition 3	Repetition 4	-.050	.269	**1.000**	-.914	.814
	Repetition 5	.050	.269	**1.000**	-.814	.914
Repetition 4	Repetition 5	.100	.269	**.998**	-.764	.964

(Table 4.12) demonstrating the comparison between each repetition in ***volunteer C (post drink)***

The above results show that the differences between each repetition in the post drink and the fasting state is not statistically significant, hence one scan is enough to obtain a reproducible threshold NPI.

2. Acquisition time test:

Normalization of data was checked by Q-Q plot. The following figures (Fig 4.16 – 4.21) demonstrate the normal distribution of data in Volunteer A (post drink).

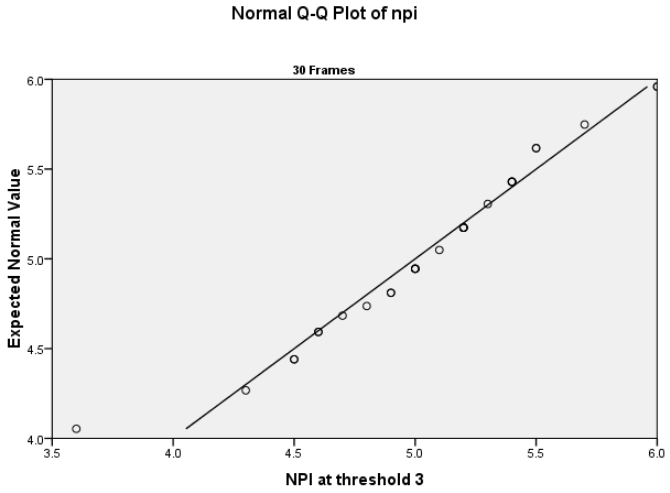

Figure (4.16) demonstrates the normal distribution of data (threshold NPIs) of the 30 frames long acquisition in volunteer A (post drink).

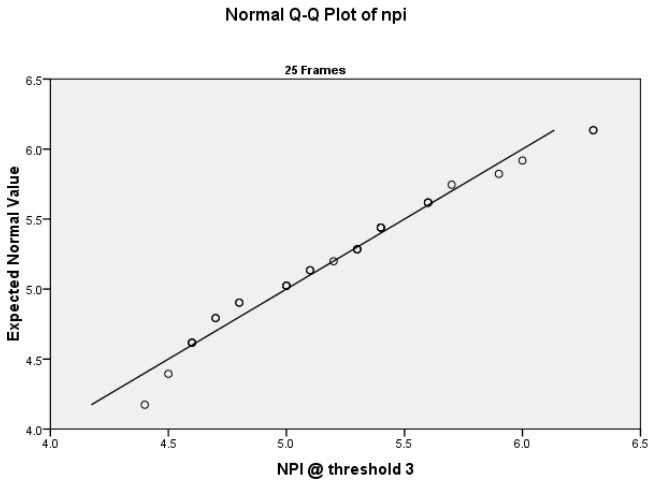

Figure (4.17) demonstrates the normal distribution of data (threshold NPIs) of the 25 frames long acquisition in volunteer A (post drink).

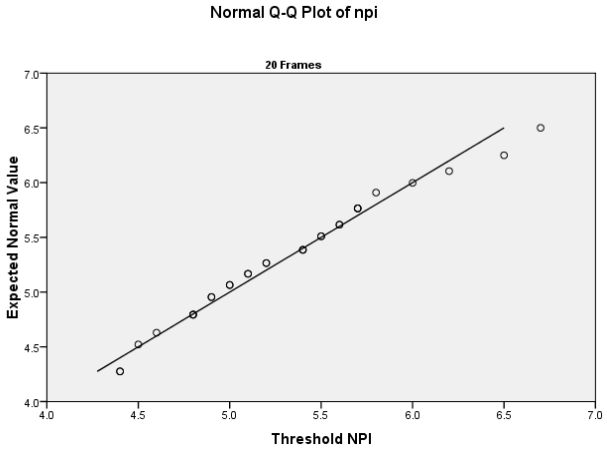

Figure (4.18) demonstrates the normal distribution of data (threshold NPIs) of the 20 frames long acquisition in volunteer A (post drink).

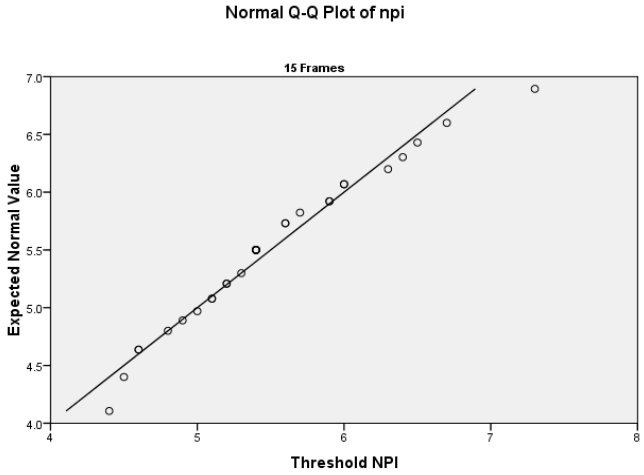

Figure (4.19) demonstrates the normal distribution of data (threshold NPIs) of the 15 frames long acquisition in volunteer A (post drink).

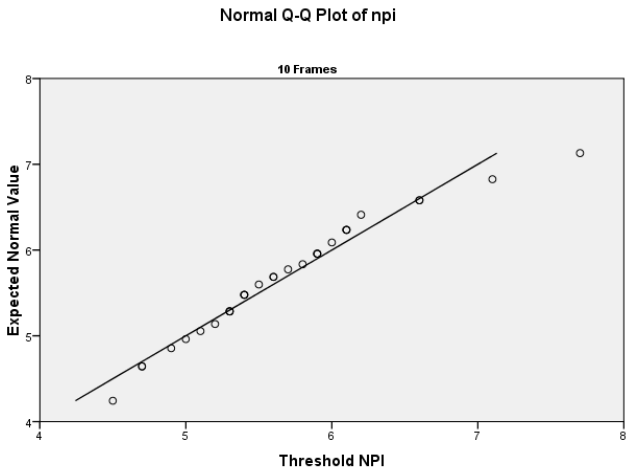

Figure (4.20) demonstrates the normal distribution of data (threshold NPIs) of the 10 frames long acquisition in volunteer A (post drink).

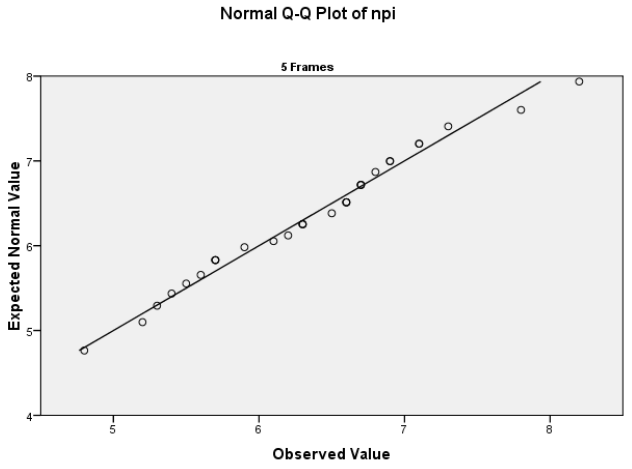

Figure (4.21) demonstrates the normal distribution of data (threshold NPIs) of the 5 frames long acquisition in volunteer A (post drink).

Data from each volunteer was plotted against time and demonstrated significant increase in variance the shorter the study time. There was a significant variation when the scan time was 10 frames or less.

The following figures (Fig 4.22 – Fig 4.26) show the change in the mean thresholded NPI per study against time for the different volunteers. ANOVA test was done between each study and demonstrated significant increase in variance for the studies of 10 frames or shorter (tables 4.13 – 4.17).

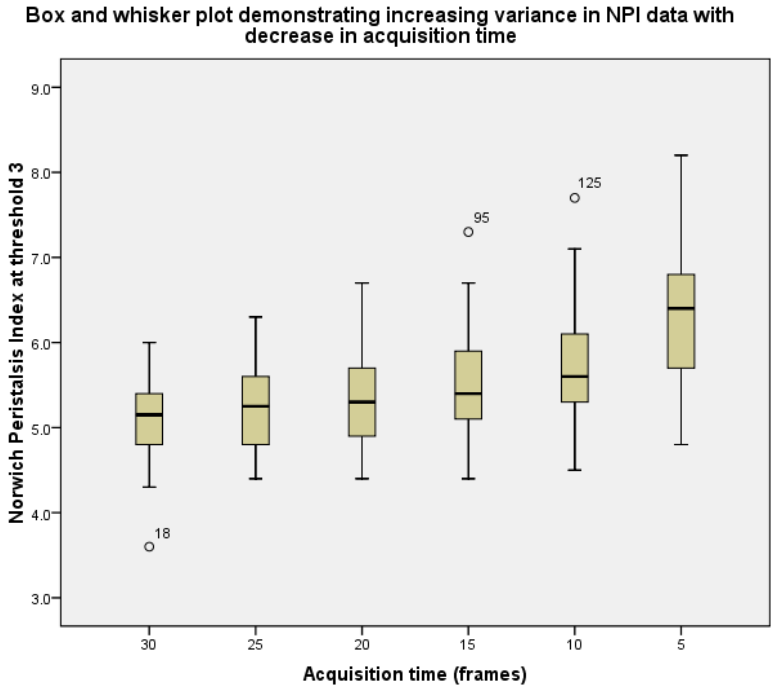

Figure (4.22) demonstrating data from volunteer A (post drink)

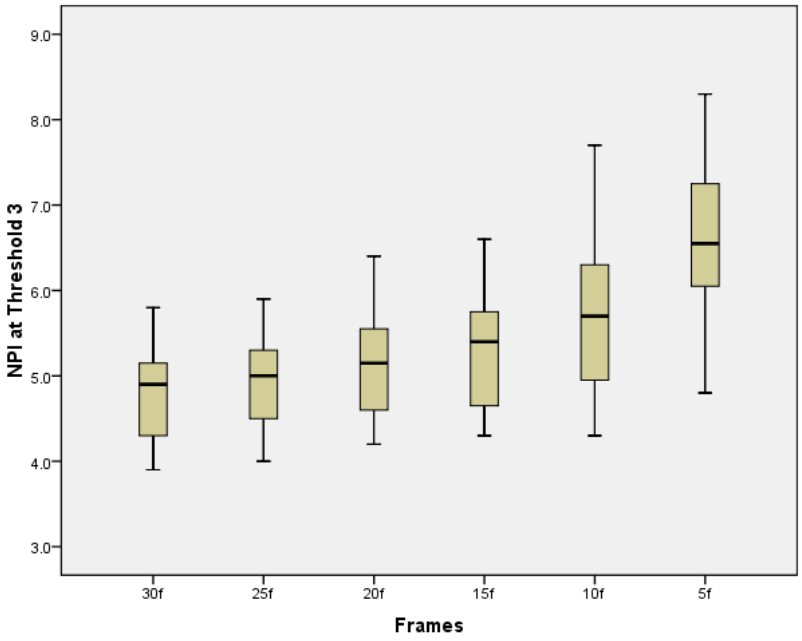

Figure (4.23) demonstrating data from volunteer A (fasting)

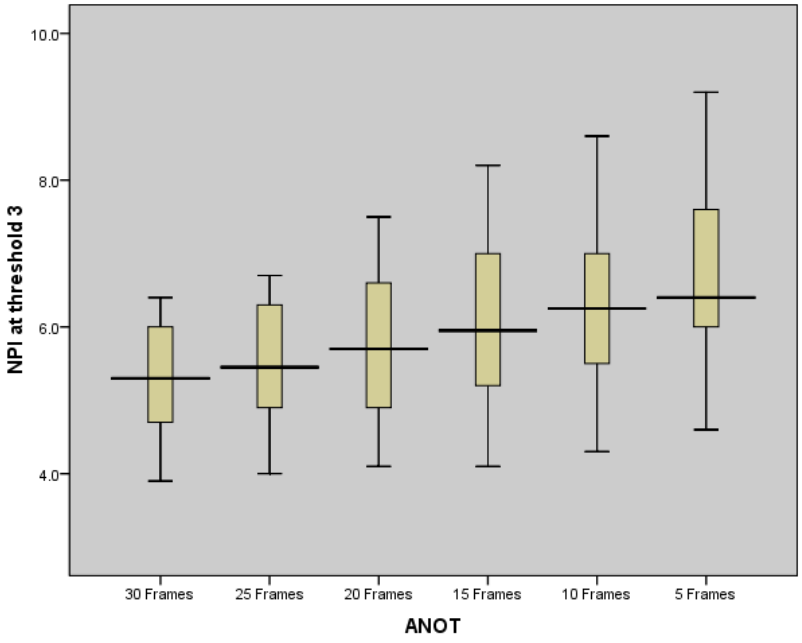

Figure (4.24) demonstrating data from volunteer B (post drink)

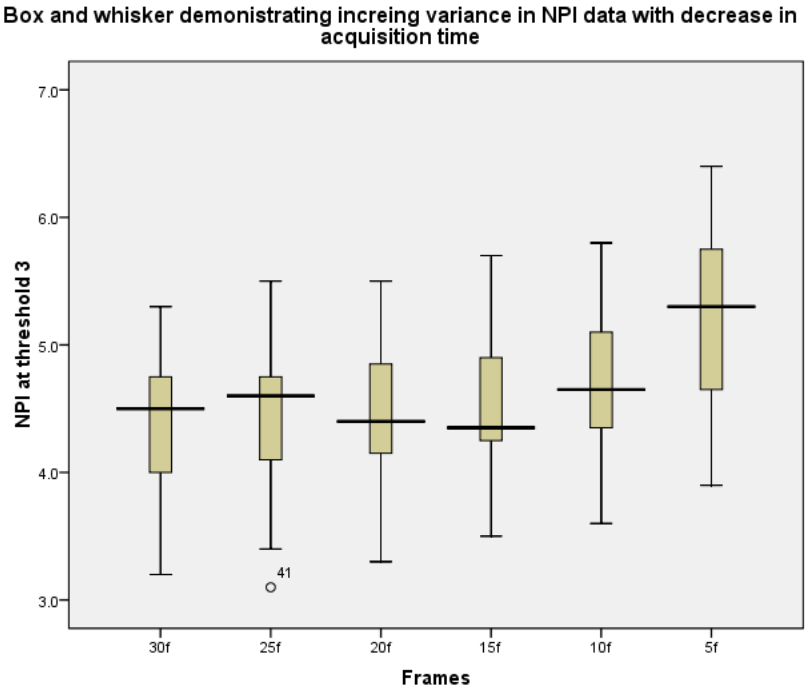

Figure (4.25) demonstrating data from volunteer B (fasting)

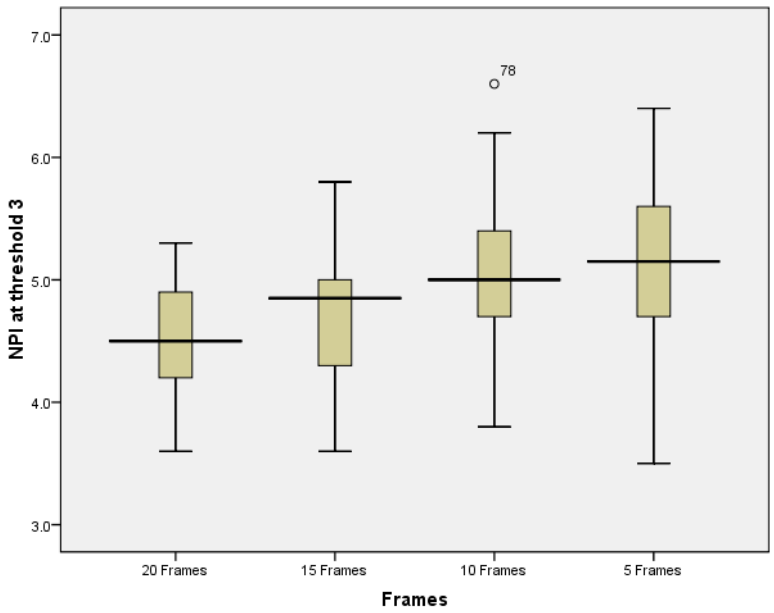

Figure (4.26) demonstrating data from volunteer B (post drink)

Multiple Comparisons

Acquisition time		Mean Difference	Std. Error	Sig.	95% Confidence Interval	
					Lower Bound	Upper Bound
30 Frames	25 Frames	-.150	.164	**.974**	-.702	.402
	20 Frames	-.243	.164	**.820**	-.795	.309
	15 Frames	-.430	.164	**.236**	-.982	.122
	10 Frames	-.617*	.164	**.018**	-1.169	-.065
	5 Frames	-1.280*	.164	**.000**	-1.832	-.728
25 Frames	20 Frames	-.0933	.164	**.997**	-.645	.459
	15 Frames	-.280	.164	**.713**	-.832	.272
	10 Frames	-.467	.164	**.157**	-1.019	.085
	5 Frames	-1.130*	.164	**.000**	-1.682	-.578
20 Frames	15 Frames	-.187	.164	**.935**	-.739	.365
	10 Frames	-.374	.164	**.398**	-.925	.179
	5 Frames	-1.037*	.164	**.000**	-1.589	-.485
15 Frames	10 Frames	-.1867	.164	**.935**	-.739	.365
	5 Frames	-.8500*	.164	**.000**	-1.402	-.298
10 Frames	5 Frames	-.6633*	.164	**.008**	-1.215	-.111

***** The mean difference is significant at the 0.05 level

Table (4.13) ANOVA test between the different acquisition times in volunteer A (post drink)

Multiple Comparisons

Acquisition time		Mean Difference	Std. Error	**Sig.**	95% Confidence Interval	
					Lower Bound	Upper Bound
30 frames	25 frames	-.113	.202	**.997**	-.793	.568
	20 frames	-.309	.202	**.800**	-.989	.372
	15 frames	-.496	.202	**.308**	-1.177	.185
	10 frames	-.892*	.202	**.002**	-1.572	-.211
	5 frames	-1.758*	.202	**.000**	-2.439	-1.078
25 frames	20 frames	-.196	.202	**.966**	-.877	.485
	15 frames	-.383	.202	**.607**	-1.064	.297
	10 frames	-.779*	.202	**.014**	-1.460	-.098
	5 frames	-1.646*	.202	**.000**	-2.327	-.965
20 frames	15 frames	-.188	.202	**.972**	-.868	.493
	10 frames	-.583	.202	**.145**	-1.264	.097
	5 frames	-1.450*	.202	**.000**	-2.131	-.769
15 frames	10 frames	-.396	.202	**.572**	-1.077	.285
	5 frames	-1.263*	.202	**.000**	-1.943	-.582
10 frames	5 frames	-.867*	.202	**.004**	-1.547	-.186

***** The mean difference is significant at the 0.05 level

Table (4.14) ANOVA test between the different acquisition times in volunteer A (fasting)

Multiple Comparisons

Acquisition time		Mean Difference	Std. Error	Sig.	95% Confidence Interval	
					Lower Bound	Upper Bound
30 Frames	25 Frames	-.204	.243	**.983**	-1.020	.614
	20 Frames	-.460	.243	**.610**	-1.277	.357
	15 Frames	-.720	.243	**.123**	-1.537	.097
	10 Frames	-.940*	.243	**.013**	-1.757	-.123
	5 Frames	-1.320*	.243	**.000**	-2.137	-.503
25 Frames	20 Frames	-.257	.243	**.952**	-1.074	.560
	15 Frames	-.517	.243	**.478**	-1.334	.300
	10 Frames	-.737	.243	**.107**	-1.554	.080
	5 Frames	-1.117*	.243	**.001**	-1.934	-.300
20 Frames	15 Frames	-.260	.243	**.949**	-1.077	.557
	10 Frames	-.480	.243	**.564**	-1.297	.337
	5 Frames	-.860*	.243	**.032**	-1.677	-.043
15 Frames	10 Frames	-.220	.243	**.975**	-1.037	.597
	5 Frames	-.600	.243	**.301**	-1.417	.217
10 Frames	5 Frames	-.380	.243	**.783**	-1.197	.437

***** The mean difference is significant at the 0.05 level

Table (4.15) ANOVA test between the different acquisition times in volunteer B (post drink)

Multiple Comparisons

Acquisition time		Mean Difference	Std. Error	Sig.	95% Confidence Interval	
					Lower Bound	Upper Bound
30 Frames	25 Frames	-.0375	.167	**1.000**	-.602	.527
	20 Frames	-.0500	.167	**1.000**	-.614	.514
	15 Frames	-.1458	.167	**.979**	-.710	.418
	10 Frames	-.3417	.167	**.526**	-.906	.222
	5 Frames	-.7917*	.167	**.001**	-1.356	-.228
25 Frames	20 Frames	-.0125	.167	**1.000**	-.577	.552
	15 Frames	-.1083	.167	**.995**	-.672	.456
	10 Frames	-.3042	.167	**.652**	-.868	.260
	5 Frames	-.7542*	.167	**.002**	-1.318	-.190
20 Frames	15 Frames	-.0958	.167	**.997**	-.660	.468
	10 Frames	-.2917	.167	**.693**	-.856	.272
	5 Frames	-.7417*	.167	**.002**	-1.306	-.178
15 Frames	10 Frames	-.1958	.167	**.926**	-.760	.368
	5 Frames	-.6458*	.167	**.014**	-1.210	-.082
10 Frames	5 Frames	-.4500	.167	**.210**	-1.014	.114

***** The mean difference is significant at the 0.05 level

Table (4.16) ANOVA test between the different acquisition times in volunteer B (fasting)

Multiple Comparisons

Acquisition time		Mean Difference	Std. Error	Sig.	95% Confidence Interval	
					Lower Bound	Upper Bound
20 Frames	15 Frames	-.173	.163	**.770**	-.636	.290
	10 Frames	-.447	.163	**.063**	-.910	.016
	5 Frames	-.524*	.163	**.019**	-.986	-.060
15 Frames	10 Frames	-.274	.163	**.426**	-.736	.190
	5 Frames	-.350	.163	**.210**	-.813	.113
10 Frames	5 Frames	-.077	.163	**.974**	-.540	.386

***** The mean difference is significant at the 0.05 level

Table (4.17) ANOVA test between the different acquisition times in volunteer C (post drink)

3. Number of slices per study

In volunteer A, Using half the dataset by selecting alternate coronal slices resulted in no significant differences in variance between the two sets of five slices (P = 0.664). On reducing the number of slices to three, there was a significant difference in variance between the three sets of three slices (p=0.012).

In volunteer B “fasting state”, there was no significant difference in variance on using half of the dataset by selecting alternate coronal slices resulting in two sets of five slices (P = 0.639). There was also no significant difference in variance on further reduction of the number of slices to three (p= 0.161) and two slices (p = 0.077).

When the study was repeated in volunteer B in the “post drink state”, there was a significant difference in variance on reduction the number of slices to five (p = 0.003).

In volunteer C “fasting”, there was a significant difference in variance on reduction the number of slices to five (p= 0.015), however, in the “post drink state” there was no significant difference in variance on reducing the number of slices to five (p= 0.514), three (P= 0.388), or two slices (p= 0.222).

The following figures and tables summarize these results.

A. Results from Volunteer A (Drink)

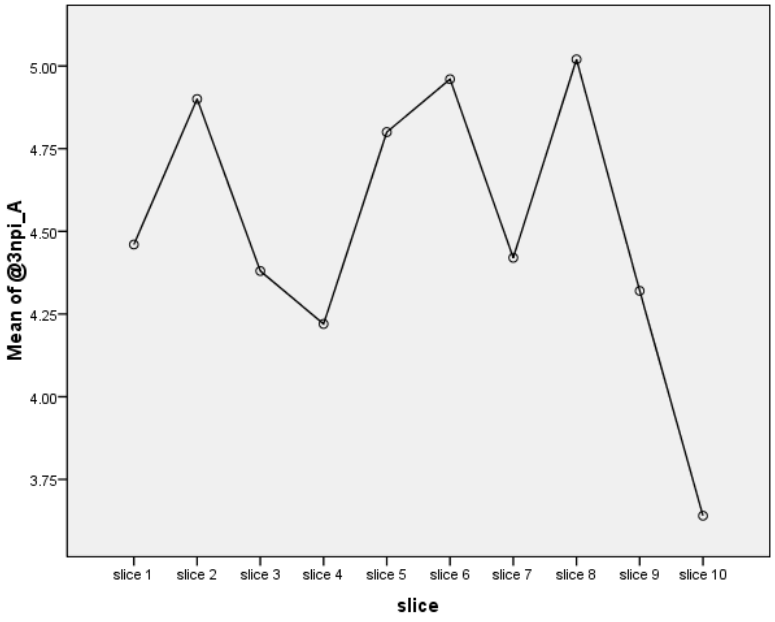

Figure (4.27) demonstrating the changes in the mean of the thresholded NPI at different slices in volunteer A (Drink)

ANOVA

Threshold_NPI	Sum of Squares	df	Mean Square	F	**Sig.**
Between Groups	.065	1	.065	.190	**.664**
Within Groups	16.328	48	.340		
Total	16.393	49			

Table (4.18) ANOVA test demonstrating the significant difference between the two sets of ***five slices*** in volunteer A (Drink status).

ANOVA

Threshold_NPI	Sum of Squares	df	Mean Square	F	**Sig.**
Between Groups	2.256	2	1.128	4.915	**.012**
Within Groups	9.640	42	.230		
Total	11.896	44			

Table (4.19) ANOVA test the variable significant difference between the three sets of ***three slices*** in volunteer A (Drink status).

B. Results from Volunteer B (Fasting)

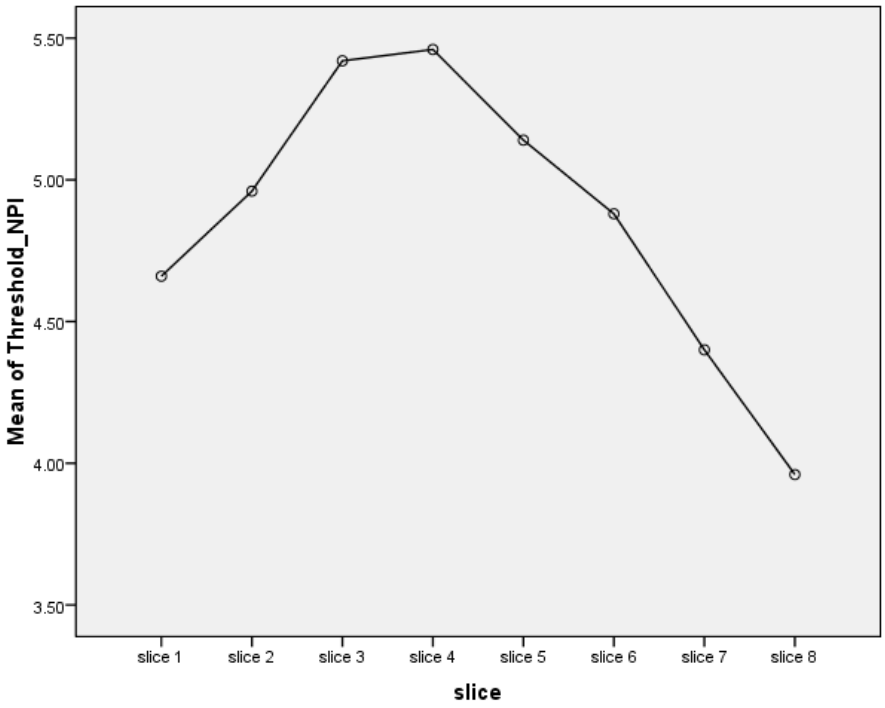

Figure (4.28) demonstrating the changes in the mean of the thresholded NPI at different slices in volunteer B (Fasting)

ANOVA

Threshold_NPI	Sum of Squares	df	Mean Square	F	**Sig.**
Between Groups	.081	1	.081	.224	**.639**
Within Groups	13.735	38	.361		
Total	13.816	39			

Table (4.21) ANOVA test the significant difference between the two sets of ***five slices*** in volunteer B (Fasting status).

ANOVA

Threshold_NPI	Sum of Squares	df	Mean Square	F	**Sig.**
Between Groups	1.298	2	.649	1.918	**.161**
Within Groups	12.518	37	.338		
Total	13.816	39			

Table (4.22) demonstrates the significant difference between the three sets of ***three slices*** in volunteer B (Fasting status).

ANOVA

Threshold_NPI	Sum of Squares	df	Mean Square	F	**Sig.**
Between Groups	2.886	4	.721	2.310	**.077**
Within Groups	10.930	35	.312		
Total	13.816	39			

Table (4.23) ANOVA test the significant difference between the five sets of ***two slices*** in volunteer B (Fasting status).

C. Results from Volunteer B (Drink)

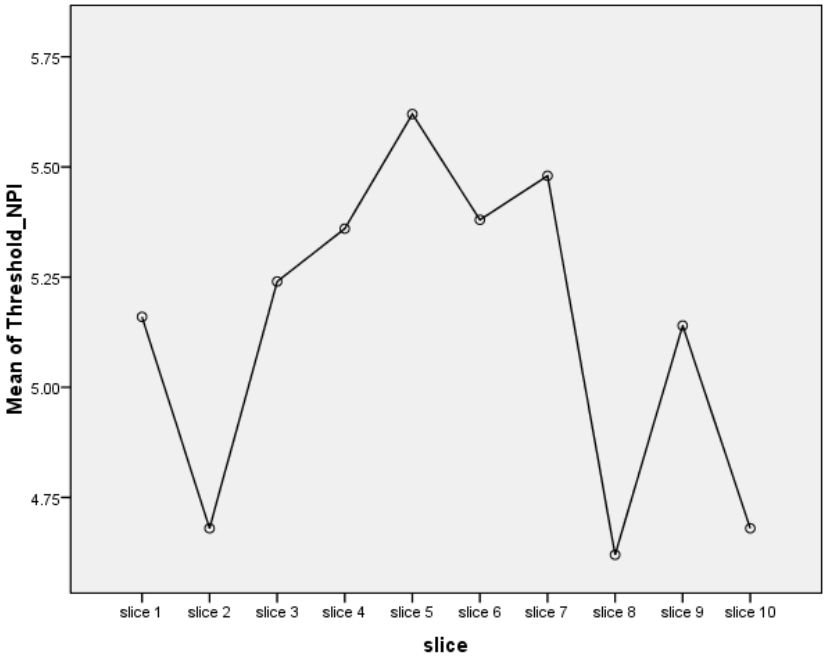

Figure (4.29) demonstrating the changes in the mean of the thresholded NPI at different slices in volunteer B (Drink)

ANOVA

Threshold_NPI	Sum of Squares	df	Mean Square	F	**Sig.**
Between Groups	1.843	1	1.843	9.460	**.003**
Within Groups	9.352	48	.195		
Total	11.195	49			

Table (4.24) ANOVA test the significant difference between the two sets of ***five slices*** in volunteer A (Drink status).

D. Results from Volunteer C (Fasting)

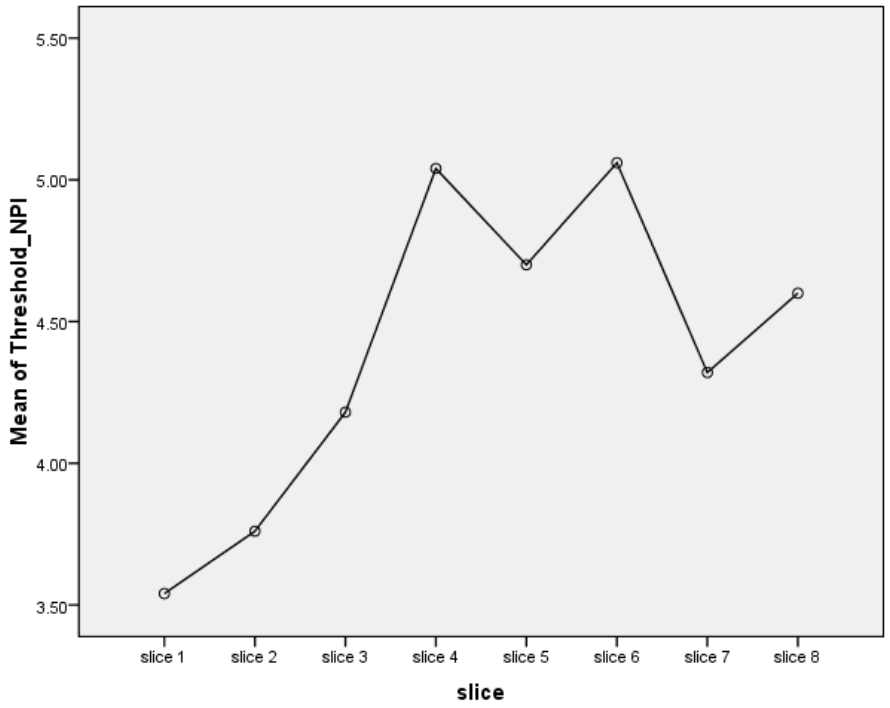

Figure (4.30) demonstrating the changes in the mean of the thresholded NPI at different slices in volunteer C (Fasting)

ANOVA

Threshold_NPI	Sum of Squares	df	Mean Square	F	**Sig.**
Between Groups	1.849	1	1.849	6.511	**.015**
Within Groups	10.791	38	.284		
Total	12.640	39			

Table (4.25) ANOVA test the significant difference between the two sets of ***five slices*** in volunteer C (Fasting status).

E. Results from Volunteer C (Drink)

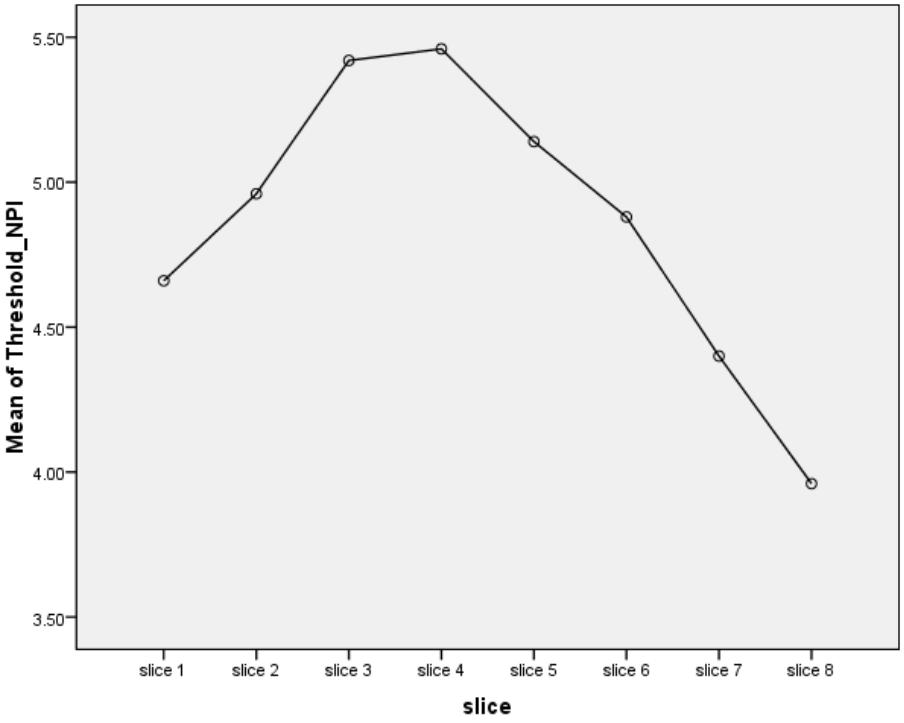

Figure (4.31) demonstrating the changes in the mean of the thresholded NPI at different slices in volunteer C (Drink)

ANOVA

Threshold_NPI	Sum of Squares	df	Mean Square	F	**Sig.**
Between Groups	.180	1	.180	.432	**.514**
Within Groups	20.000	48	.417		
Total	20.180	49			

Table (4.26) ANOVA test the significant difference between the two sets of ***five slices*** in volunteer C (Drink).

ANOVA

Threshold_NPI	Sum of Squares	df	Mean Square	F	**Sig.**
Between Groups	.833	2	.417	.968	**.388**
Within Groups	18.079	42	.430		
Total	18.912	44			

Table (4.27) ANOVA test the variable significant difference between the three sets ***of three slices*** in volunteer C (Drink status).

ANOVA

Threshold_NPI	Sum of Squares	df	Mean Square	F	**Sig.**
Between Groups	2.358	4	.589	1.488	**.222**
Within Groups	17.822	45	.396		
Total	20.180	49			

Table (4.28) ANOVA test the significant difference between the five sets of ***two slices*** in volunteer C (Drink).

4. Reliability study and quantification of the bowel activity

Normalization of data was checked by histogram of the total voxel activity (TVA) for all the slices in the first and the second studies (Fig 4.32-4.33). The data was not normally distributed (skewed to the left). There was a considerable inter-subject variation in the total voxel activity per slice and the sum of TVA per study in the test and retest studies (table 4.29 – 4.31), however the correlation coefficient demonstrated an excellent correlation between the test and the re-test studies(Fig 4.34 – 4.35).

In volunteer A, the slice-by-slice interclass correlation was 0.709, (P=0.003, 95%CI=0.269 to 0.920). In Volunteer B, the slice-by-slice interclass correlation was 0.901 (P=0.000, 95%CI=0.709 to 0.969). In Volunteer C, the slice-by-slice interclass correlation was 0.723 (P=0.002, 95%CI=0.310 to 0.906). In Volunteer D, the slice-by-slice interclass correlation was 0.625 (P=0.004, 95%CI=0.205 to 0.851). In Volunteer E, the slice-by-slice interclass correlation was 0.794 (P=0.000, 95%CI=0.490 to 0.926).

The total slice-by-slice interclass coefficient of rank correlation for the five volunteers was 0.841 (P=0.000, 95% CI = 0.754 to 0.899). The interclass coefficient of rank correlation of the sum of all slices TVA for the five volunteer was 0.985 (P=0.000, 95% CI= 0.863 to 0.998).

Volunteer	Total voxel activity per study (TVA)		SD		Mean Pixel value	
	Test	Retest	Test	Retest	Test	Retest
A	433976	500809	1.81	1.90	4.61	4.83
B	1681799	1598956	2.24	2.26	5.59	5.44
C	1272530	1117609	2.35	2.36	5.46	5.55
D	899490	860333	2.15	2.23	5.42	5.38
E	660489	565807	1.84	1.86	5.05	4.80

Table (4.29) demonstrating the Sum of TVA per study in the test and retest studies

Slice Number	Volunteer	Test	Retest
1	A	6	22
2		7247	6748
3		15647	9237
4		15125	6961
5		32447	63996
6		28602	71756
7		76975	97224
8		80352	46819
9		67994	46823
10		60341	77665
11		49240	73558

Table (4.30) demonstrating the TVA per slice for the test and retest studies in volunteer (A)

Slice Number	Volunteer	Test	Retest
1	B	25541	20781
2		62974	24267
3		26064	32231
4		83168	89262
5		146874	172496
6		205391	224513
7		291844	242109
8		256205	165818
9		181153	215563
10		128678	169502
11		121732	109843
12		95369	79190
13		56806	53381

Table (4.31) demonstrating the TVA per slice for the test and retest studies in volunteer (B)

Slice Number	Volunteer	Test	Retest	Threshold Level
1	C	5621	174	
2		34961	14295	
3		24480	60580	
4		69664	77358	
5		108396	133619	
6		200755	161237	
7		146774	154611	
8		110230	145776	
9		213243	135036	
10		177888	59880	
11		68063	60014	
12		90637	58724	
13		21818	56305	at 4

Table (4.32) demonstrating the TVA per slice for the test and retest studies in volunteer (C)

Slice Number	Volunteer	Test	Retest	Slice Number
1	D	963	1814	
2		4977	810	
3		1317	7575	
4		12145	56174	
5		43933	53829	
6		47417	128781	
7		134704	132174	
8		168657	91929	
9		165455	66882	
10		108390	71580	
11		48688	85633	
12		62151	48333	
13		58243	44857	
14		18024	53698	4.5
15		19551	10546	4.5
16		4875	5718	4.5

Table (4.33) demonstrating the TVA per slice for the test and retest studies in volunteer (D)

Slice Number	Volunteer	Test	Retest	Threshold level
1	E	9400	2787	
2		21336	12379	
3		27155	10354	
4		71924	63243	
5		94957	78516	
6		72038	79713	
7		108949	51202	
8		50709	49523	
9		60462	37539	
10		45862	50690	
11		16138	26636	4
12		25107	29213	4
13		25107	43107	4
14		21751	17011	4
15		9594	13894	4

Table (4.34) demonstrating the TVA per slice for the test and retest studies in volunteer (E)

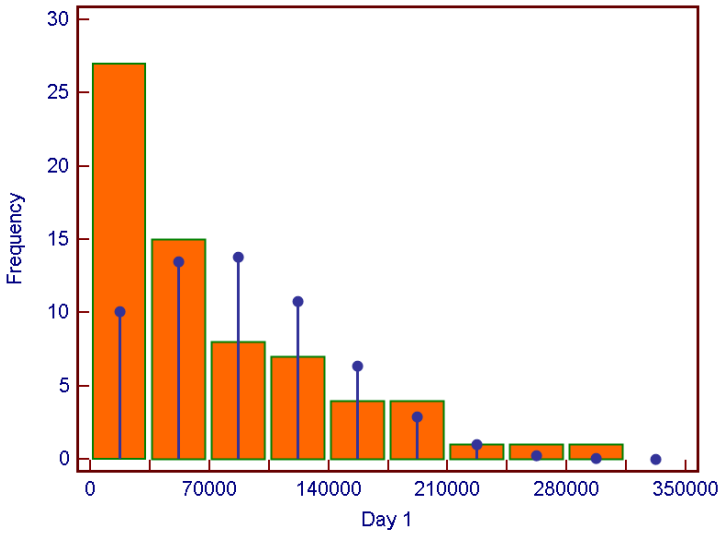

Figure (4.32) demonstrating the left skew of the distribution of the data of the test

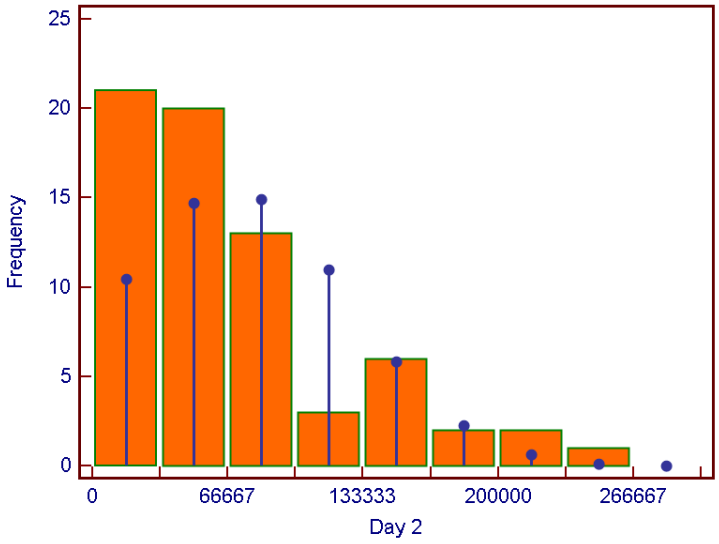

Figure (4.33) demonstrating the left skew of the distribution of the data of the retest

Intraclass Correlation Coefficient

	Intraclass Correlation[a]	95% Confidence Interval		F Test with True Value 0			
		Lower Bound	Upper Bound	Value	df1	df2	Sig
Single Measures	.841[b]	.754	.899	11.560	67	67	.000
Average Measures	.913[c]	.860	.947	11.560	67	67	.000

Two-way mixed effects model where people effects are random and measures effects are fixed.

a. Type C intraclass correlation coefficients using a consistency definition-the between-measure variance is excluded from the denominator variance.

b. The estimator is the same, whether the interaction effect is present or not.

c. This estimate is computed assuming the interaction effect is absent, because it is not estimable otherwise.

Table (4.35) demonstrating the high intraclass correlation of slice by slice TVA in the first and the second studies

Intraclass Correlation Coefficient

	Intraclass Correlation[a]	95% Confidence Interval		F Test with True Value 0			
		Lower Bound	Upper Bound	Value	df1	df2	Sig
Single Measures	.985[b]	.863	.998	130.277	4	4	.000
Average Measures	.992[c]	.926	.999	130.277	4	4	.000

Two-way mixed effects model where people effects are random and measures effects are fixed.

a. Type C intraclass correlation coefficients using a consistency definition-the between-measure variance is excluded from the denominator variance.

b. The estimator is the same, whether the interaction effect is present or not.

c. This estimate is computed assuming the interaction effect is absent, because it is not estimable otherwise.

Table (4.36) demonstrating the (almost perfect) intraclass correlation of the sum of TVA in the first and the second studies

The test-retest reliability of the technique described for quantifying small bowel peristalsis with dynamic MR is extremely good suggesting that this may be a robust technique.

5. Validation of the peristaltic index (intervention with anticholinergic para-sympatholytic agent)

The global TVA for all volunteers reduced after the Hyoscine Butylbromide (Buscopan®) injection by an average of (66%). Two volunteers demonstrated increase in their TVA after 20 minutes, however one volunteer demonstrated further reduction of TPA by 12%. The following table demonstrates the changes in the TVA, and the SD per the whole study.

	Pre-buscopan			10 minutes after Buscopan®			20 minutes after Buscopan®		
Volunteer	**TVA**	SD	Mean pixel value	**TVA**	SD	Mean pixel value	**TVA**	SD	Mean pixel value
A	**144890**	2.10	5.18	**40000**	1.93	4.86	**22664**	1.63	4.56
B	**100950**	1.93	4.87	**43383**	1.47	4.50	**59817**	2.62	5.52
C	**49996**	1.56	4.66	**16159**	1.39	4.35	**17512**	1.59	4.44
D	**72874**	2.65	5.55	**48254**	2.88	6.10	**21395**	1.95	4.87
E	**102404**	1.67	4.84	**31585**	1.09	4.13	**42101**	1.56	4.55

Table (4.37) demonstrating the changes in TVA as a result of administration of Hyoscine Butylbromide

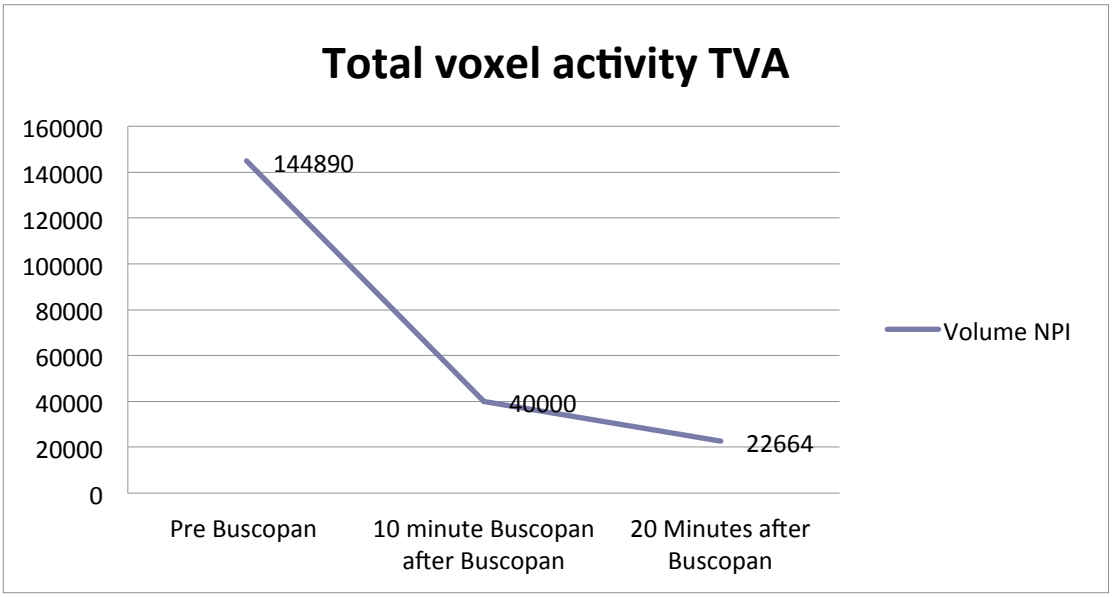

Figure (4.36) demonstrating the changes in the TPA in the three phases of the study in volunteer A

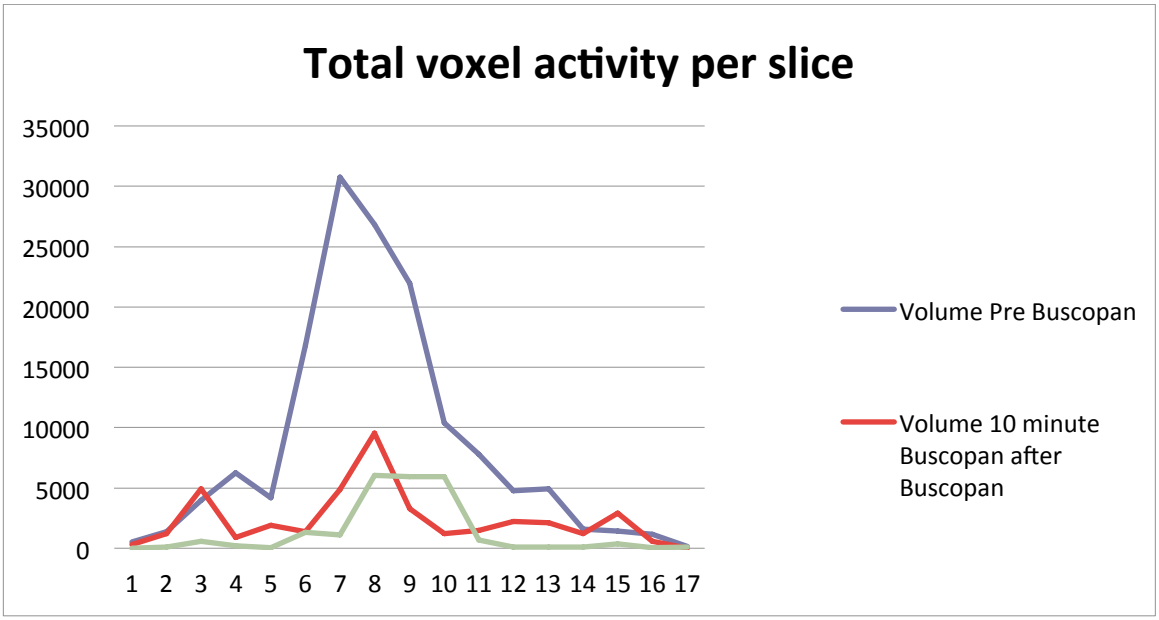

Figure (4.37) demonstrating the changes in the TPA per slice in the three phases of the study in volunteer A

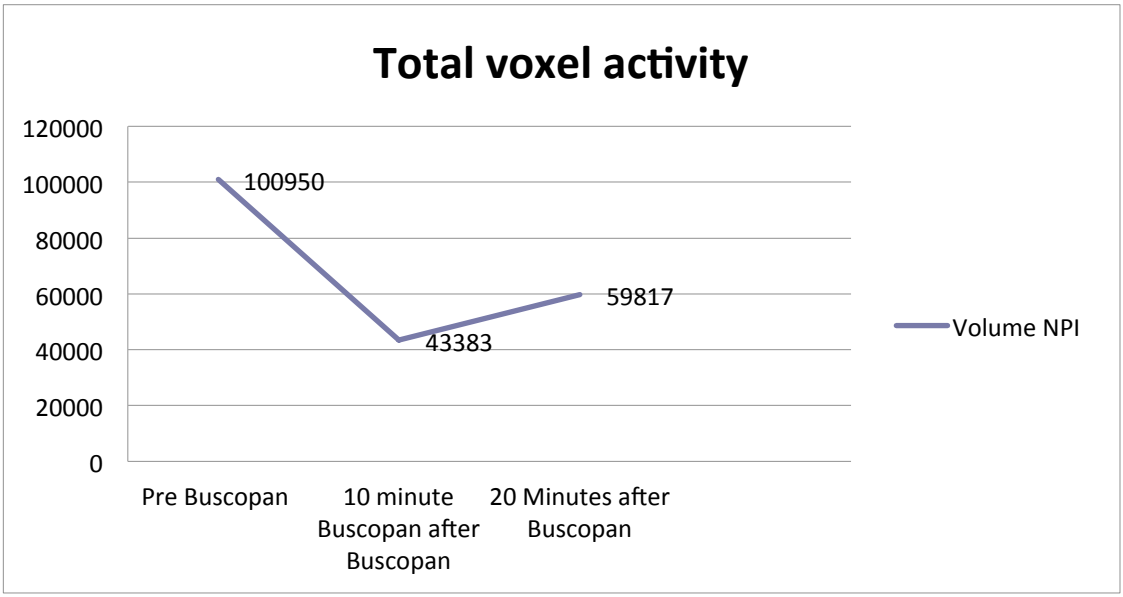

Figure (4.38) demonstrating the changes in the TPA in the three phases of the study in volunteer B

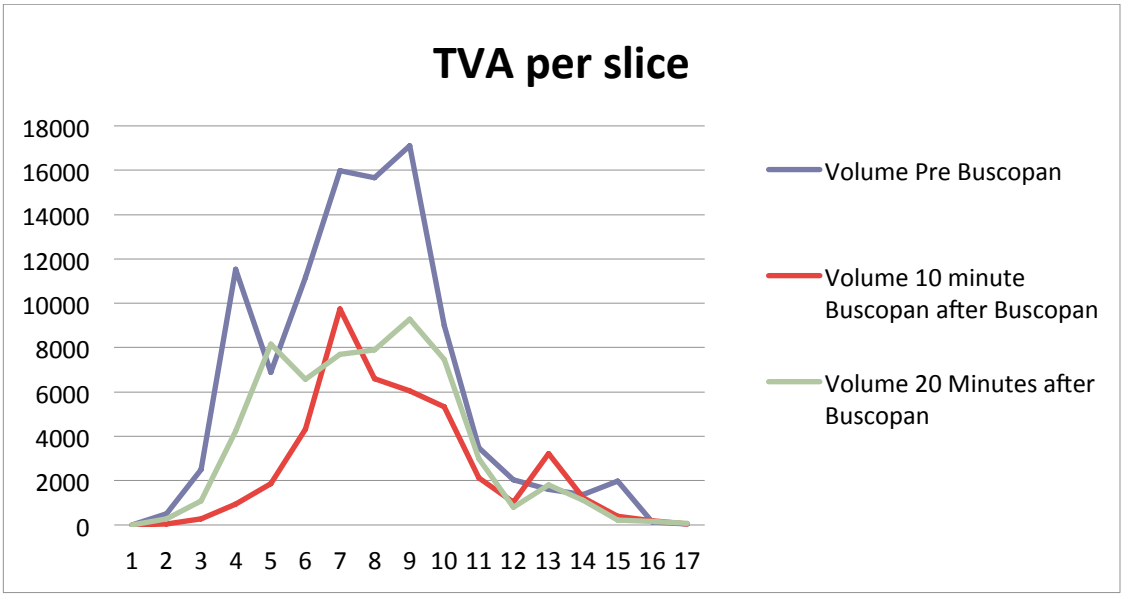

Figure (4.39) demonstrating the changes in the TPA per slice in the three phases of the study in volunteer B

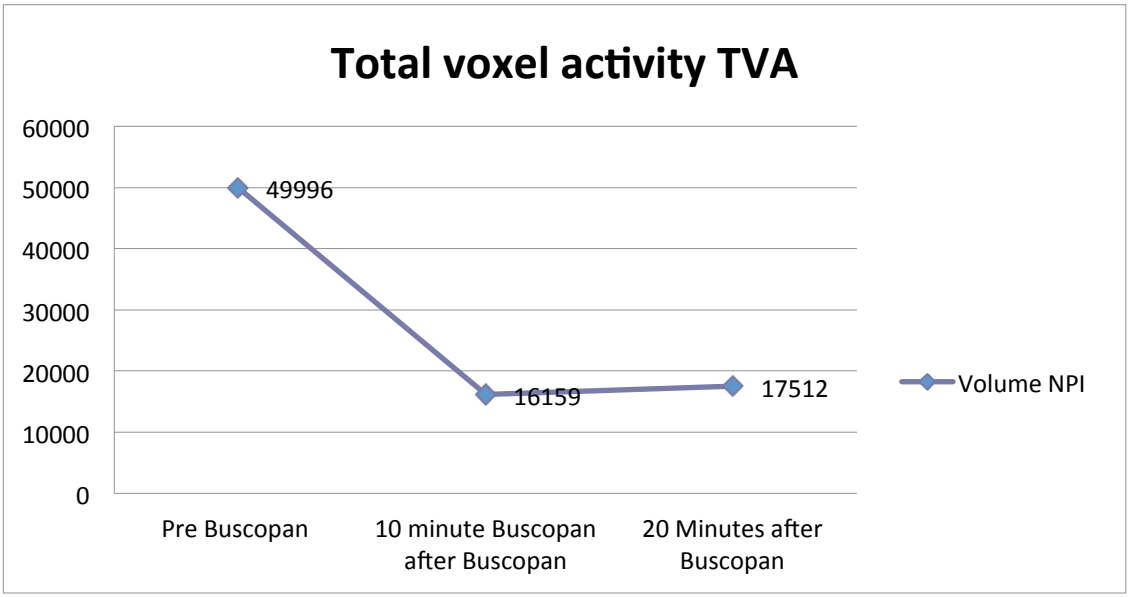

Figure (4.40) demonstrating the changes in the TPA in the three phases of the study in volunteer C

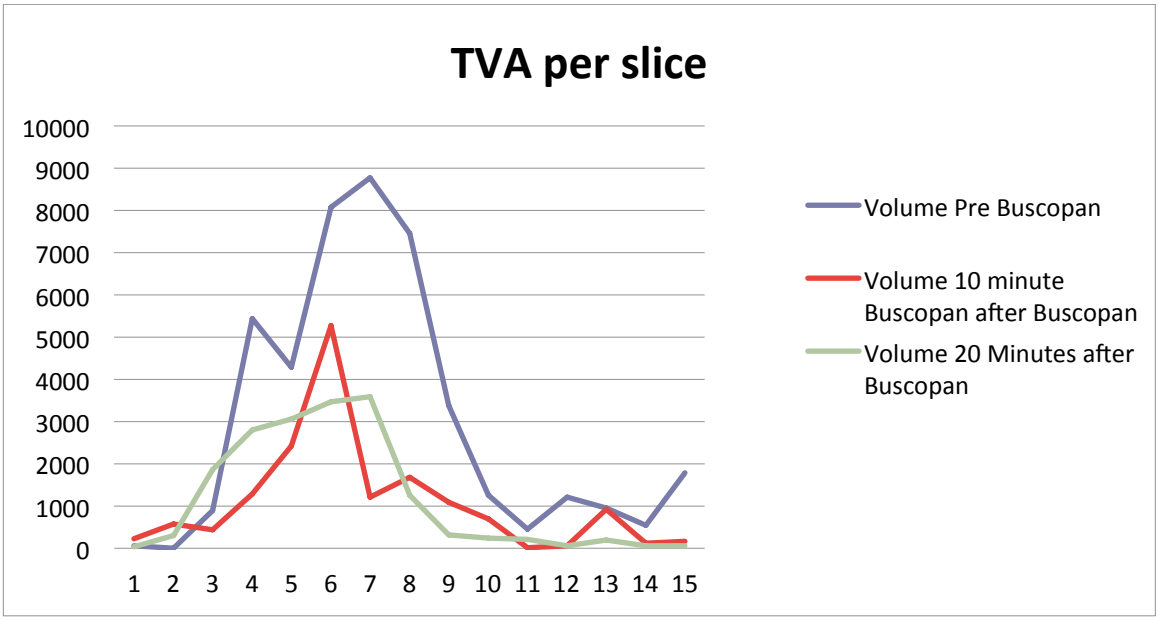

Figure (4.41) demonstrating the changes in the TPA per slice in the three phases of the study in volunteer C

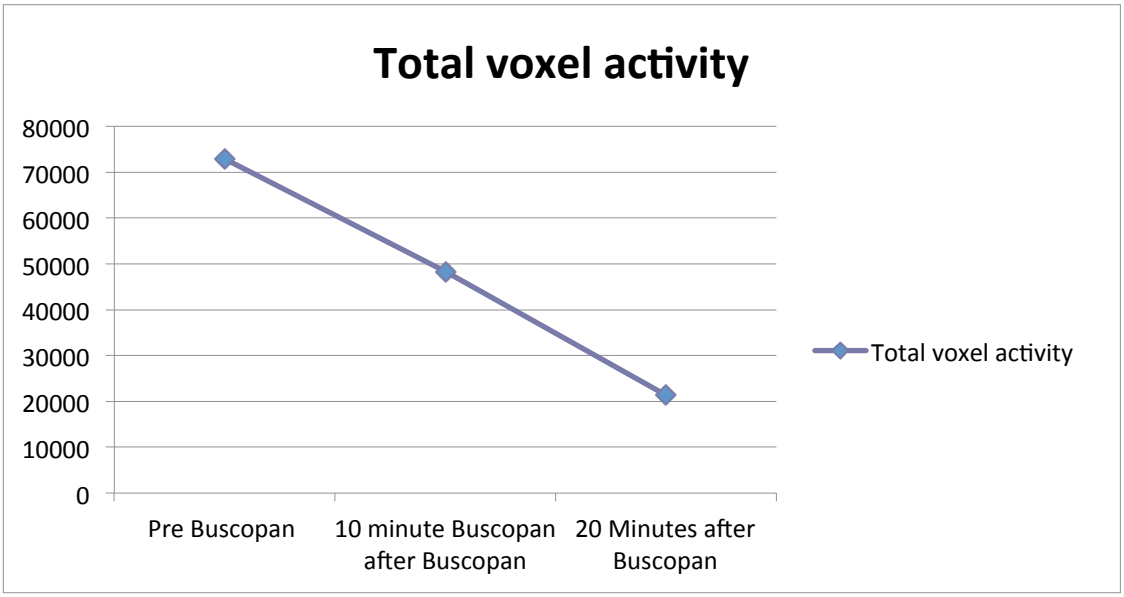

Figure (4.42) demonstrating the changes in the TPA in the three phases of the study in volunteer D

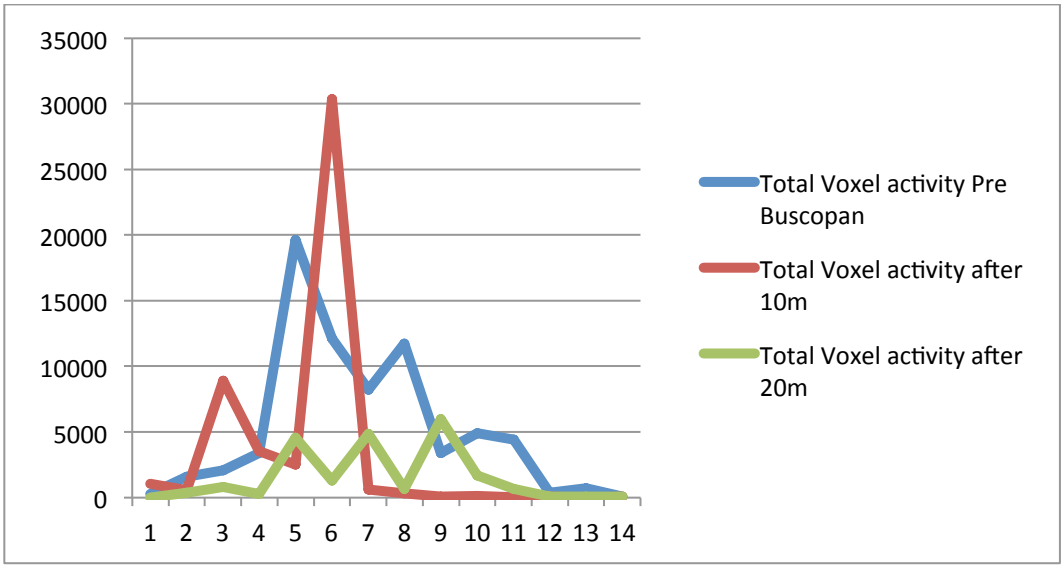

Figure (4.43) demonstrating the changes in the TPA per slice in the three phases of the study in volunteer D

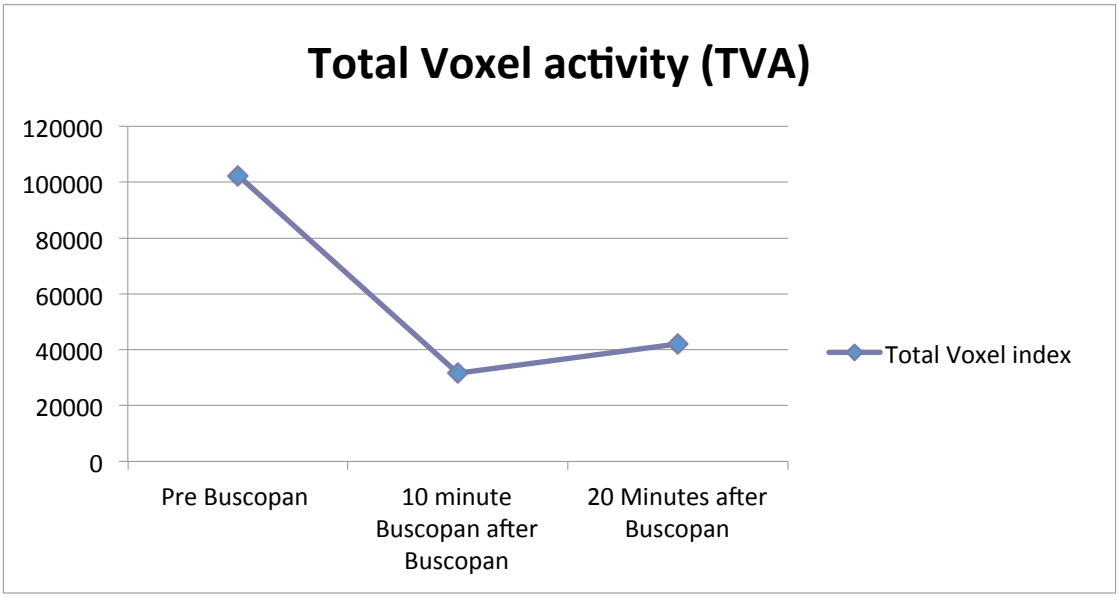

Figure (4.44) demonstrating the changes in the TPA in the three phases of the study in volunteer E

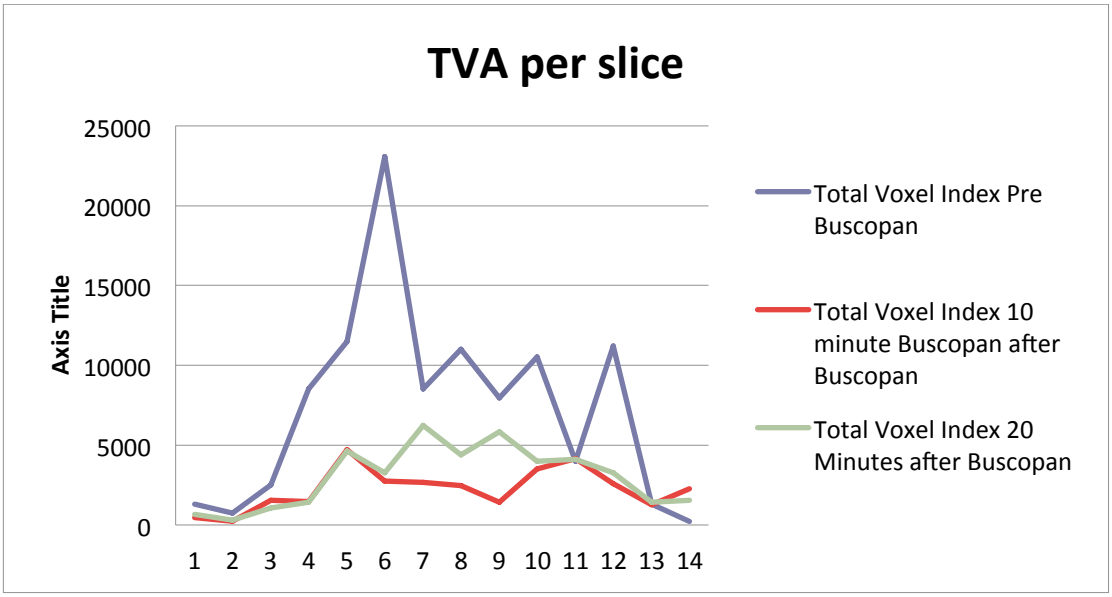

Figure (4.45) demonstrating the changes in the TPA per slice in the three phases of the study in volunteer E

Summary of results

- Dynamic MR using prospective cardiac gated True FISP appears to be a suitable sequence for assessing small bowel motility.
- Gain changes are variable between the dynamic series but constant within the series.
- Correlation of the segmented parametric map with the small bowel cine MR increased with increasing thresholds from (Moderate) to (almost perfect) (Spearman Rho range 0.4 – 0.824). Inter-observer reliability was dependant on the threshold and ranged from "moderate" to "excellent" (Kappa range 0.524 - 0.808). Applying increasing sequential thresholds on the parametric map histogram can segment out small bowel activity from other bowel movement and background noise.
- There was no statistical significance between the 30, 25, 20 and 15 frames acquisition protocols. For acquisitions of 15 frames or less there was significant variability in the data. Using half or less of the dataset by selecting alternate coronal slices resulting in significant differences in variance. There was no significant difference between a single acquisition and the combined data from up to five acquisitions.
- The intraclass correlation demonstrated (almost perfect agreement) between the test and retest in the reliability study. The slice-by-slice correlation was 0.841 (95% CI 0.754 to 0.899, p=0.000), the total abdominal correlation was 0.985 (95% CI 0.863 to 0.998, p=0.000).

- The global TVA for all volunteers reduced after the Hyoscine Butylbromide injection by an average of (66%).

Discussion

The results of this study have preformed from proof of concept, optimization, reliability and early validation studies. It appears that the new mathematical approach proposed in this thesis is practical and reliable and probably does represent a real measure of small bowel motility. This has important implications for further research and clinical care. If these early studies are supported by further studies, then this technique may offer new understanding of the physiology of small bowel in health and disease.

The aim of this thesis was to investigate a new concept of automated global measurement of small bowel activity using non-invasive dynamic MR.

1. Preparatory work:

The first research question had to be addressed in this thesis was (can we obtain acceptable set of dynamic MR data suitable for small bowel motility automated analysis?)

Water was chosen as oral contrast as we thought it was the most physiological solution we could find suitable for our study. One could argue that normal individuals normally do not drink 1L of tap water in 15 minutes, however we accepted this as a potential non-physiological factor. We also tried the fasting status on some volunteers.

The result of these initial trials demonstrated that True FISP without fat suppression was the most acceptable sequence in terms of level of noise and spatial resolution, hence was used for all the studies. As the whole technique depended on detecting the subtle changes in pixel

values, any movement not related to bowel motility was considered artefact. Breathing, cardiac and vascular movements had a negative effect on the resulting parametric image and so multiple breath hold acquisitions with cardiac gating were used. Although the application of cardiac triggering has reduced the temporal resolution from approximately 1.9 frames/second to about 1 frame/second, that was sufficient to capture the small bowel motility given that the mean contraction frequency of small bowel motility is 10.96 per minute (SD= ± 2.51/95% CI= 6.04-15.88) (Froehlich, et al.), (Fleckenstein & Oigaard). Moreover, as the bowel moves in a to and fro motion, multiple sampling of these movement at different single points in time gives the overall net of this movement regardless of the spaces between these samples as long as they are enough samples.

The dataset used for the study was a true fast imaging with steady-state precession (FISP) sequence using prospective ECG gating. Without any special preparation, it takes approximately 1 millisecond for the magnetization to reach the steady state. During the approach to steady state, the magnetization oscillates around the steady-state value and induces the (flashing artefact) in the first image if included in the MR data set (Carr, et al.).

Using prospective gating introduces a gap during the arrhythmia rejection period where the magnetization recovers (leaving the steady state). Retrospective cardiac gating is usually used in dynamic cardiac MR imaging, where the sequence runs continuously even through the arrhythmia rejection period so the magnetization is always in the steady state. The problem of applying this technique was the

unavoidable loss of timely data that is needed for the purpose of this study. Change in the overall gain within the series was another factor that generated noise in the parametric maps. These changes are not explained in the literature, but could be related to the prospective cardiac gating. Our results demonstrated that these changes were variable between the dynamic series (from slice to slice), but were persistent within the dynamic series (within each slice). In order to overcome this problem, each parametric map was corrected by histogram equalization process. In another words, the pixel values were transformed so that the histogram of each frame matched the previous. A reasonable dataset was obtained which was suitable for analysis.

2. Proof of concept study:

The second question was whether or not small bowel can be reliably identified in a coronal dynamic MR series and whether it was possible to isolate the small bowel from other signal changes in the data.

The (almost perfect) inter-rater correlation (k=0.825, 95 CI 0.61-1) in assessing the dynamic MR Cine suggested that the set of data could be used to identify the moving small bowel loops. It was also possible to segment and to separate small bowel peristalsis by using the manual thresholding technique. With increasing the manual threshold, small bowel isolation from other signals would also increase, but that came at the cost of losing some useful signal representing small bowel movement. The debate here was where to set the level of the suitable threshold? It was suggested in this study that Level 3 was suitable in this study as it was the point were two curves of bowel

overrepresentation and bowel underrepresentation decussated (Fig 4.8). This level is variable and dependant on the level of background noise, other movements in the abdomen and the spatial resolution.

The Spearman's ranked correlation coefficient comparing the dynamic MR with the parametric map at different thresholds of the first rater demonstrated (moderate agreement) in thresholds 1 to 4. This has increased to (substantial agreement) in threshold 5, and was (almost perfect agreement) in thresholds 6 to 7. These results were similar in the second rater. The positive trend of this curve (Fig 4.7) is explained by the easiness of recognizing small bowel from other structures as the background noise level decreases.

The inter-rater reliability of assessing the parametric maps was (substantial) in the extremes thresholds, however it was (moderate) at threshold 5 and 6 then (substantial) in the values from 6-7 (k range 0.525 – 0.808). This is explained by the easy distinction between the obvious noisy parametric map in threshold 1 and the under-represented one in threshold 7. The individual variability increased when it comes to the middle thresholds where bowel is mixing with other non-bowel signals. Part of this variability is also due to the relatively large size of each cell of the grid, which can accommodate varying amounts of small bowel, static or other moving tissue. The cell was designed as such for a practical purpose.

3. MR protocol optimization study

This study aimed to optimize the MR protocol that could provide a suitable set of data enabling a single endpoint measurement for small bowel activity in vivo. Four research questions were investigated in this study. The first question was what was the minimum possible number of study repetitions required to reproduce the threshold NPI. The second question was what was the minimum number of coronal slices required for a representable threshold NPI. The third question was what was the shortest possible acquisition time. The fourth question was does the threshold NPI change with fasting?

Results demonstrated:

A. Repetition Test

There was no significant statistical difference in variance (ANOVA) between each of the repetitions, which means that a single acquisition was enough to obtain a reproducible threshold NPI. There was no difference in variance between the fasting and the post drink results even when setting the significance level at 0.001. The most likely explanation for this is that the time difference between each repetition was short so the same phase of peristalsis was captured during these repetitions.

B. Acquisition time:

Results demonstrated that there was a significant increase in variance at acquisition time of 10 frames or shorter. As the dynamic MR images were acquired during multiple single breath-holds, the duration of the breath hold is particularly important when it comes to

applying this technique to sick patients who might not be able to tolerate longer breath holds. This study concluded that 15 fames were sufficient to obtain reproducible threshold NPI.

C. Number of slices per study:

There was a considerable variation in results between volunteers and also between the fasting and the post drink studies. For example in volunteer A, who was scanned in the post drink status, there was no significant difference in variance (P = 0.664) when alternate slices were analysed. On further reduction of the number of slices to three, there was a significant difference in variance between the three sets of three slices (p=0.012).

Another example was in volunteer B (in the fasting state), there was no significant difference in variance on using five slices (P = 0.639). There was also no significant difference in variance on further reduction of the number of slices to three (p= 0.161) and two slices (p = 0.077).

On reviewing the graphs representing the Threshold NPI per slice. There was a considerable variation between each slice. An explanation for these variations could be due to the variable change in position of bowel loops coming in and out of plane, which are variable from subject to subject and also depend on the luminal content and distension. So in order to obtain a robust representative and reproducible data the whole abdomen needs to be scanned.

Effect of fasting:

Fasting did not have a significant effect in the required protocol. It was possible to record the threshold NPI with un-distended bowel. This is important because it implies that ingestion of large volumes of fluid is not necessary for generating contrast resolution. This technique for the first time could open the way of non-invasive measuring of bowel peristalsis in-vivo without the need of over distending the bowel.

4. Reliability study and quantification of bowel activity

The aim for this study was to measure the global bowel activity by introducing the total voxel activity (TVA) and to assess its reliability. The results of this study demonstrated marked inter-subject variation of TVA, which could be explained by the difference in bowel activities between subjects and also the variable length of the small bowel from subject to subject. This means that this dynamic MR technique may be suited to more natural physiological challenges of food and drink.

The slice by slice TVA intraclass correlation between the test and re-test studies was moderate to strong in four volunteers (732, 0.723 , 0.794, 0.625) and very strong in one volunteer (0.901). There was almost a perfect correlation between the sum of the TVA for the whole abdomen between the test and re-test studies (0.985). This slight variation between the slice-by-slice correlation and the sum of total TVA could be explained by changing in bowel position in the two studies coming in and out of slice, giving a slight different TVA value per slice but the overall TVA for the whole abdomen was

almost the same. This study suggests the ability to quantify the global bowel function using the sum of the TVA for the whole abdomen.

5. Validation of the peristaltic index (intervention with Buscopan®)

In this study Hyoscine Butylbromide was used to validate the TVA as a mean of global assessment of small bowel activity. Results demonstrated 66% average reduction of the global TVA for all volunteers 10 minutes after the intramuscular injection of 20 mg Hyoscine Butylbromide. In three volunteers, the global TVA increased again after 20 minutes. In the other two volunteers the global TVA further reduced by 12 % after 20 minutes. This could be explained by the different response to Hyoscine Butylbromide between subjects. The anti-muscarinic effect of the intervention confirms that the TVA is a valid measure of small bowel activity.

Strengths and limitations:

This study, with no doubt, had limitations as well as its strengths. The main limitations are:

1. Due to the experimental nature of this work, selection of volunteers was biased towards medical radiology professionals who would understand the nature of this type of research and have the enthusiasm to participate. More importantly they were fully aware of the contraindication and the potential side effects of the MRI scanning and Hyoscine Butylbromide injection. No doubt they were much easy to recruit because of their availability in the department and due to the personal relationship. This bias would limit these results to a certain demographic category of volunteers.

2. The study was performed on a small number of volunteers (six volunteers). Although it was never the aim, it does limit the generalisation of these findings. This was done purely for practical and ethical purposes as multiple trial and errors had to be made before applying the technique on the large scale.

3. The non-selective way of scanning the abdomen coronally, made other moving structures such as the stomach, ureters, and large bowel contribute to the final measurement, however the small bowel was the main contributor due to its large surface area and extensive continuous motility.

4. Another limitation was the fact that all volunteers were studied either in the fasting status or following drinking water. The validity of

this technique has only been tested for limited physiological applicability.

Despite these limitations, they study has a number of strengths points:

1. This is the first study, to the best of our knowledge; to have directly studied the global small peristalsis in vivo using automated non-invasive technique. The concept of investigating the small bowel as a mathematical phenomenon rather than a discrete organ has not been offered before as an alternative to study bowel motility.

2. This study has introduced new metric measures of global small bowel activity, which were proven to be reliable, and valid in the small group of volunteers recruited in this study.

3. The optimization and reliability studies are real highlights. They are categorically clear and the results are unequivocal. Validation study had also highlighted the variations in peristalsis between individuals. This has not been fully described in the literature because of the current difficult and invasive techniques used to measure bowel peristalsis. Using this technique will enable researchers to use it as a non-invasive tool to understand and describe these variations in details.

Conclusions:

- Automated segmented quantification of small bowel peristalsis from dynamic MR is feasible and may be the basis for a novel approach to physiological imaging of the gut.
- For optimal physiological small bowel dynamic MR studies a single acquisition, with dynamic MR consisting of a minimum of 15 frames, covering the whole abdomen is satisfactory.
- The test-retest reliability of the technique described for quantifying small bowel peristalsis with dynamic MR is very strong suggesting that this may be useful technique for serial studies.
- Suppression of bowel activity with Buscopan® cause dramatic drop in the Total Voxel Activity (TVA) by approximately 66% after 10 minutes which suggests that TVA is a valid technique for measuring small bowel peristalsis.

Implications for current practice and future research:

For years in-vivo small bowel physiology was only investigated by either invasive techniques or by expensive laboratory tests. As bowel motion is extremely complex, most of these tools focused only on one side of the bowel motility. Most of these studies are performed in non-physiological conditions, for example bowel distension was required before acquiring suitable images, which could have a potential negative effect on the actual normal motility pattern. Previous studies have also focused on examining individual elements of small bowel motility, such as frequency and velocity (Froehlich, et al.).

The study has opened the door for further research in the field of bowel physiology using this direct non-invasive method.

1. This study could unable researchers to study and further explore the field of bowel peristalsis in-vivo, which for years has been dependant on invasive techniques limiting the availability of data about the distribution of normal limits.
2. Further research is needed with controlled meals and on large number of volunteers to demonstrate the different phases of peristalsis.
3. Perhaps some studies could be conducted with different formulas of food and different caloric contents to measure their effect on peristalsis. This could have a potential effect on drugs bioavailability.
4. Once normal population profile has been defined, then the effect of aging, gut diseases and systemic diseases could be evaluated against this profile.

5. Different methods of automated image segmentation could also be studied as an alternative for thresholding.

Bibliography

Abrahamsson, H., Antov, S., & Bosaeus, I. (1988). Gastrointestinal and colonic segmental transit time evaluated by a single abdominal x-ray in healthy subjects and constipated patients. *Scand J Gastroenterol Suppl, 152*, 72-80.

Appleyard, M., Fireman, Z., Glukhovsky, A., Jacob, H., Shreiver, R., Kadirkamanathan, S., et al. (2000). A randomized trial comparing wireless capsule endoscopy with push enteroscopy for the detection of small-bowel lesions. *Gastroenterology, 119*(6), 1431-1438.

Argenyi, E. E., Soffer, E. E., Madsen, M. T., Berbaum, K. S., & Walkner, W. O. (1995). Scintigraphic evaluation of small bowel transit in healthy subjects: inter- and intrasubject variability. *Am J Gastroenterol, 90*(6), 938-942.

Balzarini, L., Aime, S., Barbero, L., Ceglia, E., Petrillo, R., Reyner, J., et al. (1992). Magnetic resonance imaging of the gastrointestinal tract: investigation of baby milk as a low cost contrast medium. *Eur J Radiol, 15*(2), 171-174.

Barrett, J. A., Kim E., Ghishan, Fayez K., Merchant, Juanita L., Johnson, Leonard R., Said, Hamid M., Wood, Jackie D. (2006). Physiology of the gastrointestinal tract (pp. 936): Academic Press.

Bashar, M. K., Kitasaka, T., Suenaga, Y., Mekada, Y., & Mori, K. Automatic detection of informative frames from wireless capsule endoscopy images. *Med Image Anal, 14*(3), 449-470.

Bass, P., & Wiley, J. N. (1965). Electrical and Extraluminal Contractile-Force Activity of the Duodenum of the Dog. *Am J Dig Dis, 10*, 183-200.

Beall, D. P., & Regan, F. (1996). MRI of bowel obstruction using the HASTE sequence. *J Comput Assist Tomogr, 20*(5), 823-825.

Bestetti, A., Carola, F., Conciato, L., Marasini, B., & Tarolo, G. L. (1999). Esophageal scintigraphy with a semisolid meal to evaluate esophageal dysmotility in systemic sclerosis and Raynaud's phenomenon. *J Nucl Med, 40*(1), 77-84.

Bilbao, M. K., Frische, L. H., Dotter, C. T., & Rosch, J. (1967). Hypotonic duodenography. *Radiology, 89*(3), 438-443.

Bilecen, D., Scheffler, K., Seifritz, E., Bongartz, G., & Steinbrich, W. (2000). Hydro-MRI for the visualization of gastric wall motility using RARE magnetic resonance imaging sequences. *Abdom Imaging, 25*(1), 30-34.

Brookes, S. J., Chen, B. N., Costa, M., & Humphreys, C. M. (1999). Initiation of peristalsis by circumferential stretch of flat sheets of guinea-pig ileum. *J Physiol, 516 (Pt 2)*, 525-538.

Camilleri, M., Hasler, W. L., Parkman, H. P., Quigley, E. M., & Soffer, E. (1998). Measurement of gastrointestinal motility in the GI laboratory. *Gastroenterology, 115*(3), 747-762.

Carr, J. C., Simonetti, O., Bundy, J., Li, D., Pereles, S., & Finn, J. P. (2001). Cine MR angiography of the heart with segmented true fast imaging with steady-state precession. *Radiology, 219*(3), 828-834.

Castiglione, F., Rispo, A., Cozzolino, A., Camera, L., D'Argenio, G., Tortora, R., et al. (2007). Bowel sonography in adult celiac disease: diagnostic accuracy and ultrasonographic features. *Abdom Imaging, 32*(1), 73-77.

Connor, J. A., Mangel, A. W., & Nelson, B. (1979). Propagation and entrainment of slow waves in cat small intestine. *Am J Physiol, 237*(5), C237-246.

Dalenback, J., Abrahamson, H., Bjornson, E., Fandriks, L., Mattsson, A., Olbe, L., et al. (1998). Human duodenogastric reflux, retroperistalsis, and MMC. *Am J Physiol, 275*(3 Pt 2), R762-769.

Dell'Aquila, P., Pietrini, L., Barone, M., Cela, E. M., Valle, N. D., Amoruso, A., et al. (2005). Small intestinal contrast ultrasonography-based scoring system: a promising approach for the diagnosis and follow-up of celiac disease. *J Clin Gastroenterol, 39*(7), 591-595.

Der-Silaphet, T., Malysz, J., Hagel, S., Larry Arsenault, A., & Huizinga, J. D. (1998). Interstitial cells of cajal direct normal propulsive contractile activity in the mouse small intestine. *Gastroenterology, 114*(4), 724-736.

Diamant, N. E., & Bortoff, A. (1969). Nature of the intestinal low-wave frequency gradient. *Am J Physiol, 216*(2), 301-307.

Dietrich, C. F., Brunner, V., Seifert, H., Schreiber-Dietrich, D., Caspary, W. F., & Lembcke, B. (1999). [Intestinal B-mode sonography in patients with endemic sprue. Intestinal

sonography in endemic sprue]. *Ultraschall Med, 20*(6), 242-247.

Dietrich, O., Raya, J. G., Reeder, S. B., Reiser, M. F., & Schoenberg, S. O. (2007). Measurement of signal-to-noise ratios in MR images: influence of multichannel coils, parallel imaging, and reconstruction filters. *J Magn Reson Imaging, 26*(2), 375-385.

Diner, W. C., Hoskins, E. O., & Navab, F. (1984). Radiologic examination of the small intestine: review of 402 cases and discussion of indications and methods. *South Med J, 77*(1), 68-74.

Donald W McRobbie , E. A. M., Martin J Graves (2003). *MRI from picture to proton*: Cambridge University Press.

Ehrlein, H. J., & Schemann, M. (1987). [New methods of studying small intestine motility]. *Dtsch Tierarztl Wochenschr, 94*(1), 23-27.

Ekberg, O. (1977). Double contrast examination of the small bowel. *Gastrointest Radiol, 1*(4), 349-353.

Evans, D. F., Lamont, G., Stehling, M. K., Blamire, A. M., Gibbs, P., Coxon, R., et al. (1993). Prolonged monitoring of the upper gastrointestinal tract using echo planar magnetic resonance imaging. *Gut, 34*(6), 848-852.

Fich, A., Camilleri, M., & Phillips, S. F. (1989). Effect of age on human gastric and small bowel motility. *J Clin Gastroenterol, 11*(4), 416-420.

Fleckenstein, P., & Oigaard, A. (1978). Electrical spike activity in the human small intestine. A multiple electrode study of fasting diurnal variations. *Am J Dig Dis, 23*(9), 776-780.

Fraser, G. M., & Preston, P. G. (1983). The small bowel barium follow-through enhanced with an oral effervescent agent. *Clin Radiol, 34*(6), 673-679.

Froehlich, J. M., Patak, M. A., von Weymarn, C., Juli, C. F., Zollikofer, C. L., & Wentz, K. U. (2005). Small bowel motility assessment with magnetic resonance imaging. *J Magn Reson Imaging, 21*(4), 370-375.

Furukawa, A., Yamasaki, M., Furuichi, K., Yokoyama, K., Nagata, T., Takahashi, M., et al. (2001). Helical CT in the diagnosis of small bowel obstruction. *Radiographics, 21*(2), 341-355.

Gerson, E. (2000). The definition of small-bowel transit time. *Am. J. Roentgenol, 174*(3), 866.

Giovagnoni, A., Fabbri, A., & Maccioni, F. (2002). Oral contrast agents in MRI of the gastrointestinal tract. *Abdom Imaging, 27*(4), 367-375.

Graff, J., Brinch, K., & Madsen, J. L. (2001). Gastrointestinal mean transit times in young and middle-aged healthy subjects. *Clin Physiol, 21*(2), 253-259.

Gryback, P., Blomquist, L., Schnell, P. O., Jacobsson, H., & Hellstrom, P. M. (2002). [Scintigraphic assessment of the small intestine transit. Diagnostic investigation of dysmotility with 99mTc-HIDA]. *Lakartidningen, 99*(14), 1556-1558, 1561-1552.

Gryback, P., Jacobsson, H., Blomquist, L., Schnell, P. O., & Hellstrom, P. M. (2002). Scintigraphy of the small intestine: a simplified standard for study of transit with reference to normal values. *Eur J Nucl Med Mol Imaging, 29*(1), 39-45.

Ha, H. K., Lee, E. H., Lim, C. H., Shin, Y. M., Jeong, Y. K., Yoon, K. H., et al. (1998). Application of MRI for small intestinal diseases. *J Magn Reson Imaging, 8*(2), 375-383.

Hammer, J., Hammer, K., & Kletter, K. (1998). Lipids infused into the jejunum accelerate small intestinal transit but delay ileocolonic transit of solids and liquids. *Gut, 43*(1), 111-116.

Hansen, M. B. (2002). Small intestinal manometry. *Physiol Res, 51*(6), 541-556.

Hart, D., Haggett, P. J., Boardman, P., Nolan, D. J., & Wall, B. F. (1994). Patient radiation doses from enteroclysis examinations. *Br J Radiol, 67*(802), 997-1000.

Haruma, K., Kusunoki, H., Manabe, N., Kamada, T., Sato, M., Ishii, M., et al. (2008). Real-time assessment of gastroduodenal motility by ultrasonography. *Digestion, 77 Suppl 1*, 48-51.

Hawkes, R. C., & Patz, S. (1987). Rapid Fourier imaging using steady-state free precession. *Magn Reson Med, 4*(1), 9-23.

Hennig, J., Nauerth, A., & Friedburg, H. (1986). RARE imaging: a fast imaging method for clinical MR. *Magn Reson Med, 3*(6), 823-833.

Heppell, J., Kelly, K. A., & Sarr, M. G. (1983). Neural control of canine small intestinal interdigestive myoelectric complexes. *Am J Physiol, 244*(1), G95-100.

Herlinger, H. (1978). A modified technique for the double-contrast small bowel enema. *Gastrointest Radiol, 3*(2), 201-207.

Herlinger H, M. D., Birnbaum BA, Balthazar EJ (2001). Clinical Imaging of the Small Intestine. *Springer*, 47-77.

Herrerias, J. M., Caunedo, A., Rodriguez-Tellez, M., Pellicer, F., & Herrerias, J. M., Jr. (2003). Capsule endoscopy in patients with suspected Crohn's disease and negative endoscopy. *Endoscopy, 35*(7), 564-568.

Hung, G. U., Tsai, C. C., & Lin, W. Y. (2006). Development of a new method for small bowel transit study. *Ann Nucl Med, 20*(6), 387-392.

Husebye, E. (1999). The patterns of small bowel motility: physiology and implications in organic disease and functional disorders. *Neurogastroenterol Motil, 11*(3), 141-161.

Iddan, G., Meron, G., Glukhovsky, A., & Swain, P. (2000). Wireless capsule endoscopy. *Nature, 405*(6785), 417.

Jones, B. H., Fleischer, D. E., Sharma, V. K., Heigh, R. I., Shiff, A. D., Hernandez, J. L., et al. (2005). Yield of repeat wireless video capsule endoscopy in patients with obscure gastrointestinal bleeding. *Am J Gastroenterol, 100*(5), 1058-1064.

Karagiannis, S., Faiss, S., & Mavrogiannis, C. (2009). Capsule retention: a feared complication of wireless capsule endoscopy. *Scand J Gastroenterol, 44*(10), 1158-1165.

Kaufman, L., Kramer, D. M., Crooks, L. E., & Ortendahl, D. A. (1989). Measuring signal-to-noise ratios in MR imaging. *Radiology, 173*(1), 265-267.

Kavin, H., Berman, J., Martin, T. L., Feldman, A., & Forsey-Koukol, K. (2006). Successful wireless capsule endoscopy for a 2.5-year-old child: obscure gastrointestinal bleeding from mixed, juvenile, capillary hemangioma-angiomatosis of the jejunum. *Pediatrics, 117*(2), 539-543.

Kellow, J. E., Borody, T. J., Phillips, S. F., Haddad, A. C., & Brown, M. L. (1986). Sulfapyridine appearance in plasma after salicylazosulfapyridine. Another simple measure of intestinal transit. *Gastroenterology, 91*(2), 396-400.

Kim, S. K. (1968). Small intestine transit time in the normal small bowel study. *Am J Roentgenol Radium Ther Nucl Med, 104*(3), 522-524.

King, C. E., & Toskes, P. P. (1986). Comparison of the 1-gram [14C]xylose, 10-gram lactulose-H2, and 80-gram glucose-H2 breath tests in patients with small intestine bacterial overgrowth. *Gastroenterology, 91*(6), 1447-1451.

King, C. E., Toskes, P. P., Spivey, J. C., Lorenz, E., & Welkos, S. (1979). Detection of small intestine bacterial overgrowth by means of a 14C-D-xylose breath test. *Gastroenterology, 77*(1), 75-82.

King, P. M., Adam, R. D., Pryde, A., McDicken, W. N., & Heading, R. C. (1984). Relationships of human antroduodenal motility and transpyloric fluid movement: non-invasive observations with real-time ultrasound. *Gut, 25*(12), 1384-1391.

Kitazume, Y., Satoh, S., Hosoi, H., Noguchi, O., & Shibuya, H. (2007). Cine magnetic resonance imaging evaluation of peristalsis of small bowel with longitudinal ulcer in Crohn disease: preliminary results. *J Comput Assist Tomogr, 31*(6), 876-883.

Kivelitz, D., Gehl, H. B., Heuck, A., Krahe, T., Taupitz, M., Lodemann, K. P., et al. (1999). Ferric ammonium citrate as a positive bowel contrast agent for MR imaging of the upper abdomen. Safety and diagnostic efficacy. *Acta Radiol, 40*(4), 429-435.

Kraus, B. B., Rappaport, D. C., Ros, P. R., & Torres, G. M. (1994). Evaluation of oral contrast agents for abdominal magnetic resonance imaging. *Magn Reson Imaging, 12*(6), 847-858.

Kruis, W., Azpiroz, F., & Phillips, S. F. (1985). Contractile patterns and transit of fluid in canine terminal ileum. *Am J Physiol, 249*(2 Pt 1), G264-270.

Lang, R. A., Buhmann, S., Hopman, A., Steitz, H. O., Lienemann, A., Reiser, M. F., et al. (2008). Cine-MRI detection of intraabdominal adhesions: correlation with intraoperative findings in 89 consecutive cases. *Surg Endosc, 22*(11), 2455-2461.

Larson, M., & Schulze, K. (2002). Appearance of peristaltic reflex in isolated guinea pig ileum in response to boluses of air, water, oil, and cellulose. *Dig Dis Sci, 47*(12), 2644-2650.

Laubenberger, J., Buchert, M., Schneider, B., Blum, U., Hennig, J., & Langer, M. (1995). Breath-hold projection magnetic resonance-cholangio-pancreaticography (MRCP): a new method for the examination of the bile and pancreatic ducts. *Magn Reson Med, 33*(1), 18-23.

Lawrance, I. C., Welman, C. J., Shipman, P., & Murray, K. (2009). Small bowel MRI enteroclysis or follow through: which is optimal? *World J Gastroenterol, 15*(42), 5300-5306.

Li, B., & Meng, M. Q. (2009). Computer-based detection of bleeding and ulcer in wireless capsule endoscopy images by chromaticity moments. *Comput Biol Med, 39*(2), 141-147.

Lieb, J. G., & Draganov, P. V. (2008). The lactulose breath test (LBT): modified, but still a lot of hot air? *J Clin Gastroenterol, 42*(10), 1067-1069.

Lin, H. C., Zhao, X. T., & Wang, L. (1996). Jejunal brake: inhibition of intestinal transit by fat in the proximal small intestine. *Dig Dis Sci, 41*(2), 326-329.

Lomas, D. J. (2002). Techniques for magnetic resonance imaging of the bowel. *Top Magn Reson Imaging, 13*(6), 379-387.

Lomas, D. J., & Graves, M. J. (1999). Small bowel MRI using water as a contrast medium. *Br J Radiol, 72*(862), 994-997.

Low, R. N., & Francis, I. R. (1997). MR imaging of the gastrointestinal tract with i.v., gadolinium and diluted barium oral contrast media compared with unenhanced MR imaging and CT. *AJR Am J Roentgenol, 169*(4), 1051-1059.

Ma, M., Zhang, B. L., Chen, C. X., Li, F. B., Huang, X. L., Wang, P. X., et al. (2009). [Clinical value of wireless capsule endoscopy in diagnosis of small bowel disease in children]. *Zhonghua Er Ke Za Zhi, 47*(10), 745-749.

Maglinte, D. D., Lappas, J. C., Heitkamp, D. E., Bender, G. N., & Kelvin, F. M. (2003). Technical refinements in enteroclysis. *Radiol Clin North Am, 41*(2), 213-229.

Mako, E. K., Mester, A. R., Tarjan, Z., Karlinger, K., & Toth, G. (2000). Enteroclysis and spiral CT examination in diagnosis and evaluation of small bowel Crohn's disease. *Eur J Radiol, 35*(3), 168-175.

Malagelada, J. R., Robertson, J. S., Brown, M. L., Remington, M., Duenes, J. A., Thomforde, G. M., et al. (1984). Intestinal transit of solid and liquid components of a meal in health. *Gastroenterology, 87*(6), 1255-1263.

Marik, F., & Code, C. F. (1975). Control of the interdigestive myoelectric activity in dogs by the vagus nerves and pentagastrin. *Gastroenterology, 69*(2), 387-395.

Marshak, R. H., Maklansky, D., & Lindner, A. E. (1976). The radiology corner. Sigmoid-appendiceal fistula in diverticulitis. *Am J Gastroenterol, 66*(3), 292-296.

Martin, D. R., Danrad, R., Herrmann, K., Semelka, R. C., & Hussain, S. M. (2005). Magnetic resonance imaging of the gastrointestinal tract. *Top Magn Reson Imaging, 16*(1), 77-98.

Mazzeo, S., Caramella, D., Battolla, L., Melai, L., Masolino, P., Bertoni, M., et al. (2001). Crohn disease of the small bowel: spiral CT evaluation after oral hyperhydration with isotonic solution. *J Comput Assist Tomogr, 25*(4), 612-616.

McCoy, E. J., & Baker, R. D. (1968). Effect of feeding on electrical activity of dog's small intestine. *Am J Physiol, 214*(6), 1291-1295.

Mirowitz, S. A., & Susman, N. (1992). Use of nutritional support formula as a gastrointestinal contrast agent for MRI. *J Comput Assist Tomogr, 16*(6), 908-915.

Mishkin, D. S., & Mishkin, S. (2004). Sorbital H2 breath testing when screening for malabsorption/ intolerance and untreated celiac disease: understanding the dose and concentration issues. *Am J Gastroenterol, 99*(6), 1196.

Mugler, J. P., 3rd, & Brookeman, J. R. (1996). Off-resonance image artifacts in interleaved-EPI and GRASE pulse sequences. *Magn Reson Med, 36*(2), 306-313.

Nagi, B., Rana, S. S., Kochhar, R., & Bhasin, D. K. (2006). Sonoenteroclysis: a new technique for the diagnosis of small bowel diseases. *Abdom Imaging, 31*(4), 417-424.

Naslund, E., Bogefors, J., Gryback, P., Jacobsson, H., & Hellstrom, P. M. (2000). Gastric emptying: comparison of scintigraphic, polyethylene glycol dilution, and paracetamol tracer assessment techniques. *Scand J Gastroenterol, 35*(4), 375-379.

Negaard, A., Paulsen, V., Sandvik, L., Berstad, A. E., Borthne, A., Try, K., et al. (2007). A prospective randomized comparison between two MRI studies of the small bowel in Crohn's disease, the oral contrast method and MR enteroclysis. *Eur Radiol, 17*(9), 2294-2301.

Negaard, A., Sandvik, L., Berstad, A. E., Paulsen, V., Lygren, I., Borthne, A., et al. (2008). MRI of the small bowel with oral contrast or nasojejunal intubation in Crohn's disease: randomized comparison of patient acceptance. *Scand J Gastroenterol, 43*(1), 44-51.

Nieuwenhuijs, V. B., Verheem, A., van Duijvenbode-Beumer, H., Visser, M. R., Verhoef, J., Gooszen, H. G., et al. (1998). The role of interdigestive small bowel motility in the regulation of

gut microflora, bacterial overgrowth, and bacterial translocation in rats. *Ann Surg, 228*(2), 188-193.

Nolan, D. J., & Traill, Z. C. (1997). The current role of the barium examination of the small intestine. *Clin Radiol, 52*(11), 809-820.

Pallotta, N., Baccini, F., & Corazziari, E. (1999). Ultrasonography of the small bowel after oral administration of anechoic contrast solution. *Lancet, 353*(9157), 985-986.

Pallotta, N., Baccini, F., & Corazziari, E. (2000). Small intestine contrast ultrasonography. *J Ultrasound Med, 19*(1), 21-26.

Pallotta, N., Baccini, F., & Corazziari, E. (2001). Small intestine contrast ultrasonography (SICUS) in the diagnosis of small intestine lesions. *Ultrasound Med Biol, 27*(3), 335-341.

Parikh, D. A., Parikh, J. A., Albers, G. C., & Chandler, C. F. (2009). Acute small bowel perforation after wireless capsule endoscopy in a patient with Crohn's disease: a case report. *Cases J, 2*, 7607.

Patak, M. A., Froehlich, J. M., von Weymarn, C., Breitenstein, S., Zollikofer, C. L., & Wentz, K. U. (2007). Non-invasive measurement of small-bowel motility by MRI after abdominal surgery. *Gut, 56*(7), 1023-1025.

Penning, C., Gielkens, H. A., Hemelaar, M., Lamers, C. B., & Masclee, A. A. (2001). Reproducibility of antroduodenal motility during prolonged ambulatory recording. *Neurogastroenterol Motil, 13*(2), 133-141.

Pham, D. L., Xu, C., & Prince, J. L. (2000). Current methods in medical image segmentation. *Annu Rev Biomed Eng, 2*, 315-337.

Raptopoulos, V., Schwartz, R. K., McNicholas, M. M., Movson, J., Pearlman, J., & Joffe, N. (1997). Multiplanar helical CT enterography in patients with Crohn's disease. *AJR Am J Roentgenol, 169*(6), 1545-1550.

Rubesin, S. E., & Maglinte, D. D. (2003). Double-contrast barium enema technique. *Radiol Clin North Am, 41*(2), 365-376.

Sadik, R., Abrahamsson, H., & Stotzer, P. O. (2003). Gender differences in gut transit shown with a newly developed radiological procedure. *Scand J Gastroenterol, 38*(1), 36-42.

Sarna, S. K. (1987). Giant migrating contractions and their myoelectric correlates in the small intestine. *Am J Physiol, 253*(5 Pt 1), G697-705.

Sarna, S. K., Soergel, K. H., Harig, J. M., Loo, F. D., Wood, C. M., Donahue, K. M., et al. (1989). Spatial and temporal patterns of human jejunal contractions. *Am J Physiol, 257*(3 Pt 1), G423-432.

Scholz, F. J. (1989). Manual compression device for fluoroscopy. *Radiology, 170*(2), 564-565.

Schreyer, A. G., Geissler, A., Albrich, H., Scholmerich, J., Feuerbach, S., Rogler, G., et al. (2004). Abdominal MRI after enteroclysis or with oral contrast in patients with suspected or proven Crohn's disease. *Clin Gastroenterol Hepatol, 2*(6), 491-497.

Schwizer, W., Fox, M., & Steingotter, A. (2003). Non-invasive investigation of gastrointestinal functions with magnetic resonance imaging: towards an "ideal" investigation of gastrointestinal function. *Gut, 52 Suppl 4*, iv34-39.

Sellink, J. L. (1971). [Thoughts on the radiologic study of the small intestine]. *Ned Tijdschr Geneeskd, 115*(17), 743-748.

Sharma, N., & Aggarwal, L. M. Automated medical image segmentation techniques. *J Med Phys, 35*(1), 3-14.

Sharpstone, D., Neild, P., Crane, R., Taylor, C., Hodgson, C., Sherwood, R., et al. (1999). Small intestinal transit, absorption, and permeability in patients with AIDS with and without diarrhoea. *Gut, 45*(1), 70-76.

Silverman, P. M., Kalender, W. A., & Hazle, J. D. (2001). Common terminology for single and multislice helical CT. *AJR Am J Roentgenol, 176*(5), 1135-1136.

Soffer, E. E., Thongsawat, S., & Ellerbroek, S. (1998). Prolonged ambulatory duodeno-jejunal manometry in humans: normal values and gender effect. *Am J Gastroenterol, 93*(8), 1318-1323.

Suzuki, N., Prosser, C. L., & Dahms, V. (1986). Boundary cells between longitudinal and circular layers: essential for electrical slow waves in cat intestine. *Am J Physiol, 250*(3 Pt 1), G287-294.

Tasaka, K., & Farrar, J. T. (1969). Mechanics of small intestinal muscle function in the dog. *Am J Physiol, 217*(4), 1224-1229.

Theoni, R. F. (1987). Radiography of the small bowel and enteroclysis. A perspective. *Invest Radiol, 22*(12), 930-936.

Thompson, W. M., Halvorsen, R. A., Shaw, M., Bates, W. M., & Shemano, I. (1982). Evaluation of intramuscular ceruletide for

shortening small bowel transit time. *Gastrointest Radiol, 7*(2), 141-147.

Torkzad, M. R., Vargas, R., Tanaka, C., & Blomqvist, L. (2007). Value of cine MRI for better visualization of the proximal small bowel in normal individuals. *Eur Radiol, 17*(11), 2964-2968.

von Schonfeld, J., Evans, D. F., Renzing, K., Castillo, F. D., & Wingate, D. L. (1998). Human small bowel motor activity in response to liquid meals of different caloric value and different chemical composition. *Dig Dis Sci, 43*(2), 265-269.

Vu, H., Echigo, T., Sagawa, R., Yagi, K., Shiba, M., Higuchi, K., et al. (2009). Detection of contractions in adaptive transit time of the small bowel from wireless capsule endoscopy videos. *Comput Biol Med, 39*(1), 16-26.

Wang, X. Y., Sanders, K. M., & Ward, S. M. (1999). Intimate relationship between interstitial cells of cajal and enteric nerves in the guinea-pig small intestine. *Cell Tissue Res, 295*(2), 247-256.

Wright, J., Evans, D., Gowland, P., & Mansfield, P. (1999). Validation of antroduodenal motility measurements made by echo-planar magnetic resonance imaging. *Neurogastroenterol Motil, 11*(1), 19-25.

Appendix 1

Volunteer information sheet

Norfolk and Norwich University Hospital NHS

NHS Trust

Department of Respiratory Medicine
Level 3, East Block
Colney Lane
Norwich
NR4 7UY

Physiological MR imaging of small bowel: Implementation, validation and interpretation- Volunteer information sheet

What is the purpose of the study?

The aim of this study is to investigate techniques of mathematical modelling of dynamic MRI of small bowel; in particular the optimal imaging parameters will be evaluated, the reliability of the technique will be validated, and the application of various mathematical analyses will be assessed.

Why have I been chosen?

The research team do not consider it appropriate to use healthy volunteers from outside the research team for ethical reasons. As you are part of the research team you understand the process of trial and errors needed for establish a robust technique to be used in future on volunteers.

Do I have to take part?

No, it is up to you to decide whether to take part. If you do decide to take part, you will be given this information sheet to keep and be asked to sign a consent form. If you decide to take part, you are still free to withdraw at any time without giving a reason. A decision to withdraw at any time, or a decision not to take part, will not affect your current clinical work, training or further research projects.

What will happen to me if I agree to take part?

If you are happy to take part, and are satisfied with the explanations from the research team, you will be asked to sign a consent form. And then asked to come to be scanned in the MRI for about 6-6 sessions each will be around 2 hours long. We will also give in one of the sessions a 20 mg of Buscopan Intramuscular.

What are the possible disadvantages and risks of taking part?

MRI is a relatively safe investigation, which does not use ionizing radiation. Absolute contraindications include:

Cardiac pacemakers

Certain implanted medical devices

Intra-ocular metallic foreign bodies

Common adverse effects, which do not pose a serious health risk, include:

- Acoustic noise
- Peripheral nerve stimulation
- Light flashes

- Claustrophobia

Buscopan is regularly used in the department of radiology paralysing bowel during fluoroscopy and MR examinations of the pelvis. Contra-indications to its use include glaucoma, history of angina or allergy. Serious side effects are uncommon the most common being blurring of vision and dry mouth.

What are the possible benefits of taking part?

There are no clinical benefits to taking part. However, the information we get from this study may help us diagnose and hence manage future patients with small bowel disorders.

What if something goes wrong?
We would not expect anything to go wrong with this study
If you have a concern about any aspect of this study, you should ask to speak to the researchers who will do their best to answer your questions.

If you are harmed by taking part in this research project, there are no special compensation arrangements. If you are harmed during the research due to someone's negligence then you may have grounds for legal action for compensation against the hospital, but you may have to pay your legal costs. The normal NHS complaints mechanisms will still be available to you.

Will taking part in this study be kept confidential?

Your data will be collected by members of the research team. All information that is collected about you during the course of this study will be kept strictly confidential. Representatives of the sponsor or the Trust R&D department will have access to identifiable data to ensure the study is being corrected properly. This anonymised information will be accessible to the research team and may also be looked at by representatives of regulatory authorities and by authorized people to check that the study is being carried out correctly. All will have a duty of confidentiality to you as a research participant. It will be stored securely and Dr Farghal will be the custodian. It will be kept for 15 years after which it will be disposed of securely. Use of your data will be in compliance with the Data Protection Act.

What will happen to the results of the research study?

It is hoped that the results of the study will be presented at a medical meeting or reported in a scientific journal. We can forward the report of the study to you if you wish.
You will not be named or identified in any report or publication.

Who is organising and funding the research?

This study is being carried out by doctors from the Norfolk & Norwich NHS Trust and University of East Anglia. It is being funded by departmental funds.

Who has reviewed the study?

The study has been reviewed by East Norfolk & Waveney Research Governance Committee and Norfolk Research Ethics Committee

Contact for Further Information

Dr Aser Farghal at the address given above, 07909901719 e-mail: **aser.farghal@nnuh.nhs.uk**

We would like to thank you for taking time to read this sheet and considering taking part.

Appendix 2

Consent form

Norfolk and Norwich University Hospital NHS
NHS Trust

Centre Number:
Study Number:
Patient Identification Number:

CONSENT FORM

Title of Project: Physiological MR imaging of small bowel: implementation, validation and interpretation

Name of Researchers: Dr Andoni Toms Dr Paul Malcolm
Dr Iean Beals Dr Aser Farghal

Volunteer Details:

Name: DOB: Address: Tel: GP:

Please initial box

1. I confirm that I have read and understand the information sheet dated ..... (version .....) for the above study and have had the opportunity to ask questions. ☐
2. I understand that my participation is voluntary and that I am free to withdraw at any time, without giving any reason, without my medical care or legal rights being affected. ☐
3. I agree to take part in the above study. ☐

_____	_____	_____
Name of Volunteer	Date	Signature
_____	_____	_____
Researcher	Date	Signature

1 for Volunteer; 1 for researcher

Appendix 3

Ethics approval

NHS
National Research Ethics Service

Norfolk Research Ethics Committee
c/o The Norfolk & Norwich University Hospitals NHS Foundation Trust
East of England REC Office [2]
Room 2.08 First Floor
Aldwych House
57 Bethel Street
NORWICH
NR2 1NR

Telephone: 01603 289813
Facsimile: 01603 286573

24 February 2009

Dr Aser Farghal
Specialist Registrar In Radiology
Norfolk and Norwich University Hospitals NHS Foundation Trust
Department of Radiology
Colney Lane, Norwich NR4 7UY

Dear Dr Farghal

Full title of study: **Physiological MR imaging of small bowel: implementation, validation and interpretation**
REC reference number: **09/H0310/3**

Thank you for your letter of 31 January 2009, responding to the Committee's request for further information on the above research and submitting revised documentation.

The further information has been considered on behalf of the Committee by the Chair in consultation with selected Members.

Confirmation of ethical opinion

On behalf of the Committee, I am pleased to confirm a favourable ethical opinion for the above research on the basis described in the application form, protocol and supporting documentation as revised, subject to the conditions specified below.

Ethical review of research sites

The favourable opinion applies to the research sites listed on the attached form.

Conditions of the favourable opinion

The favourable opinion is subject to the following conditions being met prior to the start of the study.

Management permission or approval must be obtained from each host organisation prior to the start of the study at the site concerned.

Management permission at NHS sites ("R&D approval") should be obtained from the relevant care organisation(s) in accordance with NHS research governance arrangements. Guidance on applying for NHS permission is available in the Integrated Research Application System or at http://www.rdforum.nhs.uk.

Approved documents

The final list of documents reviewed and approved by the Committee is as follows:

Document	*Version*	*Date*
checklist		
Participant Consent Form: Small Bowel	AF/01	31 December 2008
Compensation Arrangements	S Steel, UEA	15 December 2008
Peer Review		
Covering Letter		
Protocol	6	15 December 2008
Investigator CV	Aser S Farghal	
Application	7123/18366/ 1/329	15 December 2008
Application [SSI Form]	7123/18375/ 6/102/4271/7 3156 [NNUH]	15 December 2008
Response to Request for Further Information	Letter from Dr Aser Farghal	31 January 2009
Participant Information Sheet: Information Sheet about Buscopan	02	31 December 2008
Participant Information Sheet: Volunteer	AF/01	31 January 2009

Statement of compliance

The Committee is constituted in accordance with the Governance Arrangements for Research Ethics Committees (July 2001) and complies fully with the Standard Operating Procedures for Research Ethics Committees in the UK.

After ethical review

Now that you have completed the application process please visit the National Research Ethics Website > After Review

You are invited to give your view of the service that you have received from the National Research Ethics Service and the application procedure. If you wish to make your views known please use the feedback form available on the website.

The attached document "After ethical review –guidance for researchers" gives detailed guidance on reporting requirements for studies with a favourable opinion, including:

- Notifying substantial amendments
- Progress and safety reports
- Notifying the end of the study

The NRES website also provides guidance on these topics, which is updated in the light of changes in reporting requirements or procedures.

We would also like to inform you that we consult regularly with stakeholders to improve our service. If you would like to join our Reference Group please email referencegroup@nres.npsa.nhs.uk.

This Research Ethics Committee is an advisory committee to East of England Strategic Health Authority

The National Research Ethics Service (NRES) represents the NRES Directorate within the National Patient Safety Agency and Research Ethics Committees in England

09/H0310/3	**Please quote this number on all correspondence**

With the Committee's best wishes for the success of this project

Yours sincerely

Co-ordinator

Michael Sheldon, MA PhD
Chair

Email: janette.guymer@nnuh.nhs.uk

Enclosures: "After ethical review – guidance for researchers" *[SL- AR2]*
Site approval form [SF1] Issue 1

Copy to: *Mrs Sue Steel, UEA*
NNUH R&D Department

This Research Ethics Committee is an advisory committee to East of England Strategic Health Authority
The National Research Ethics Service (NRES) represents the NRES Directorate within the National Patient Safety Agency and Research Ethics Committees in England

Norfolk Research Ethics Committee

LIST OF SITES WITH A FAVOURABLE ETHICAL OPINION

For all studies requiring site-specific assessment, this form is issued by the main REC to the Chief Investigator and sponsor with the favourable opinion letter and following subsequent notifications from site assessors. For issue 2 onwards, all sites with a favourable opinion are listed, adding the new sites approved.

REC reference number:	09/H0310/3	**Issue number:**	1	**Date of issue:**	24 February 2009
Chief Investigator:	Dr Aser Farghal				
Full title of study:	Physiological MR imaging of small bowel: implementation, validation and interpretation				

This study was given a favourable ethical opinion by Norfolk Research Ethics Committee on 28 February 2009. The favourable opinion is extended to each of the sites listed below. The research may commence at each NHS site when management approval from the relevant NHS care organisation has been confirmed.

Principal Investigator	*Post*	*Research site*	*Site assessor*	*Date of favourable opinion for this site*	*Notes [1]*
Dr Aser Farghal	Specialist Registrar In Radiology	Norfolk and Norwich University Hospitals NHS Foundation Trust	Norfolk Research Ethics Committee	24/02/2009	

Approved by the Chair on behalf of the REC:

..... (Signature of ~~Chair~~/Co-ordinator)

(delete as applicable)

..... (Name)

(1) *The notes column may be used by the main REC to record the early closure or withdrawal of a site (where notified by the Chief Investigator or sponsor), the suspension of termination of the favourable opinion for an individual site, or any other relevant development. The date should be recorded.*

This Research Ethics Committee is an advisory committee to East of England Strategic Health Authority

The National Research Ethics Service (NRES) represents the NRES Directorate within the National Patient Safety Agency and Research Ethics Committees in England

NHS
National Patient Safety Agency
National Research Ethics Service

RESEARCH IN HUMAN SUBJECTS OTHER THAN CLINICAL TRIALS OF INVESTIGATIONAL MEDICINAL PRODUCTS

After ethical review – guidance for sponsors and investigators

This document sets out important guidance for sponsors and investigators on the conduct and management of research with a favourable opinion from a NHS Research Ethics Committee. Please read the guidance carefully. A failure to follow the guidance could lead to the committee reviewing its opinion on the research.

1. Further communications with the Research Ethics Committee

1.1 Further communications during the research with the Research Ethics Committee that gave the favourable ethical opinion (hereafter referred to in this document as "the Committee") are the personal responsibility of the Chief Investigator.

2. Commencement of the research

2.1 It is assumed that the research will commence within 12 months of the date of the favourable ethical opinion.

2.2 In the case of research requiring site-specific assessment (SSA) the research must not commence at any site until the Committee has notified the Chief Investigator that the favourable ethical opinion is extended to the site.

2.3 The research must not commence at any site until the local Principal Investigator (PI) or research collaborator has obtained management permission or approval from the organisation with responsibility for the research participants at the site.

2.4 Should the research not commence within 12 months, the Chief Investigator should give a written explanation for the delay. It is open to the Committee to allow a further period of 12 months within which the research must commence.

2.5 Should the research not commence within 24 months, the favourable opinion may be suspended and the application would need to be re-submitted for ethical review.

3. Duration of ethical approval

3.1 The favourable opinion for the research generally applies for the duration of the research. If it is proposed to extend the duration of the study as specified in the application form, the Committee should be notified.

3.2 Where the research involves the use of "relevant material" for the purposes of the Human Tissue Act 2004, authority to hold the material under the terms of the ethical approval applies until the end of the period declared in the application and approved by the Committee.

4. Progress reports

4.1 Research Ethics Committees are expected to keep a favourable opinion under review in the light of progress reports and any developments in the study. The Chief Investigator should submit a progress report to the Committee 12 months after the date on which the favourable opinion was given. Annual progress reports should be submitted thereafter.

4.2 Progress reports should be in the format prescribed by NRES and published on the website (see www.nres.npsa.nhs.uk/applicants/after-ethical-review/).

4.3 The Chief Investigator may be requested to attend a meeting of the Committee or Sub-Committee to discuss the progress of the research.

5. Amendments

5.1 If it is proposed to make a substantial amendment to the research, the Chief Investigator should submit a notice of amendment to the Committee.

5.2 A substantial amendment is any amendment to the terms of the application for ethical review, or to the protocol or other supporting documentation approved by the Committee, that is likely to affect to a significant degree:

(a) the safety or physical or mental integrity of the trial participants
(b) the scientific value of the trial
(c) the conduct or management of the trial.

5.3 Notices of amendment should be in the format prescribed by NRES and published on the website, and should be personally signed by the Chief Investigator. The agreement of the sponsor should be sought before submitting the notice of amendment.

5.4 A substantial amendment should not be implemented until a favourable ethical opinion has been given by the Committee, unless the changes to the research are urgent safety measures (see section 7). The Committee is required to give an opinion within 35 days of the date of receiving a valid notice of amendment.

5.5 Amendments that are not substantial amendments ("minor amendments") may be made at any time and do not need to be notified to the Committee.

6. Changes to sites *(studies requiring site-specific assessment only)*

6.1 Where it is proposed to include a new site in the research, there is no requirement to submit a notice of amendment form to the Committee. The SSI Form together with the local Principal Investigator's CV should be submitted to the relevant local REC for site-specific assessment (SSA).

6.2 Similarly, where it is proposed to make significant changes in the management of a site (in particular, the appointment of a new PI), a notice of amendment form is not required. A revised SSI form for the site (together with the CV for the new PI if applicable) should be submitted to the relevant local REC for SSA.

6.3 The relevant local REC will notify the Committee whether there is any objection to the new site or Principal Investigator. The Committee will notify the Chief Investigator of its opinion within 35 days of receipt of the valid application for SSA.

6.4 For studies designated by the Committee as exempt from SSA, there is no requirement to notify the Committee of the inclusion of new sites.

7. Urgent safety measures

7.1 The sponsor or the Chief Investigator, or the local Principal Investigator at a trial site, may take appropriate urgent safety measures in order to protect research participants against any immediate hazard to their health or safety.

7.2 The Committee must be notified within three days that such measures have been taken, the reasons why and the plan for further action.

8. Serious Adverse Events

8.1 A Serious Adverse Event (SAE) is an untoward occurrence that:

(a) results in death
(b) is life-threatening
(c) requires hospitalisation or prolongation of existing hospitalisation
(d) results in persistent or significant disability or incapacity
(e) consists of a congenital anomaly or birth defect
(f) is otherwise considered medically significant by the investigator.

8.2 A SAE occurring to a research participant should be reported to the Committee where in the opinion of the Chief Investigator the event was related to administration of any of the research procedures, and was an unexpected occurrence.

8.3 Reports of SAEs should be provided to the Committee within 15 days of the Chief Investigator becoming aware of the event, in the format prescribed by NRES and published on the website.

8.4 The Chief Investigator may be requested to attend a meeting of the Committee or Sub-Committee to discuss any concerns about the health or safety of research subjects.

8.5 Reports should not be sent to other RECs in the case of multi-site studies.

9. Conclusion or early termination of the research

9.1 The Chief Investigator should notify the Committee in writing that the research has ended within 90 days of its conclusion. The conclusion of the research is defined as the final date or event specified in the protocol, not the completion of data analysis or publication of the results.

9.2 If the research is terminated early, the Chief Investigator should notify the Committee within 15 days of the date of termination. An explanation of the reasons for early termination should be given.

9.3 Reports of conclusion or early termination should be submitted in the form prescribed by NRES and published on the website.

10. Final report

10.1 A summary of the final report on the research should be provided to the Committee within 12 months of the conclusion of the study. This should include information on whether the study achieved its objectives, the main findings, and arrangements for publication or dissemination of the research including any feedback to participants.

11. Review of ethical opinion

11.1 The Committee may review its opinion at any time in the light of any relevant information it receives.

11.2 The Chief Investigator may at any time request that the Committee reviews its opinion, or seek advice from the Committee on any ethical issue relating to the research.